# Investigation of the Potential Use of the Root-Zone Storage Concept in Hydrological Modelling under South African Conditions

**ROBYN HORAN**

**214582108**

**Submitted in fulfilment of the academic requirements of**

**Master of Science**

in Hydrology

School of Agricultural, Earth and Environmental Sciences

University of KwaZulu-Natal

Pietermaritzburg

South Africa

November 2019

# PREFACE

The research contained in this thesis was completed by the candidate while based in the Discipline of Hydrology, School of Agricultural, Earth and Environmental Sciences of the College of Agriculture, Engineering and Science, University of KwaZulu-Natal, Pietermaritzburg, South Africa. The research was financially supported by the Water Research Commission of South Africa.

The contents of this work have not been submitted in any form to another university and, except where the work of others is acknowledged in the text, the results reported are due to investigations by the candidate.

_____

Signed: Robyn Horan

Date: 21/11/2019

_____

Signed: Dr ML Toucher

Date: 21 November 2019

# DECLARATION: PLAGIARISM

I, Robyn Horan, declare that:

(i)     the research reported in this dissertation, except where otherwise indicated or acknowledged, is my original work;

(ii)     this dissertation has not been submitted in full or in part for any degree or examination to any other university;

(iii)     this dissertation does not contain other persons' data, pictures, graphs or other information, unless specifically acknowledged as being sourced from other persons;

(iv)     this dissertation does not contain other persons' writing, unless specifically acknowledged as being sourced from other researchers. Where other written sources have been quoted, then:

   a)     their words have been re-written but the general information attributed to them has been referenced;

   b)     where their exact words have been used, their writing has been placed inside quotation marks, and referenced;

(v)     where I have used material for which publications followed, I have indicated in detail my role in the work;

(vi)     this dissertation is primarily a collection of material, prepared by myself, published as journal articles or presented as a poster and oral presentations at conferences. In some cases, additional material has been included;

(vii)     this dissertation does not contain text, graphics or tables copied and pasted from the Internet, unless specifically acknowledged, and the source being detailed in the dissertation and in the References sections.

_____

Signed: Robyn Horan

Date: 21/11/2019

# ABSTRACT

Hydrological models are currently an accepted method used in determining the impacts of Streamflow reduction activities (SFRA) in South Africa. However, the limited availability of soils and rooting depth data create high uncertainty within hydrological modelling exercises. Following poor simulations of streamflow, evaporation and soil water by the ACRU model at Two Streams and Cathedral Peak Catchment VI, the root- zone storage capacity was calculated for both catchments using three internationally published over the period 2007 to 2013 and 2014 to 2018, respectively.

The input and calibration data used in the running of the ACRU model was undertaken using observed data commonly available for research catchments in South Africa. Additional data that was available for these specific catchments (observed evaporation and soil water at Two Streams and evaporation at Cathedral Peak Catchment VI) were used in the validation of results.

The three methods produced similar mean root- zone storage capacities in both catchments but the Nijzink and DiCaSM methods produced the deepest root-zone storage capacity in the summer months. The results of the Nijzink method were the most variable and DiCaSM the least variable in both catchments. The Nijzink method was most sensitive to the actual evaporation in both summer and winter and sensitive to the precipitation in summer. The Wang method most sensitive to precipitation in summer. The DiCaSM method was found to not be sensitive to the rainfall in either season but highly sensitive to the actual evaporation year-round.

The root-zone storage concept better reproduced the observed soil water throughout the soil profile at the Two Streams catchment than the ACRU model. The validation of the root- zone storage capacity against observed soil water illustrated that the root zone storage capacity reflects climate conditions rather than the soil depth and is independent of vegetation, soils and rooting characteristics. This study found that traditional methods of estimating the actual evaporation does not always capture the variability in timing and magnitude of evaporation.

3

The most significant finding is that simple climate driven water balance routine could provide a better representation of soil water than a complex, layered model under South African conditions. The root-zone storage capacity could be a valuable tool in the improvement of hydrological modelling and fundamental in improving the precision of SFRA assessments in South Africa.

# ACKNOWLEDGEMENTS

**TABLE OF CONTENTS**

6

# LIST OF TABLES

# LIST OF FIGURES

14

15

# CHAPTER 1: INTRODUCTION

## 1.1  Rationale for the Research

The declaration of streamflow reduction activities (SFRA) and the implications of licensing these activities continue to be a complicated and tedious task to execute and uncertainty remains in their accuracy and fairness (Dye and Versfeld, 2007). The environmental and socio-economic impacts of commercial afforestation are a prominent political debate amongst the role- players affected by SFRA policies in South Africa (Scott and Gush, 2017). A clear, accurate and fair procedure to declare and manage SFRAs needs to be established with the collaboration from participating sectors (DWAF, 2003). The use of hydrological models, such as the Agricultural Catchments Research Unit (ACRU) model, are currently an accepted method used in determining the impacts of SFRAs in South Africa. However, the improvement and refinement of a number of input parameters, including the soils data, is necessary.

Soils play a critical role in the regulation and generation of catchment hydrological responses. Hydrological models require detailed catchment scale soils data to generate satisfactory results (Schulze and Pike, 2004). There is no universal soils map for South Africa although, the use of Land Type maps and small areas of available intensive soils information are commonly used in modelling exercises. Land Type maps provide complete coverage of the country but alone have limited hydrological application. Work has been performed to assign hydrological parameters to the Land Type maps for the purpose of hydrological modelling. An identified problem has been the lack of detailed root depth estimates and understanding of their establishment over time to input into dynamic hydrological models. Typically coarsely averaged values from literature are used along with the assumption that porosity drives the root-zone storage capacity.

A possible alternative to intensive soils mapping is the incorporation of the root-zone storage concept into hydrological modelling. Root-zone storage capacity is considered to be the volume of water per unit area within the range of plant roots and available for transpiration. There are many methodologies used in the estimation of the root-zone storage concept. The water balance derived methods have proven the most successful internationally. The water balance derived root-zone storage capacity considers climate variables (effective precipitation, total evaporation and streamflow) and the permanent wilting point to determine the soil water fluxes

through the entire soil profile. The vegetation growth is considered through the interception component of the effective precipitation. This concept introduces additional vegetation growth parameters through this proxy and may provide more appropriate parameters and algorithms to result in a better representation of the system. This concept could be appropriate in regions were climate data is available however, detailed, multi- horizon, soils data (eg. depth, texture, field capacity, saturated hydraulic conductivity etc) are unavailable.

Successful studies have been performed in Asia, the Boreal region and New Zealand using this concept but not as yet in South African conditions. Additionally, Nijzink *et al.* (2016), detected the change in root-zone storage with deforestation but little work has been performed on the root-zone storage capacity under commercial afforestation. The utilization of the root-zone storage capacity under commercial afforestation could potentially be useful in the improvement of modelling for SFRA purposes.


## 1.2   Justification

The South African timber industry is reliant on fast- growing, high water using exotic tree species for economically viable pulp and timber production. These exotic trees are favourable over the slower growing and sparsely located indigenous species.

South Africa has a limited area of natural forest (Scott and Gush, 2017). Indigenous forests constitute an area less than 0.4 % of South Africa. The highly fragmented nature of these indigenous forests increases their vulnerability to changing land use, climate change and unsustainable usage (Berliner, 2009). For the protection of the remaining indigenous forests and more economically viable timber production, it is necessary to have introduced exotic fast-growing species into suitable regions (DAFF, 2003). The large scale planting of fast- growing exotic trees has the potential to reduce the available runoff (Brown *et al.*, 2005) and groundwater within the catchment due to changes in total evaporation and deeper rooting depths. Most plantations in South Africa are established in the high rainfall escarpment areas which act as the headwaters for major rivers. Literature shows that commercial forestry in headwater catchments reduces the volume of water available to feed the catchment and provide for downstream usage (Armstrong and Hensbergen, 1996 and Brown *et al.*, 2005).

The establishment of exotic forests in the humid escarpment of the country can lead to conflict with downstream water users (Scott and Gush, 2017) and intense competition over the limited water resources in South Africa (DWAF, 2003). The South African Ministry of Water Affairs and Forestry (DWAF, 1996) estimated that commercial forestry consumed approximately 1.2 billion additional cubic meters of water than pre-existing natural vegetation. The environmental concerns over commercial forestry are however not new. The South African government has been aware of the potential long term environmental effects of introduced forestry since 1920. Despite continuing controversy over the effect of forestry on water resources, research pertaining to the water-use characteristics of timber has received significant attention (Scott and Lesch, 1997).

An intensive forest hydrology research program was established in 1936 with results being utilised between 1970 and 1995 into management policies for plantations (Scott and Gush, 2017). The first permit system was introduced in 1972 (Afforestation Permit System) which allowed plantations to be developed in areas where it was seen to have the least environmental effect (Tewari, 2001). Under this system, approximately five thousand square kilometres of plantation forests were authorised from the ten thousand square kilometres that were established for forestry before the requirement for permits (Van der Zel, 1995). This system made use of the classification of primary catchments into three categories based on the percentage of expected reduced streamflow from the afforestation of the catchment. The percentage of expected reduction in streamflow was derived from an agreed formula developed from Nänni (1970a, 1970b) and modified by van der Zel (1982). The method of determining the reduction of streamflow under afforestation is determined from the estimated vegetation characteristics of mid-age trees. It does not account for the variance of the tree water use throughout the growth cycle. Following the determination that afforestation has a marked reduction in the catchment streamflow of a varying percentage, the practise was declared an SFRA in 1998.

There has been a stagnation of commercial forestry expansion in the last two decades due to policy regulating plantations through estimated regional water use and the declaration of plantations as the only SFRA under the National Water Act (1998) which requires existing and new commercial forest stands to be licensed. Under the National Water Act (1998) the Afforestation Permit Policy Committee was appointed to develop and improve on the

Afforestation Permit System and to guide the development of SFRA declaration and licensing procedures.

To undertake the SFRA declaration and licensing procedures, the Department of Water and Sanitation (DWAF 2003a – d) required an extensive tool to assess the impacts of commercial afforestation on water resources and incorporate the findings into water use authorisation and allocation processes. Hydrological modelling has become the accepted method of assessing the impact of commercial afforestation on water resources (Greenwood *et al.*, 2011). Although many hydrological models such as SWAT (Govender and Everson, 2005 and von Stackelberg *et al.*, 2007), SWIM (Wattenbach *et al.*, 2007) and SIMHYD (Li *et al.*, 2012) models give good estimations of the impacts of afforestation, there is a need for improvement and refinement of specific parameters. In many international studies reviewed by Vereecken *et al.* (2016), the conclusions have pointed to inaccurate soils information as a common shortcoming in modelling endeavours. In a South African context, Jewitt and Schulze (1999) give evidence that the ACRU model along with the forest decision support system is a viable application in estimating the impacts of commercial afforestation. Furthermore, the conclusions presented from this study show that there are shortcomings with this approach such as poor simulations in catchments with limited input data and when modelling very small scale catchments. Despite this, it is generally accepted that the ACRU model and the forest decision support system provide a useful tool for SFRA assessments (Jewitt and Schulze, 1999).

Gush et al. (2002) identified the ACRU model as a possible option for simulation of the effects of commercial afforestation on a national level. The paragraph which follows summarises the relevant findings of Gush et al. (2002) for this study. The effects of afforestation are determined by comparing the catchment under a baseline scenario, consisting of the natural vegetation, and the changed catchment under varying afforestation intensity. The ACRU model was run, using the natural vegetation (Acocks 1988 Veld types) and 100% afforestation of eucalyptus, pine and wattle for 843 quaternary catchments. The difference in streamflow was attributed to tree water use. This estimation of forestry water use from the ACRU model proved successful when comparing the simulations to observed data from paired catchment studies in catchments where such data was available. It was concluded that with improvement to the quaternary catchment

database (soils, baseline vegetation and climate data) the results could have been improved further.

In 2009, Jewitt *et al.* made a number of improvements to the ACRU2000 model in order to address identified shortcomings in the simulations of catchments under commercial afforestation. The inclusion of the intermediate soil zone and consideration of the hillslope into the model proved successful and improved the estimation of the low flows under forestry. It was suggested that there needed to be ongoing testing of the model in a wider range of catchments and improved knowledge of soil depth and hillslope lengths which are not widely available on a national scale. The application of the modified model was sufficient in small detailed studies where the above- mentioned parameters were available but proved inadequate on a national scale. The project concluded that the incorporation of both the SFRA Assessment Utility and the BEEH Quinary Catchments Database provided a valuable tool for SFRA assessments. The integration, improvement and better spatial representation of rainfall, soils, potential evaporation and baseline vegetation data is required to reduce uncertainty.

The implications of licensing and declaration procedures remain a grey area and are complex and time-consuming to execute (Dye and Versfeld, 2007). The uncertainty with regards to the impacts of forestry in South Africa has become a high- level political debate (Scott and Gush, 2017). There continues to be an ongoing debate amongst role-players affected by SFRAs as to the most effective way to declare and manage these activities (DWAF, 2003).

There has been extensive work undertaken at the University of the Free State to provide refined Land Types Soils (van Tol *et al.*, 2013). The refinement is to potentially provide a more accurate representation and conceptualisation of modelled catchments. A need has arisen for alternative methods of conceptualising the soil water budget and soil water within hydrological models to be considered due to the immense labour and cost of intensive soils mapping. An idea that has emerged in recent literature is the incorporation of the root-zone storage capacity into hydrological modelling. Studies undertaken in Asia, the Boreal region and New Zealand have proven successful (Zhao *et al.*, 2016; Nijzink *et al.*, 2016 and Wang- Erlandsson *et al.*, 2019). These successful studies provide reason to test the root-zone storage capacity concept in South Africa under a natural grassland and commercial afforestation.

## 1.3   Aims and Objectives

The aims and objectives evolved throughout the duration of this project based on findings of the preceding aim. The initial aim was to project is to produce a good simulation of the streamflow, total evaporation and soil water component of the hydrological cycle in both the Cathedral Peak Catchment VI (pristine grassland) and Two Streams (commercial forestry) using the ACRU model (Aim 1). Following a fair simulation of streamflow at Cathedral Peak Catchment VI and a poor simulation of streamflow at Two Streams, the second aim is to validate (using observed data) various simulated components of the water balance to potentially isolate routines or parameters producing poor simulations within the ACRU model (Aim 2). The soil water and total evaporation were identified as components poorly simulated by ACRU.

Following the isolation of the soil water routine and total evaporation estimation as potential sources of uncertainty, the next objective was to set up an investigation into the use of three internationally verified water balance derived root-zone storage capacity methods under South African pristine grassland and commercial forestry conditions.(Aim 3) and to undertake a sensitivity analysis to determine the effect of the total evaporation derivation on the estimation of the root-zone storage capacity (Aim 4). And finally to determine the application of the root-zone storage capacity in addressing the uncertainty within ACRU (Aim 5).

# CHAPTER 2: LITERATURE REVIEW

## 2.1　Introduction

South Africa's timber industry is dependent on the cultivation of exotic water- thirsty commercial tree species as the country has a limited area of natural forest (Scott and Gush, 2017). The change in land use to the exotic forest stands can lead to conflict with downstream water users (Scott and Gush, 2017) and promote intense competition over the fair allocation of the limited water resources in South Africa (DWAF, 2003). The potential for commercial tree growth is determined by the sunshine hours, the soil fertility and the availability of soil water for root uptake (Richardson *et al.*, 2002). Experiments by Benson *et al.* (1992); Clinton *et al.* (2003) and McMurtrie *et al.* (1992) have shown that tree growth is limited when there is a deficit in root-zone water. Physical and conceptual models have the potential to assist with such extrapolations but have often been criticised for requiring detailed input and parameterisation and being too complex (Richardson *et al.*, 2002).

Hydrological modelling has become the accepted method of assessing the impact of commercial afforestation on water resources (Jewitt and Schulze, 1999). This literature review discusses the strengths and weaknesses associated with the conceptualisation of soil routines within hydrological modelling and areas of potential improvement and refinement.　The concept of the root-zone storage capacity is explored and investigated as an alternative to the necessary intensive soils data for current hydrological modelling.

## 2.2　Below Ground Processes within Hydrological Modelling

The hydrological regime and the partitioning of water fluxes within a catchment is altered by the continuous adaption of vegetation to change in the biosphere (Black, 1997; Wagener *et al*., 2007; Nijzink *et al*., 2016). Vegetation survives by extracting plant available water between the field capacity and wilting point of their immediate soil (Vietz, 1972). Within their sphere of influence, vegetative roots create a moisture storage volume known as the root-zone storage capacity (Moore and Heilman, 2011). The root-zone storage capacity exists in the unsaturated soil and is a vital component of the hydrological regime (Rodriguez-Iturbe *et al.,* 2007 and Nijzink *et al*., 2016). The following sections focus on the role soils play within the hydrological cycle and the conceptualisation of soil routines within hydrological models before discussing the source of soils information for hydrological modelling and finally the root-zone.

## 2.2.1 The Role of Soils in the Hydrological Cycle

Streamflow lag time is eminently dependent on the soil properties, the size of the catchment, the drainage network density and the slope (Bugan, 2014). Amongst the various input data requirements for most hydrological models, the soils data remains critical in determining the nature of the hydrological response (Manus *et al.*, 2009).

The soil water is a determinant in the partitioning of net radiation energy into upward latent and sensible heat fluxes, providing water for vegetative growth and groundwater recharge (Jewitt, 2002) and controlling runoff processes. Soil water constitutes only 0.05 % of the global freshwater store and is considered a relatively minor hydrological component compared with the likes of precipitation and evaporation (Chapagain *et al.*, 2008). However, the soil water dictates the nature and magnitude of hydrological responses in the immediate atmosphere, land surface and groundwater (Gerten *et al.*, 2007). Soil water conditions reflect the past occurrence of precipitation (Eltahir, 1998), immediate percolation, plant uptake and evaporation whilst control future runoff, infiltration and evaporation capacities (Castillo *et al.*, 2003). The soil-atmosphere interface is a highly complex system and the soil water dynamics within the top metre of the soil are a central but often overlooked component of the hydrological cycle (Legates *et al.*, 2011).

Soil water has a direct effect on the albedo of the soil surface (Taha *et al.*, 1998). Wet soil conditions darken the soil hue and increase effective solar radiation (Baumgardner *et al.*, 1986). The consequent enhanced net terrestrial radiation at the surface reduces the upwards transmission of terrestrial radiation and simultaneously increases the atmospheric water vapour content (Coulson, 2012). Subsequently the Bowen ratio increases (Eltahir, 1998). If these processes occur over a large enough area, the enhanced heat flux from the surface should favour a large magnitude of moist static energy per unit mass thus increasing evaporation and soil water loss to the atmosphere resulting in the reduction of infiltration into lower soil horizons (Eltahir, 1998).

Additionally, soil water controls the soil physical properties and the carbon and nitrogen fluxes within the soil and at the soil- atmosphere interface (Koehler *et al.,* 2009). Soil physical properties play a determining role in soil suitability and capability and govern both the chemical and biological properties of the soil (Gregorich *et al.*, 1994). Long term soil water patterns have an influence on the texture and the structure of the soil profile (Sala *et al.*, 1992).

The infiltrability and pore sizes within the profile are both created by the soil water regime whilst being key in determining the soil water regime itself (Phogat *et al.*, 2016).

The understanding of nitrogen and carbon fluxes within the soil structure is critical in the comprehension of plant ecosystems (D'Odorico *et al*., 2003). The available mineral nitrogen is important for several ecological processes and is primarily determined by the hydrological regime, including but not limited to, root uptake, biological growth, litter decomposition and biogenic emission of carbon dioxide. The nitrogen cycle within the soil is closely interlinked with the soil carbon budget (Quinton *et al*., 2010) and is dependent on the soil water content (D'Odorico *et al*., 2003). Graeff (2012) determined that improvement to parameters associated with the soil water would improve ecological, agricultural, hydrological understanding and modelling.

Soil hydrological properties can be defined by estimating soil water characteristics for water potential and hydraulic conductivity using the soil texture, organic matter content and structure (Dexter, 2004 and Saxton and Rawls, 2006). Statistical correlations and laboratory analyses of the soil texture, soil water potential and hydraulic conductivity can provide sufficient estimates for the hydrologic properties of a soil profile (Saxton and Rawls, 2006).  The analysis of hydrological properties, within the soil, include the evaluation of water infiltration, conductivity, storage and plant-water relationships (Van Genuchten, 1980 and Saxton and Rawls, 2006). Laboratory and field measurements have proven to be difficult, expensive and impractical for the estimation and analysis of hydrological properties (Saxton and Rawls, 2005; Feki and Slimani, 2015; Ibrahim and Aliyu, 2016).  Estimations of soil properties and the subsequent parameterisation increases uncertainty within hydrological modelling (Pechlivanidis *et al*., 2011).

### 2.2.2. *Increased Modelling Uncertainty due to Below ground Parameter Estimation and Process Parameterisation*

The root profile distribution acts as the primary control of water uptake through the soil horizons. In current modelling methods, the root depth and root vertical profile, are pivotal in determining the movement of water through the soil-vegetation-atmosphere continuum (Gu *et al.*, 2007). The depth and structure of the root system determines the maximum amount of soil water that can potentially be taken up by the plant xylem and transpired by the vegetation (Tron

*et al*., 2015). The ability to uptake water is critically important during the dry season and prolonged drought (Lobet *et al*., 2014). Root growth and the process of root water uptake is spatially and temporally dynamic and reacts to the availability of water within the soil profile (Bleby *et al*., 2010 and Jung and McCouch, 2013)

Models considering below- ground vegetation began to emerge in the early 1970s. These models were based on mathematical representations of root depth distribution in soil. Over the last two decades, more complex architectural models have been developed and the use of more computer-intensive methods have been utilised (Dupuy *et al*., 2010). Most catchment-scale models are originally developed to address stationary scenarios and are not well equipped to deal with predicting the variance in hydrological parameters due to change (Nijzink *et al.,* 2016). Although modelling studies have been performed with the attempt to incorporate temporal change, most or all of the changes to the hydrological parameters have been assumed or estimated (Legesse *et al*., 2003; Mahe *et al*., 2005; Fenicia *et al*., 2009). More systematic approaches have only recently gained momentum, with the incorporation of temporal change into the model formulation (Nijzink *et al.,* 2016 and Zhang *et al*., 2016).

In most hydrological models, two plants of the same species growing in two different soils would be considered to have the same average rooting depth. This would subsequently mean that the plants have access to different volumes of water because of the difference in the porosity of the two soils. Research by Milly (1994); Schymanski *et al*. (2008) and Troch *et al.* (2009), has shown that this is not the case and that plants design their root systems to access similar volumes of water and limit unnecessary carbon investment in root growth. Recently this consideration has been supported by de Boer-Euser *et al*. (2016), who showed that in most environments the water balance- derived estimates for the root-zone storage capacity are as accurate as the soil- derived estimates and concluded that the maximum rooting depth controls the transpiration of the plants and the soil drainage.

Soil and rooting depth are key parameters in hydrological and land-surface modelling (Fan *et al*., 2017). The global distribution of soil and rooting depths are largely unknown due to the difficulties in measurement and the high variance between soil type, plant species and combinations thereof within modelling units (Yang *et al*., 2016). A common trait amongst many plant species is a deep complex rooting system. The rooting systems are essential in the

determination of the soil pedogenesis, soil water partitioning and soil chemistry processes (Pierret *et al.*, 2016). Current research efforts are focussed towards shallow root systems whist the study of deep root systems remain disproportionate, due to challenging procedures to observe and measure deep systems.

The rooting depth of a plant directly affects their resilience to environmental stresses (Maeght *et al.,* 2013). Deep roots enhance many functions such as bedrock weathering, determination of the soil water and regulation of chemical cycles. However, little is known about the limits to which roots grow and the factors that determine this limit (Beerling and Berner, 2005). A study by Fan *et al*. (2017), showed that in well-drained uplands, the rooting depth followed the infiltration depth to the capillary fringe. In waterlogged lowlands, the roots remained shallow to avoid anaerobic respiration conditions. These results suggest that the variation in rooting depths observed under the same climate for the same species is due to different topographic positions.

Large portions of continental landmasses are characterised by shallow soils overlying weathered bedrock and cemented soil layers (Schwinning, 2010; Zhao *et al*., 2017). Studies show that the majority of the soils are deeper than 1.2 meters and many plants grow beyond this depth. However, the depth of 1.2 meters is often considered as the maximum soil depth in literature and hydrological modelling (Richter and Markewitz, 1995; FAO, 2006). The drivers of deep root growth remain poorly understood (Maeght *et al*., 2013). Deep rooting could be a more prevalent and a more important trait due to the overall distribution of root biomass through the deeper layers (da Silva *et al.*, 2011). The misrepresentation of soil and root depths in hydrological models causes uncertainty in hydrological prediction and land- surface modelling (Schwinning, 2010 and Vrettas and Fung, 2017). Schwinning (2010) suggested that further research is necessary to improve the characterization of dynamic water recharge and depletion throughout the root-zone. It is important to understand the functionality, purpose and input criteria of different types of models when selecting a hydrological model that is fit for purpose. Within Section 2.3 the types of hydrological model groupings and examples of the

soil routines of some available hydrological models will be discussed with a special focus on the ACRU model.

## 2.3    Hydrological Models

Hydrological models are commonly used to estimate soil water at different spatial and temporal scales (Schaake *et al*., 1996 and Martínez-Fernández, and Ceballos, 2005). Hydrological models use similar sets of equations for simulating the water and energy balance and as a residual the soil moisture (Salvucci *et al*., 1994). Different hydrological models use different structures for simulating each of the components of the water and energy balances, however, the main governing balance equations are the same (Arnold *et al*., 1998). In Sections 2.3.1-2.3.3 the ways in which various models conceptualise and simulate soil water fluxes is explored. The accuracy of soil water data generated from the model is strongly dependent on the model selected and the quality of input data and observations (Dee *et al*., 2011). Hydrological models can be classified into three broad categories; conceptual, physical and a combination of both (Refsgaard and Storm, 1990; Chen and Adams, 2006; Jajarmizadeh *et al*., 2012).

### *2.3.1    Conceptual models*

Conceptual models (grey-box models) describe the catchment processes' underlying controls using states, parameters and fluxes and are based on theoretical storages and model parameters that require calibration (Vrugt *et al*., 2008). Conceptual models are subject to considerable uncertainty (Beven, 1989). Some examples of conceptual models are the Variable Infiltration Capacity Model (VIC) (Liang *et al*., 1994) and Hydrologiska Byråns Vattenbalansavdelning Model (HBV) (Lindström *et al*., 1997).

In the VIC model, there is an arbitrary number (normally three) of soil layers. The infiltration into and between the layers is controlled by the variable infiltration capacity. Water is lost from the top layer due to soil evaporation and plant uptake and lost to lower layers by gravity. The model uses a gridded configuration and assigns a sand, silt and clay percentage and the bulk density to each grid cell and each soil layer. The model internally assigns a hydraulic parameter to each grid cell based on the user input texture and bulk density data. The hydraulic parameter is then utilised to determine the movement of water within the soil profile (Liang *et al*., 1994).

This model requires extensive soils data at a grid level, which is not always available, particularly in developing countries, remote areas and regions of inaccessible terrain, and thus estimates and averaging across grid cells provides sources of uncertainties.

The HPV model uses a modified bucket theory to determine the soil water and assumes a statistical distribution of storage capacities within a basin, which in turn is the main concept controlling runoff formation. This routine is based on three parameters: a soil parameter, the limit for potential evaporation and the maximum soil storage. The soil parameter controls the contribution to the response function or the increase in soil moisture storage from each millimetre of rainfall. The limit for potential evaporation is the soil water value above which evapotranspiration reaches its potential value, and the maximum soil storage is the maximum soil water storage in the model (Lindström *et al*., 1997). Bucket-type models require detailed calibration data and bring about a high uncertainty especially in areas where a limited number of observations are available (Etter *et al*., 2018).

### 2.3.2. *Physical Models*

Physical models are based on understood scientific principles of water and energy fluxes which mimic physical processes in a simplified manner. The hydrological cycle is often modelled by the finite difference approximation of the partial differential equation, representing the mass, momentum and energy balance of the catchment, or conversely by empirical equations (Abbott *et al*., 1986). Conventionally physical models describe water partitioning using the Darcy-Richards' approach. Physical models provide a reliable estimate of the effect local change in system properties has on the local process patterns and the partitioning of water into integral hillslope and catchment responses (Quinn *et al*., 1991).The performance of models predicting water fluxes are more likely to be uncertain and difficult to judge fully (Salvucci, 2001).  Some examples of physically- based hydrological models are the Soil and Water Assessment Tool (SWAT) (Neitsch *et al.,* 2011) and Système Hydrologique Europeén (SHETRAN) (Ewen *et al*., 1995).

SWAT directly simulates saturated flow within the soil profile. The model uses conventionally calculated water content variables within the different soil layers but ultimately assumes that the water is distributed uniformly throughout the soil profile. Once the water throughout the

profile exceeds that of the field capacity the water will move downwards into deeper layers and the groundwater. Unsaturated flow is accounted for in the modelling by the distribution of plant water uptake and soil water evaporation. The model needs the clay content percentage, the bulk density and the plant available water as minimum input (Neitsch *et al.,* 2011). The SWAT model requires a high level of spatially explicit detailed soils information to yield the most confident results. The lack of this data compromises the model's performance and assumptions increase the uncertainty in the model simulations.

The SHETAN model simulates three-dimensional flow in saturated and unsaturated multi-layers of porous media. The soil layers can be laterally extensive, discontinuous, or of limited lateral extent. The input variables used in this model are the pressure potential, saturated hydraulic conductivity, porosity and specific storage over time across three dimensions (Figure 2.1). The calculated hydraulic head is used for defining the boundary conditions and the relationship between the hydraulic head and pressure potential is found in a user- defined list of parameters (Ewen *et al*., 1995).
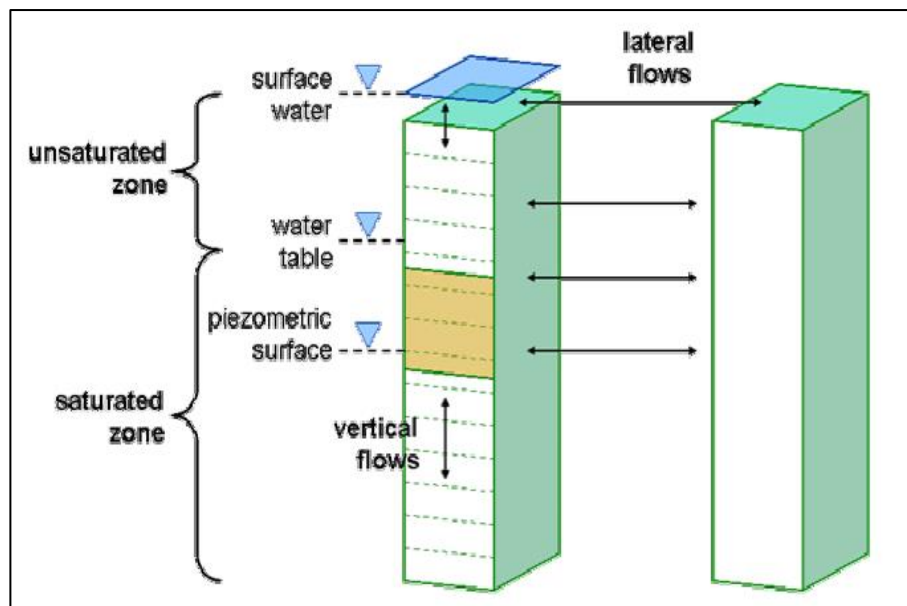


Figure 2.1:    A schematic diagram of the processes modelled in the variably saturated subsurface module (Ewen *et al*., 1995).

### *2.3.3    Physical-Conceptual Models*

Physical-conceptual models are designed to simulate various components of the hydrological cycle in a simplified manner across a range of time scales (Schmidt *et al*., 1987) but are not parameter fitting or optimizing models (Wallner *et al*., 2012). All variables are estimated from

the physical characteristics of the catchment. If input variables are not available, they are estimated within physically meaningful ranges. These ranges are based on either available literature, complex GIS analysis or local expert knowledge (Chowdary *et al*., 2012).

An example of a physical-conceptual model is the ACRU agrohydrological model. ACRU (Smithers and Schulze, 1995) integrates the various components of the hydrological cycle including runoff, at a daily time step water budget (Figure 2.2; Schulze 1995). ACRU is an operational model which has been conceptualised and structured to be used with the available national databases of climate, soils, and land use to produce acceptable results (Malan, 2016) and to simulate the time distribution (Royappen, 2002) of streamflow in ungauged catchments across varying hydro-climatic regimes (Malan, 2016). To account for the many fluxes involved within the hydrological cycle, the model had to integrate the processes in a physical way to best mimic the real-world movement of water and ultimately the runoff of the system.

The ACRU model was developed in the 1970s to provide an integrated evapotranspiration model to assess high altitude evaporation and transpiration occurring in the headwaters of important catchments (Schulze, 1995). As a result, the model contains a complex water budgeting routine and specific "rules" for the partitioning of water to evaporative processes. The model has been expanded from its original form to a model that now incorporates many other facets of the water cycle and catchment operations. The ACRU model has become the widely accepted model for modelling catchment- scale processes in South Africa and more specifically modelling of the effects of afforestation on catchment hydrology (Gush *et al.*, 2002). An understanding of the internal processes, assumptions and functionality of the model is important when investigating the various components and fluxes of the hydrological cycle simulated by the model. The particular soil budgeting and total evaporation estimation functionality of the ACRU model will be described in Section 2.4.
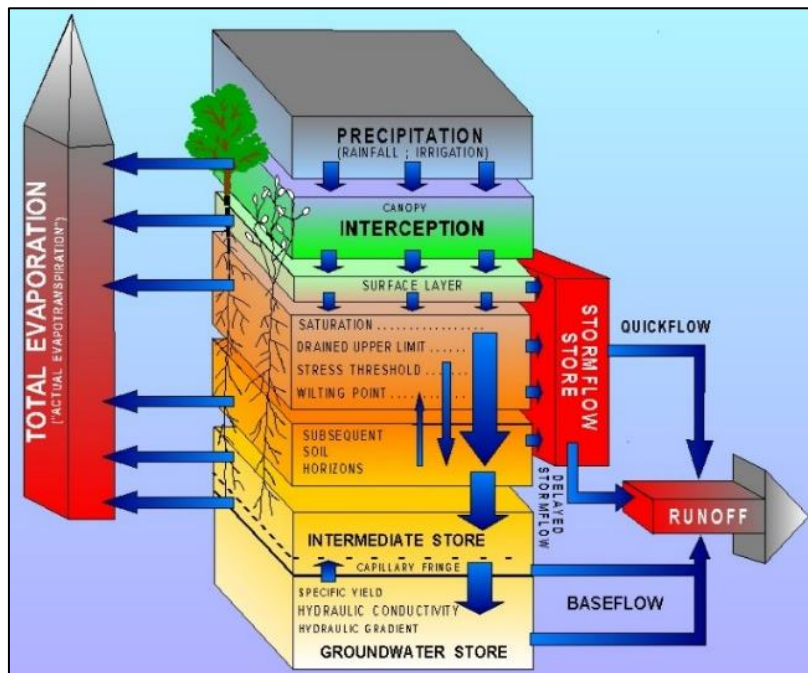
Figure 2.2: The conceptualisation of the ACRU model (Schulze, 1995)

## 2.4 Soil Water Budgeting and Total Evaporation Partitioning in the ACRU Model

In the ACRU model, the estimation of total evaporation is dependent on the water available for both transpiration and soil water evaporation determined by the internal soil water budgeting processes.

### 2.4.1 Determining Interception and Residual Reference Evaporation

The sequencing and processing to determine the daily soil water budget is detailed by Schulze (1995) as follows:

"The ACRU model initially calculates the intercepted water stored on the plant canopy from the previous day (if it was a rain day the value will be positive if not, there will be no water stored). This stored intercepted water is evaporated first, either at the atmospheric demand for short crops or at a greater rate for forests. The amount of potential evaporation that is remaining is allocated to meeting the soil water evaporation and plant transpiration demands for that day, and is referred to as the residual reference evaporation."

### 2.4.2 Determining Maximum Evaporation, Transpiration and Soil Evaporation

The maximum evaporation for the day is determined by first obtaining the crop coefficient for the day (or the LAI, if available). This value is calculated either by a Fourier analysis of the

user input monthly values or by calculation of the daily value based on the preceding days of stress / no stress that the vegetation has encountered. The maximum evaporation is calculated by multiplying the residual reference potential evaporation and the crop coefficient for the day.

Depending on the point within the growth cycle, the maximum evaporation is portioned into soil water evaporation and transpiration. This is determined by using a relationship between the crop coefficient and the canopy cover of the vegetation, according to a relationship proposed by Childs and Hanks (1975). Where if a plant surface is at full canopy cover and the effects of maximum ground shading prevail, then the maximum total evaporation is partitioned as 95% transpiration loss and 5% soil water evaporation. On the contrary, if no canopy cover exists, there is assumed no transpiration loss and maximum total evaporation is composed entirely of soil water evaporation. The extent of the canopy assumed in this relationship is derived from the crop coefficient and the concept that a crop coefficient of 1 will denote a full canopy cover, whilst that of 0.2 or less would imply no measurable canopy.

If LAI is available, then this is used to determine the maximum transpiration. When daily LAI values are available, these values are input directly into the model. When only monthly values are available, the monthly LAI values are converted to daily values internally using Fourier Analysis. The fraction of the maximum evaporation apportioned to transpiration is given by the formula:

$$F_t = 0.7 \, LAI_D^{\,0.5} - 0.21$$

Where $LAI_D$ is the daily value of the leaf area index. This equation is constrained, however, such that the upper and lower limits are 0.0 and 0.95. The evaporation through transpiration cannot exceed 95% of the residual maximum calculated for the day.

Following the allocation of maximum water for transpiration and soil evaporation by either method, the maximum transpiration water is further allocated into the various contributing soil horizons in proportion to the percentage distribution of the root mass within each layer. The maximum soil evaporation is determined for the topsoil only.

### 2.4.3 *Determining Soil Water content, actual soil water evaporation and plant transpiration*

The atmosphere puts an evaporative demand on the vegetation. The transpiration demand to the atmosphere is satisfied from the root active soil horizon layers in proportion to the rooting densities. The roots absorb the water from the soil water that is accessible to the roots. The actual transpiration can be equal to or less than the maximum transpiration for the horizon depending on the state of water deficiency or excess in the root-zone. When the root-zone becomes depleted and permanent wilting point is reached, the roots cannot absorb the water at a sufficient rate to meet atmospheric demand and plant stress sets in. This stress causes a reduction in the growth rate and the crop coefficient. The determination of soil hydraulic properties, such as drained upper limit and permanent wilting point, is important in the estimation of the total evaporation and the partitioning of the soil water budget.

The actual transpiration is calculated, firstly from the topsoil and then from the subsoil. The actual amounts are calculated as a function of the soil water content. At "day end" the soil water contents are adjusted after accounting for the actual total evaporation. The soil water contents within the soil layers are compared. If either layer is under a water deficit, compensations are made to the transpiration allocations from each layer.

The maximum soil water available for evaporation is estimated either as a residual of the available energy not used in the estimation of maximum transpiration or from the assumed effects of shading on the soil surface. The first approach is used within the dryland routine and the latter is of importance in water loss routines especially under irrigation. Under any above-ground vegetation conditions, it is assumed that a minimum of 5% of the available energy is allocated to soil water evaporation. The maximum soil water evaporation can be suppressed by litter, mulching or a rocky surface. Under these conditions, a linear relationship between the surface cover and soil water evaporation is assumed with a total surface cover allowing up to 20% soil evaporation to take place. If the monthly percentage of the surface cover is available then a revised maximum soil water evaporation is determined based on the surface cover percentage.

The actual total evaporation from the soil surface is calculated in two phases. The first phase is evaporation from the soil surface when the soil is wet, and therefore energy and not water is the limiting factor. In this phase, the soil water evaporation is limited to the maximum potential

soil water evaporation. When the accumulated soil water evaporation exceeds the maximum potential soil water evaporation and therefore water becomes the limiting factor, the next phase commences. This phase predicts the soil water evaporation using the number of days since this phase began and the maximum potential soil water evaporation. In theory, once the second phase begins the soil should dry out rapidly.

### 2.4.4   Rainfall, Stormflow and Baseflow

On a rain day, the effective precipitation and canopy interception are calculated from the net precipitation. The effective precipitation is available for subsequent addition to the soil water budget. The soil water deficit is determined for the critical stormflow soil depth, which is either a depth of the topsoil or a threshold input soil depth. The soil water deficit is the difference between the soil water content at porosity and that held by the soil profile at the critical stormflow depth on that day.

From the rainfall event, if the net rainfall is less than that required to meet the initial abstractions and critical soil layer deficit, no stormflow will be generated, if the net rainfall exceeds this threshold then stormflow will be generated. Any stormflow generated will be added to the residual stormflow from previous events to provide a total stormflow for the day.

The soil water content of the topsoil horizon is then calculated by the addition of the effective rainfall from either the stormflow producing or non-stormflow producing rainfall event. If the soil water exceeds that of the topsoil's drained upper limit then the volume of water exceeding the drained upper limit drains into the subsoil layer. The same process occurs in the subsoil horizon, but the excess water trains into the intermediate storage zone rather than a physical soil layer.

The baseflow generation routine operates to convert the water in the intermediate zone into a river carried baseflow. If there is no drainage into the intermediate zone from the overlying horizons, then baseflow releases are determined by the drainage coefficient acting on the intermediate store. The drainage coefficient is an experimentally determined exponential decay function releasing water from the intermediate store daily. If there is drainage into the intermediate zone then this is controlled by a drainage response variable derived from the soil properties of the lower horizon. The baseflow amount is calculated as a release from the total

35

amount of water held in the intermediate zone on that day. The total runoff for a day would be the sum of the released stormflow from the stormflow generated from an event, combined with the baseflow release calculated for that day.

Final values for the components of the soil water budget, soil water evaporation and transpiration, stormflow, baseflow, quickflow and baseflow store amounts are used as initial values for the following time step.

### 2.4.5    *Soil data processing*

If soils information is uncertain or lacking, the model requests two inputs, soil texture and soil depth. The soil texture is then assigned ACRU's pre-programmed default values for the hydraulic properties of the designated soil texture. The soil depth class is determined by the model from the inputted soil depth. There are six default soil depth classes that determine topsoil and subsoil horizon thickness. This option is effective when soils data is severely lacking but in turn, it produces no distinction between the hydraulic properties of the various soil horizons. If adequate data is available (soil thickness, retention constants and rates of the saturated redistribution for both soil horizons) the values can be inputted directly into the model. Inputted or hardcoded soils information is processed in three ways.

a) **Menubuilder**

Used when a single soil dominates a sub-catchment and when an area weighting of the soil properties has been undertaken outside of the model.

b) **Area-weighting**

This is used when two or more soil types are present in a sub-catchment. The respective percentages of the various soils that are present in the sub-catchment are used to area weight the soil properties and the model returns a single area- weighted value for each soil characteristic.

c) **AUTOSOILS**

AUTOSOILS software created for the ACRU modelling system by Pike and Schulze (1995) converts Land Type soils input to information useable in the model. The area-

weighting of the soils is carried out automatically and a single set of soils input is determined per sub-catchment.

Soils data are necessary for the running of all hydrological models, some more detailed than others. However, often the optimal detail of soils information is not available for the area of interest and indirect sources are needed to bridge the data gap.

## 2.5    Sources of Soils Information

Soil data are critical for a variety of functions (Balestrini *et al.,* 2015; Greiner e*t al*., 2017). Soils, however, can differ vastly over short distances (Lin, 2012), resulting in difficulties in obtaining accurate soils data (Paterson, 2015). Refined soil information is challenging to obtain due to the extent of surveys required to account for the spatial variability of soils, the cost of equipment, and the labour intensity of skilled technicians to perform such studies and the lack of accurate pre-existing records. The first South African national scale soil survey was undertaken in the 1920s and the resulting soil map produced in 1940. During the 1960s, several regional studies were performed that ultimately contributed to the completed Land Type Survey in 2002. Access to this South African Land Type data is costly, and the more detailed field scale results are often held strategically by the commercial bodies who commissioned the surveys.

There is no universal soil map for South Africa, so often, the broad-scale soil information contained within the Land Type survey are used (Land type survey staff, 1972-2006). A Land Type (Land Type Survey Staff, 1972 – 2001) is a class of land over which macroclimate, terrain form and soil patterns each display a level of uniformity. The Land Type surveys consist of memoirs and areal maps delineating the Land Types, where the fieldwork was undertaken at a scale of 1:50 000, but final mapping is at 1:250 000 resolution (Schulze, 2012; Van Zijl *et al.*, 2013 and Rowe, 2015). Each Land Type memoir (SIRI, 1987) provides details about each Land Type, including, but not exclusively:

- The percentage of each of the five terrain units within the Land Type.
- The percentages of each of the soil series occurring (both by terrain unit and total Land Type unit).
- The soil series' thickness for each series occurring.
- Details regarding any soil depth limiting layers or material.

- Clay content.
- Soil clay models.
-  Soil series textures.

The classification of Land Types was based predominantly on agricultural potential rather than hydrological or soil properties (Rowe, 2015). For the assessment, representative soil pits were dug and augur samples taken between the pits to aid interpolation. These pedological findings were combined with detailed climatic maps to chart the first Land type mapping units. This information was augmented by visual inspection of the landscape for changes in terrain and vegetation to further assist with the Land Type boundary delineation. Each Land Type is accompanied by terrain, soil and climate inventories collected from the data analysed for each Land Type (Rowe, 2015). This inventory includes details of the climate within the climatic zones as well as the location of and specific soils information from the dug pits and auger samples. There are approximately 22 000 Land Type polygons classified for South Africa. There are nine broad groups based on soil patterns and sub- groups representing soil colour, base status and soil depth, A, B, C…etc. (Schulze, 2012 and Rowe, 2015) which were then further sub-divided into map units coded  Aa, Ab, Ac... Ai etc., with a mapping unit representing soils of a certain uniformity in regards, inter alia, to colour, base status, depth range and other factors. Land Types within the broader classification with specific local properties were then identified, where for example, Ab12 would be the 12th  ocal unit within the broader Ab mapping unit.

Uncertainties stem from how the original survey was conducted. Many pits were dug, but given the spatial extent of the country, interpolation of the pit and augur sample results was necessary. Interpolation, combined with the use of other indicators to estimate the potential soil changes and the percentages of soil types, such as vegetation and topography leads to uncertainty. There are numerous methods of interpolation available, none of which is perfect, thus the further a mapped unit is away from a sample pit, the more the level of uncertainty surrounding the results. Land Type maps have limited hydrological applications because the Red Book classification used in the inventory excludes the acknowledgement of signs of wetness in the subsoil (Van Zijl *et al.*, 2013) and due to their agricultural potential focus. As the Land Type database provides complete coverage of the country; it is commonly used for the extraction of soils information for surveys (Thompson *et al.,* 2012).

The advancement of technology into the digital age has allowed for the manual processes of map interpretation to have been replaced with Geographic Information Systems technology (Longley *et al*., 2005). This digital advance has led to the establishment of the Soil Information System. A continuous Land Type coverage for South Africa which has been produced by digitising and edge matching the Land Type field maps (Hudak, and Wessman, 1998). The Land Type soil inventories have been captured fully in electronic formats, along with the addition of soil analyses and profile descriptions (Thompson *et al.,* 2012). Detailed surveys from a range of studies have been digitised and further included in the system (Van Zijl *et al.*, 2013).

## 2.6    Hydrological Properties of Land Type Data

Following the digitisation of the Land Type maps, hydrological responses, soil infiltration rates and permeability rates of the soils in each Land Type were assigned. As produced the Land Type maps are of little use to hydrologists. For them to become a source of useful data, all the data contained in the maps, the working rules and the various working assumptions that come with such a dataset, have been consolidated into the Soils Decision Support System (DSS). The DSS is linked to the digitised Land Type inventories in ACRU to convert Land Type inventory information into hydrological variables for both the A and B horizons, necessary for the running of the ACRU model using AUTOSOILS (Schulze and Pike, 2004). The Land Type information can be converted in three ways. The first as an individual soil series of the terrain units within a single Land Type, the second as a weighted average of the values comprising an individual Land Type. Or finally at a catchment scale, which comprises of a percentage of all the Land Types delimited within it. An example of this is work undertaken to extrapolate the ACRU hydrological soils variables by area weighting to provide values for each of the 5838 Quinary catchments making up South Africa (Schulze, 2012).

Schulze (2012) found that the permanent wilting point of the soil was dependent on soil texture, clay content and particle distribution through the soil profile. Schulze (2012) then used the soil water content at the permanent wilting point to reflect the stormflow potential of soil using the soil properties such as texture and change in texture with depth. The permanent wilting point values were mapped for the extent of the country in five categories representing the distribution of clay (Rowe, 2015). A clay distribution category was then assigned to each soil series in the

South African Binomial Classification using the description and definition of each (Schulze, 2012 and Rowe, 2015). Equations developed by Hutson and Cass (1984) and Schulze *et al.* (1985) were then used to calculate typical values of soil water content at the permanent wilting point and the drained upper limit for each clay distribution category (Rowe, 2015). The 22 000 Land Types polygons were transformed into maps of permanent wilting point, drained upper limit, soil depths, soil porosity and drainage rates for both the A and B horizon by Pike and Schulze (1995) and later revised by Schulze and Horan (2005), for input into the ACRU model (Rowe, 2015).

## 2.7    Consequences of Poor Soils Data when using the ACRU Model

The soil characteristics and critical points not only determine the soil budgeting but control the evaporation processes. Incorrect soils data or data that has been over-averaged can lead to inaccurate soil budgeting and the over- or under- estimation of the potential evaporation and in turn discrepancies in the actual total evaporation estimation. Soils and the relevant data play an important role in the water partitioning processes within the model. The influence of vegetation on the hydrological regime is accounted for using above, below and ground surface biomass and characteristics to determine the uptake and distribution of precipitation (Schulze, 1995; McNamara, 2018). The below- ground vegetation parameters are determined by the plant type and soil attributes and are used to determine the fluxes of the ground surface partitioning point (McNamara, 2018). The below- ground vegetation parameters are solely based on the effective rooting depth of the soil profile, the seasonal variation in the rooting depth, the fraction of roots found in each horizon (Schulze, 1995).

The ACRU model along with land surface models, Community Land Model and Integrated Biosphere Simulator (Lawrence and Chase, 2009), and hydrological models, Soil and Water Assessment Tool (Arnold *et al.*, 1998) and the Global Water Assessment Tool (Meigh *et al.*, 1999) do not accurately reflect the dynamic nature of the root system over the growth cycle nor do they consider the area of influence of the root-zone within the soil profile. The lack of detailed soils information and uncertainties associated when soils information is available, especially in developing countries, provides an opportunity for the various methods of estimating the root-zone storage capacity to be explored.

## 2.8  The Root-zone

Root-zone storage capacity can be considered as a volume of water per unit area within the range of plant roots and available for transpiration (Zhu *et al.*, 2008; de Boer-Euser *et al.*, 2016; Mao and Liu, 2019). Vegetation survives by extracting plant available water between the field capacity and wilting point of their immediate soil (Coppin and Richards, 1990; Irmak and Djaman, 2016). Within their sphere of influence, vegetative roots create a moisture storage volume known as the root-zone storage capacity (Schenk and Jackson, 2002). It is a vital component of the hydrological regime (Nijzink *et al.*, 2016).

Vegetation has a significant influence on the hydrological cycle (Bates, 1921; Zegre, 2008). The vegetative roots structurally adapt to establish an equilibrium resulting in the avoidance of water shortage within the ecosystem (Eagleson, 1982). Research suggests that root systems are designed for the most efficient extraction of water from the soil to meet the transpiration demands of the canopy while minimising the root growth necessary to sustain these demands (Milly, 1994). Studies, for example by Reynolds *et al.* (2000); Laio *et al.* (2001); Schenk and Jackson (2002), show that climate has a strong influence on the hydrologically active root-zone, whist periods of drought and flood are critical situations that affect the establishment of the root-zone.

The root-zone storage capacity currently cannot be physically measured in the field (Gao *et al.*, 2014). Within hydrological models, if the root-zone is considered, it is normally treated as a calibration parameter or a range of soil parameters estimated on assumed knowledge about the in-situ soil characteristics and estimates of the rooting depth (Liu *et al.*, 2006). Generally, this parameter is conceptually considered to change with season but not over the growth cycle of the plant (Figure 2.3). This does not reflect the real-world processes accurately and could be a potential source of error when modelling non- stationary conditions (Blasone *et al.*, 2008). Models account for the seasonal change in effective rooting depth and the colonisation of each horizon but do not account for the change in the root collar diameter or volume of roots (Figure 2.3).
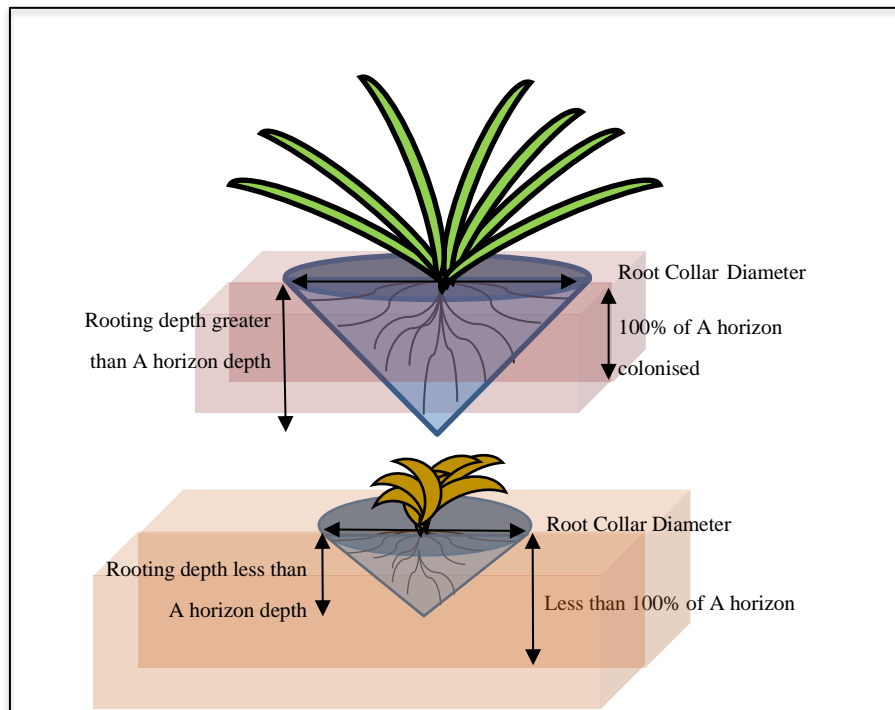
Figure 2.3: A basic conceptualisation of the root-zone storage within common hydrological models in wet and dry periods under grassland conditions

Recently there have been an increased number of studies focussed on determining the root-zone storage capacity. Summarising available literature, six methods of estimating the root-zone storage capacity have been identified for application in hydrological modelling.

### 2.8.1 Field Observation

The first of these approaches is the field observation approach (Wang- Erlandsson, 2014). This approach estimates the rooting depth using the rooting depth measurements taken by removing vegetation from the soil profile and measuring the length of the longest rooting structure (Zeng, 2001). This method is advantageous as it relies on actual observations and measurements of vertical root distributions. One study using this technique was Schenk and Jackson (2002), where using an empirical regression model, the in-situ rooting depth measurements were upscaled in conjunction with mean biome rooting depths obtained from literature. This method is handicapped by data scarcity, location bias, vegetation and soil heterogeneity and the assumption that water uptake is from a set portion of the soil profile.

### 2.8.2   Lookup Table Approach

This approach is favoured in hydrological modelling to parameterise the root-zone storage capacity. Mean biome rooting depths and soil texture are determined from literature (Wang-Erlandsson *et al*., 2014). This approach is useful in land- use change studies and can be verified by literature but assumes that the root-zone storage is solely based on vegetation and soil type, with no climatic consideration other than those indirectly expressed through vegetation and soil characteristics. This is a major downfall of this method, as the same species of vegetation can show large variations in root-zone storage capacities under different climatic conditions (Collins and Bras, 2007; Wang-Erlandsson *et al*., 2014).

### 2.8.3   The Optimisation Approach

This approach predicts the rooting depth based on existing soil, vegetation and climate variables, including but not limited to soil hydraulic properties and root distribution. This method can potentially incorporate complex algorithms, complicated eco-hydrological modelling and analytical modelling (Collins and Bras, 2007). Although these tools need further development and streamlining, they have proven valuable for the understanding of root profile development when detailed root distributions information is available.

### 2.8.4   The Inverse Modelling Approach

This method makes use of satellite data to estimate the rooting depth using either absorbed photosynthetically active radiation or total terrestrial evaporation along with different rooting depth parameterisations (Kleidon, 2004). This approach is highly dependent on ground-truthed soil information and accurate evaporation estimations. However, is useful because it is an indirect measurement and can be used over a large spatial coverage (Campos *et al*., 2016).

### 2.8.5   The Calibration Approach

This is a common approach, whereby a hydrological model is calibrated on the root-zone storage capacity using records of precipitation, runoff and evaporation and for use only at a catchment scale.  It is of importance to note that these parameters are strictly tied to the model used and not transferable between models as they compensate for uncertainties in the model structure. The calibration becomes more uncertain when only discharge data is available as the parameterisation absorbs the uncertainty in data (Pappenberger and Beven, 2006).

### 2.8.6    *The Water Balance Approach*

The root-zone storage capacity is strongly related to climate variables utilised in the estimation (Kleidon and Heimann, 1998; Gentine *et al*., 2012; Gimbel *et al*., 2015) an alternative approach to parameterization of the root-zone storage capacity and allow for temporal variability is based a water balance approach (de Boer-Euser *et al*., 2016; Gao *et al*., 2014; Wang-Erlandsson *et al*., 2016, Nijzink *et al*., 2016). This approach is climate- driven and thus incorporates climatic and vegetation conditions in a dynamic hydrological parameter (de Boer-Euser *et al.*, 2019). It should be noted that this method estimates a catchment representative root-zone storage capacity, which reflects the root-zone storage capacity for all the combinations of vegetation that exist in a catchment (de Boer-Euser *et al.*, 2019). The currently published studies are discussed in chronological order below.

The first published paper was that of Zhu *et al*. (2008) who performed one of the first root-zone storage studies. This study considered the temporal variation of the root-zone storage capacity under natural undershrub in China. The root-zone storage capacity was modelled using a two-layer soil water balance model. This model comprised of a shallow surface layer and a root-zone layer. Model results from this study were found to simulate the observed data sufficiently well.

Following the work of Zhu *et al*. (2008), at the Centre for Ecology and Hydrology, a simple root-zone storage routine was developed and integrated into the in-house Distributed Catchment Scale Model (DiCaSM). The model utilises a routine based on a root-zone water balance to determine the storage. Precipitation, streamflow and interception are used to calculate the infiltration into the root-zone. The total evaporation and recharge are calculated as water fluxes out of the root-zone and the remaining water is considered to be storage (Figure 2.4). Although there are no studies that have specifically isolated the root-zone storage routine, there are many studies that have used the DiCaSM model successfully as a whole entity, these include D'Agostino *et al*. (2010), Montenegro and Ragab (2010), Montenegro and Ragab (2012), Ragab (2012) and Afzal *et al*. (2018).
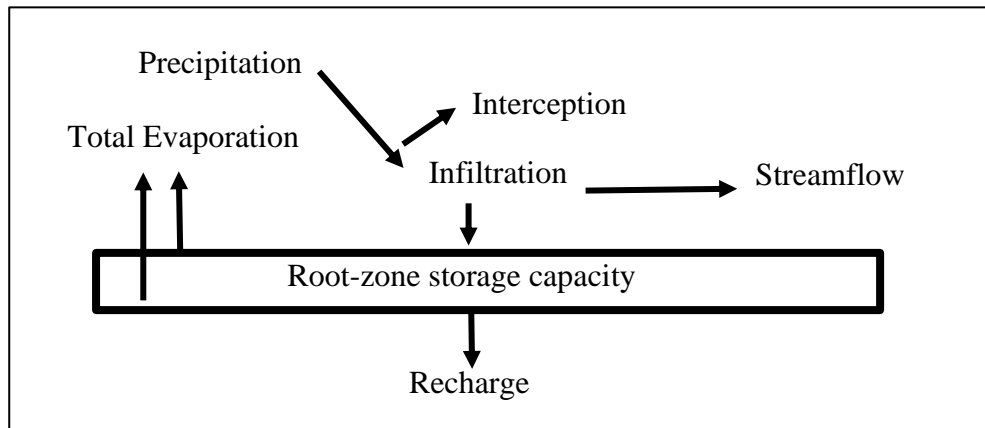
Figure 2.4:     A basic conceptualisation of the root-zone storage routine within DiCaSM

Wang- Erlandsson *et al*. (2014) calculated the root-zone storage capacity by estimating the soil moisture deficit constructed from a time series of water inflow and outflow through the root-zone storage system (Figure 2.5). A simple method using remotely sensed data, which can be adapted for in-situ observed data, was developed for the estimation of the root-zone storage capacity.  It is assumed that the vegetation optimises the root-zone storage capacity and does not require any vegetation and soils data. The method is additionally model- independent. The advantages of the Wang- Erlandsson *et al*. (2014) technique over field-based studies is that it can be utilised with remotely sensed data. Remotely sensed data can reduce the dependence on human and financial capital, limit the need for intrusive measuring techniques, compliment modelling methods that make use of indirect observation data and contribute to the understanding of areas with limited direct observational studies. The Wang- Erlandsson *et al*. (2014) technique allows for the inclusion of irrigation and additional variables if they are available to adjust the root-zone storage.
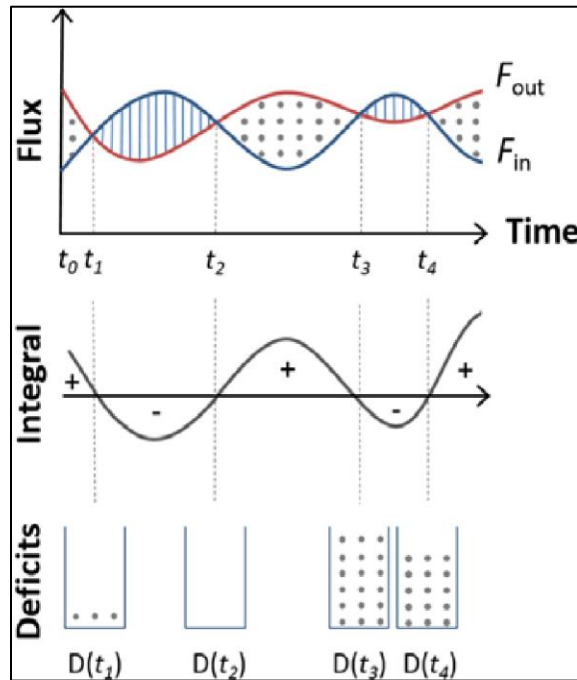
Figure 2.5:    The soil moisture deficit constructed from a time series of water inflow and outflow through the root-zone storage system (Wang- Erlandsson *et al*, 2014)

Building on the work of Wang- Erlandsson *et al*. (2014), Gao *et al*. (2014) tested a theory of treating the root-zone as a reservoir. The mass curve technique, an engineering method for reservoir design, was applied to over 300 catchments and was used to estimate catchment-scale root-zone storage capacity from effective rainfall and plant transpiration. It was found that the mass curve technique derived root-zone storage capacities reflected the model-derived estimates well. The estimates of root-zone storage capacity derived by Gao *et al*. (2014) could be used to constrain hydrological models. Furthermore, they concluded that root systems are controlled by climate and that ecosystems can potentially dynamically design their root systems to combat periods of drought.

Zhao *et al*. (2016) improved the mass curve technique for the root-zone of Gao *et al*. (2014) by incorporating a snowmelt module. Zhao *et al*. (2016) found the root-zone storage capacity estimates to vary greatly with changes in climatic conditions and soil characteristics whilst being most sensitive to changes in the transpiration of ecosystems. The adjusted mass curve technique proved to be a simple but effective tool for the root-zone storage capacity estimation in different climatic regions of China, however, the inclusion of additional climatic regions will improve knowledge on the variability of the storage capacity.

de Boer-Euser *et al*. (2016) undertook a study to investigate the nature of vegetative adaption to the root-zone storage capacity, especially under drought conditions. Precipitation and evaporative demand data were used in this methodology. The climate-based calculations were compared with a proportion of soil water measurements and modelled data within 32 catchments in New Zealand. It was found that the range of values between the catchments was greater for the climate-based calculations compared with those of the soil derived data in humid climates but was similar in arid climates. Using a model, it was shown that the climate-derived root-zone storage capacity better reproduced the hydrological regime signatures for humid catchments. However, in arid climates, the model produced similar results. de Boer-Euser *et al*. (2016) concluded that the climate-based root-zone storage capacity is a valuable addition in the process of understanding the root-zone storage capacity and reducing hydrological model uncertainty.

Nijzink *et al*. (2016) introduced a catchment-scale root-zone storage capacity estimation method using climatic data to reproduce the temporal evolution of root-zone storage capacity over the growth cycles and multiple seasons. This method considers the maximum deficit between daily precipitation and transpiration as a proxy for root-zone storage capacity. The calculated values from this method were validated against model results from four different hydrological models over a two year period. The calculated water-balance root-zone storage capacities were found to be similar to the values obtained from the hydrological models and proved a promising method to reflect the time-dynamic behaviour of a catchment.

de Boer-Euser *et al*. (2019) extended on the de Boer-Euser *et al*. (2016) study using a water balance based method to estimate the root-zone storage capacity in Boreal forests. The study investigated the relationship between catchment and vegetation characteristics and the root-zone storage capacity. The intention was to further understand the physical meaning of the root-zone storage capacity parameter. A climate-derived root-zone storage capacity parameter was compared with climate variables and vegetation characteristics. It was concluded that the dynamic root-zone storage capacity gives additional information about the hydrological characteristics as of a catchment and represents climatic and vegetation conditions in a single dynamic hydrological parameter. This could be valuable in the assessment of changing conditions.

Lastly, Mao and Liu (2019) developed a hydrological model to simulate the root-zone storage capacity on a global scale. They claimed that most root-zone storage studies are focussed on the soil water at a certain depth rather than the water stored within the rooting system. The root-zone storage capacity was integrated into a well- validated lumped model to reflect the natural spatial heterogeneity of the plant rooting system across the globe. The model mimicked the observed root-zone storage capacity in most regions well, however, the regions of high latitudes were not considered and thus results from these regions cannot be justified.

## *2.9 Summary*

The declaration of streamflow reduction activities and well as the implications of licensing them continue to be complicated and tedious to carry out and remain uncertain in their accuracy and fairness (Dye and Versfeld, 2007). The environmental and socioeconomic impacts of commercial afforestation are a prominent political debate amongst the role- players affected by SFRA policy (Scott and Gush, 2017). A clear, accurate and fair way to declare and manage SFRAs needs to be established with the collaboration with all sectors involved (DWAF, 2003). The use of hydrological models, such as ACRU, is currently an accepted method used in determining the impacts of SFRAs. However, many parameters, namely the soils data and rooting depth as discussed above, need to be improved and refined.

Models require detailed catchment scale soils data to generate accurate results as soils play a critical role in the regulation and generation of catchment hydrological responses (Schulze and Pike, 2004). ACRU specifically requires soils input data to determine how water is partitioned in the soil water budget and furthermore to determine the water allocation for total evaporation. In South Africa, total evaporation is a considerable component of the landscape water budget. Thus the ability to calculate and model this component accurately both in quantity and temporally is critical. Although soils play a large role in South African hydrological modelling, there is no universal soils map for South Africa. The use of Land Type maps and small areas of available intensive soils information are often used. Land Type maps provide complete coverage of the country but alone have limited hydrological application in their initial output format. Intensive work has been performed to convert the information from the Land Type maps to hydrological properties useful for ACRU input.

Along with uncertainty in inputted soils data, further uncertainty in modelling stems from a lack of available soil and rooting depth data. Soil depths tend to be estimated based on soil type and slope gradients and the rooting depth based on the soil depth assumptions and estimated growth curves for the plant species. Although this data tends to be lacking in a South African context, the data itself is difficult, time- consuming and invasive to measure in the field.

A possible alternative to intensive soils mapping is the use or incorporation of the root-zone storage concept into hydrological modelling. This concept will overcome the problems associated with the lack of or inaccurate rooting and soil depths and the uncertainty of vegetative growth curves. Successful studies have been performed internationally using this concept but not as yet in South African conditions. There are several ways to estimate the root-zone storage capacity. Currently, the most accurate and popular method is using the water balance principle. The root-zone storage capacity is a core component in determining a dynamic hydrological response and could be a valuable concept in improving the development of dynamic models. The concept of root-zone storage in hydrological modelling would need to be treated as a dynamically evolving parameter as a function of vegetation and climate. A number of successful studies using the various variations of the water balance approach have recently been published. The strength of this approach is that the dynamic nature of the climate and vegetation temporally and across a catchment can be represented in a single parameter. The input data can be remotely sensed data or in-situ measurements of commonly measured climate variable and limited below ground information is necessary. The approach has been proven successful across a range of climate zones however, performs better in humid environments. At the time of this study, there were no published results from high altitude catchments.

Of the eight current studies using the water balance method, the methods by Nijzink *et al*. (2016), Wang- Erlandsson *et al*. (2014) and the DiCaSM routine are the most appropriate under South African conditions and for the potential use in ACRU.  The Nijzink *et al*. (2016) method was tested under commercial afforestation in New Zealand thus it is the best choice of method to test under South African commercial forestry.  Wang- Erlandsson *et al*. (2014) was developed for grassland conditions and thus it is a strong choice for comparison between grassland and afforestation conditions in South Africa.  Although this method was developed for remotely sensed data, the nature of the fundamental equations allows for the input of in-

situ point observations. The DiCaSM method provides a strong opportunity to test an existing routine in a small scale catchment model that is similar to ACRU in its functioning. The utilization of the root-zone storage capacity could not only improve modelling in regions of limited below ground data but additionally, under commercial afforestation, it could potentially be useful in the improvement of modelling for SFRA purposes.

# CHAPTER 3: METHODOLOGY

Two catchments (Two Streams and Cathedral Peak Catchment VI) will be used in this study. Both catchments are well monitored and had a sufficient length of data available. It must be noted that the ACRU model was set up and calibrated for both catchment using data that is commonly available (ie observed maximum and minimum temperature, precipitation and streamflow) to identify the weaknesses within a common modelling environment. As the purpose was to use commonly available information as a way of determining the model adequacy under typical conditions, the observed evaporation and soil moisture data that was available in this case was used solely for the purpose of validation and not in the model calibration. A summary of the steps followed in the methodology, with a detailed explanation, is provided below.

1. The ACRU model was run using daily observed precipitation and maximum and minimum temperatures. Hargreaves and Samani daily was used internally to estimate the potential evaporation. The daily observed streamflow was used in the calibration of the model.

2. As observed actual evaporation and soil moisture are not commonly available, these were not use in the calibration of the model. In the calibration process, only parameters were that there known or could be reasonable estimated with use of the ACRU manual were adjusted.

3. The calibration statistics were calculated on the best fit of streamflow obtained only from commonly available input data and parameters. Once all the parameters and information that would be commonly available for South African catchments were adjusted, the calibration process ceased.

4. The simulated actual evaporation and soil water was validated against observed data.

5. The calculation of potential evaporation by ACRU has high uncertainty as there is a Apan equivalent conversion factor and a crop coefficient multiplication. Therefore the potential evaporation was calculated outside of the model using Hargreaves and Samani (R script in APPENDIX C), the PENPAN factor and the crop coefficient. This potential evaporation was fed into the ACRU model to generate the actual evaporation. It was discovered that the actual evaporation calculated with both sets of potential evaporation

has no significant difference and thus the ACRU calculated potential evaporation was deemed adequate and used to produce the ACRU simulated actual evaporation.

6. The root zone storage calculations were undertaken with both the observed and the simulated actual evaporation, observed precipitation, interception and observed streamflow. This was to test the robustness of the methodology to data scarcity.

7. The observed gravimetric water content, permanent wilting point and field capacity were converted to a depth of water using the soil depth before being compared to the root- zone storage capacity. To validate the root- zone storage capacity estimations, the estimations needed to be adjusted to reflect a water content within the soil profile using the permanent wilting point as the lower limit of the water in the root zone.

## 3.1 Site Description

Both the Cathedral Peak Catchment VI and the Two Streams Catchment are located in KwaZulu- Natal, South Africa (Figure 3.1) and are intensely monitored by the South African Environmental Observation Network (SAEON).
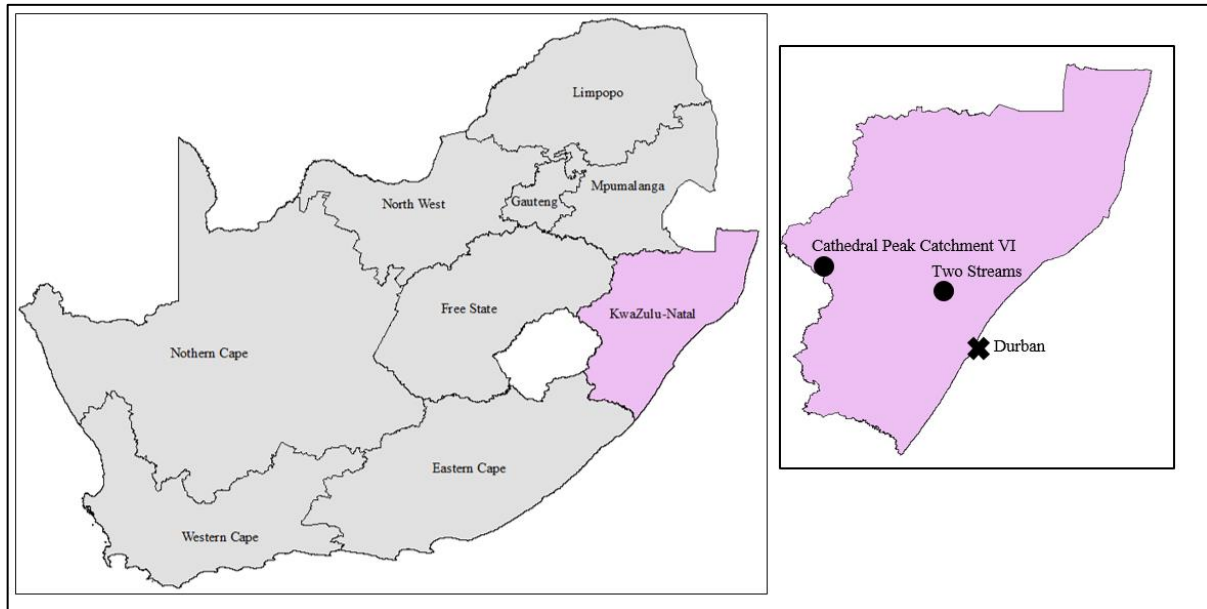


Figure 3.1:    Location of Two Streams and Cathedral Peak Catchment VI within South Africa.

### *3.1.1    Two Streams research Catchment*

The 0.65 km$^2$ Two Streams Research Catchment, established in 1999, (30.67°S, 29.19°E) is situated 70 km North North-East of Pietermaritzburg in the province of KwaZulu-Natal (Figure 3.2; Everson *et al.*, 2018). The catchment is in the 'midlands mistbelt grassland' bioregion (Clulow, 2011). The area experiences a humid climate with predominantly summer rainfall. The annual rainfall ranges from 659 to 1139 mm (Everson *et al.*, 2018). The dominant soil forms are apedal and plinthic with dolerite dykes and sills present in the area. The Two Streams Catchment forms part of the Mistley-Canema Estate belonging to Mondi Forestry and was afforested with *Acacia mearnsii* until November 2017 (Everson *et al.*, 2018).

The catchment rainfall is monitored by two Texas high-intensity rain gauges with a 0.254 mm resolution. One rain gauge is located above the tree canopy (Partial AWS) and the other at the automatic weather station (AWS) in a short grassland area near the site (Clulow, 2011). Relative humidity, temperature and wind are monitored above the tree canopy. The evaporation

is estimated using an eddy covariance tower situated within the stand (EC system). The streamflow has been monitored continuously since 1999 using a 457.2 mm 90° V-notch weir, logger (CR200X, Campbell Scientific) and pressure transducer (CS451, Campbell Scientific) (Clulow, 2011). Groundwater is monitored at four boreholes located in the centre, western, northern and eastern corners of the plantation. Soil water (Soil water pit) is monitored using time- domain reflectance probes to a depth of 2.4m in the centre of the plantation (Figure 3.2).



Figure 3.2:      The location the monitoring instrumentation within the Two Streams catchment.

### *3.1.2.    Cathedral Peak Catchment VI*

The Cathedral Peak research catchments, situated within the uKhahlamba Drakensberg Park, are ideal research sites as four of the catchments are pristine sites (Figure 3.3). The vegetation is fire maintained grasslands. The majority of the rainfall (85%) falls within the summer months, October to March (Morris *et al*., 2016). An estimated 50% of the rain originates from

thunderstorms whilst some less intense longer events can last for several days. The MAP is 1400 mm (Morris *et al.,* 2016).
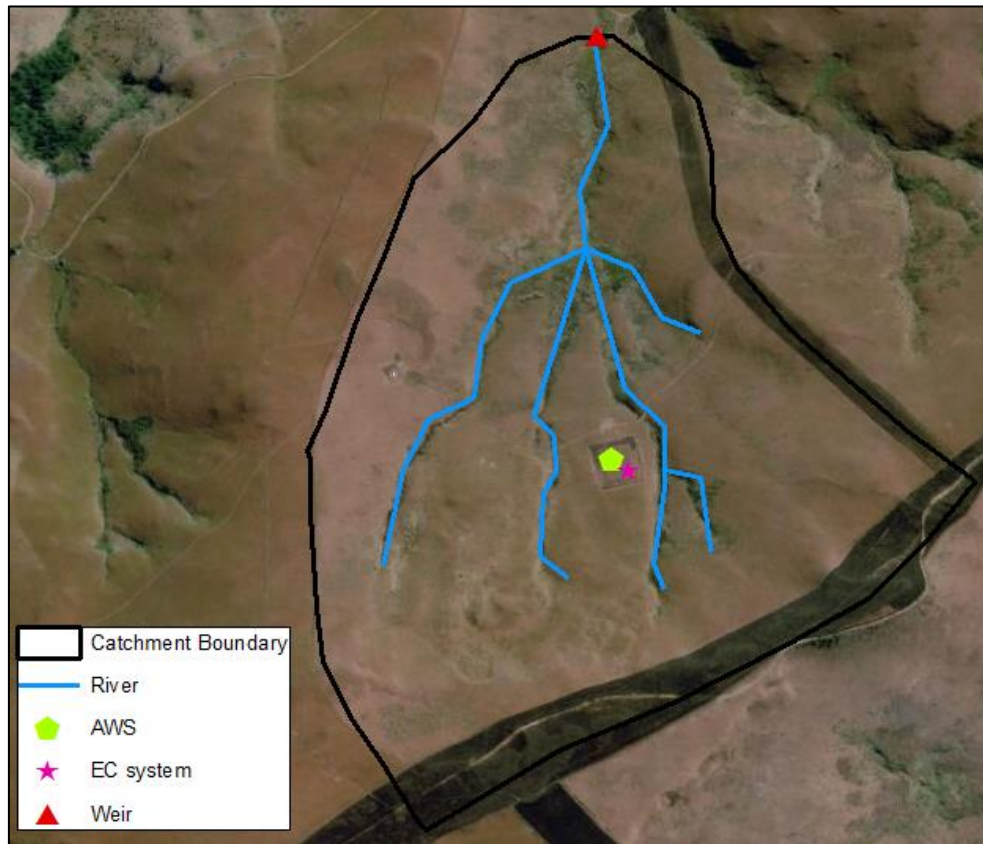


Figure 3.3:  The location the monitoring instrumentation within the Cathedral Peak Catchment VI.

All of the research catchments comprise of Drakensberg Basalt Group. It intermittently overlies the Clarens Formation Sandstone. There are two types of lava flow, amygdaloidal basalt and non-amygdaloidal basalt that occur in the research area (Kuenene *et al*., 2009). Three 3 m post-Karoo dolerites dykes cut across the research area, but exert no hydrological influence (Kuenene *et al*., 2009). An erosion feature of basalt is the terraces on the steeper slopes, with lengths of 6m and vertical steps of 0.46 m.

The individual catchments are well-defined and are hydrologically separated except for catchments IV and V (Kuenene *et al*., 2009). All the sampled soils are moderately weathered and can be considered immature. The profiles are at least 1.5 m deep and have an average pH of 5.5 in the surface horizon and 6.6 in partly decomposed rock. The dominant soil forms are Hutton and Griffin (Kuenene *et al*., 2009). Schulze (1979) found that the average soil depth was 0.8 m, whilst on the contrary Scott (1999) found that the average soil depth was 0.5 m

when including results from catchment VI. It is of vital importance that although the catchments spatially do not differ much, the soil form and depth differs over this relatively small area because of the high spatial variability and complexity of soils.

## 3.2 Data Acquisition

The physical characteristics of the catchments were obtained from various sources and used in the modelling exercises whilst the observed and estimated climate data, interception and recharge estimations and streamflow measurements, were assembled into a time series for each catchment extending from March 2007 until October 2013 and from July 2014 until August 2018 for both the Two Streams and Cathedral Peak catchment VI, respectively.

### 3.2.1 Physical Parameters

The Two Streams catchment is a $0.73km^2$ area upstream of the weir. As with the ACRU modelling of Two Streams by Clulow *et al*. (2011), the catchment was sub-divided into two subcatchments. The set up consisted of a $0.08$ km$^2$ riparian zone and $0.65$ km$^2$ under *Acacia mearnsii*. The position of the riparian zone was delineated using Google Earth imagery to identify the area cleared of *Acacia mearnsii* along the stream. From pre-existing work, in the catchment, the elevation and the slope were known to be 1000 m and 12.3% respectively. The soils information for the area were extracted from the Institute of Soil Climate and Water (ISCW) (1993) land type maps using the AUTOSOILS technique derived by Pike and Schulze (1995). A permanent wilting point and field capacity were established for both the A and B horizon along with the A-B and B-F response rates. The land cover was selected to be *Acacia mearnsii* (ACRU crop number 6030303). The parameters for this species at the mature stage of the growth cycle were pre-existing in the model and all input parameters to the model set up can be found in Appendix A.

The ACRU model was set up for Cathedral Peak catchment VI. An HRU (hydrological response unit) was added to the catchment. In this case, there was only one HRU in the catchment because of the similar land use throughout the catchment. The catchment contains Highland and Dohne Sourveld, based on the work of Hill (1996) and Scott *et al*. (2000), which is represented as Acocks number 44 and ACRU crop number 2030306. The soils data was obtained from the new Soils Database (Pike and Schulze, 1995). The following land use type

A265 fell within the catchment. A description of these land types can be found in Appendix B from Land Type Survey Staff (2002) along with additional information regarding the survey. The soils data such as total soil depth, wilting point, porosity and potential available water were extracted from the abovementioned database. All the input parameters to the model set up can be found in Appendix A.

### 3.2.2. Climate

**a)      Rainfall**

Two Texas high- intensity rain gauges with a 0.254 mm resolution are installed in the Two Streams catchment. One rain gauge is located above the tree canopy and the other at the Campbell Scientific automatic weather station in a short grassland area near the site. Several times over the monitoring period either gauge has failed, but it has been seldom that both gauges have failed at the same time. A full rainfall record was compiled by using the records from both stations (Figure 3.4).
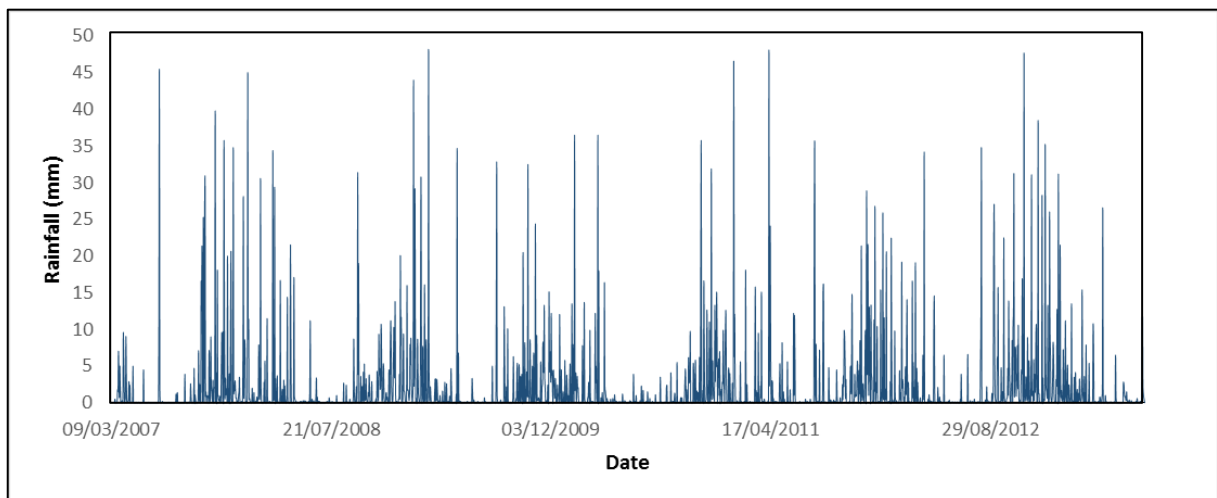


Figure 3.4:      Daily rainfall for the Two Streams catchment from March 2007 to October 2013

Daily rainfall measurements for Cathedral Peak Catchment VI were obtained from the South African Environmental Observation Network (SAEON). The rainfall was measured using a Texas high- intensity rain gauge with a 0.254 mm resolution (Figure 3.5). For the purpose of infilling, rainfall data from rain gauges in the neighbouring catchment VII, 7C and 7B, in

closest proximity to the raingauge in Catchment VI were utilised to produce a complete record (Figure 3.5). A rainfall correction factor is 1.254 was applied to the rainfall for the modelling exercises to account for a point- based rainfall measurement over the spatial extent of the high altitude catchment as well as to account for the under- catch of the rain gauge in the high intensity rainfall region. The rainfall correction factor was determined by comparing the mean monthly gauged values with the long term mean rainfall surfaces as created by Lynch (2003).
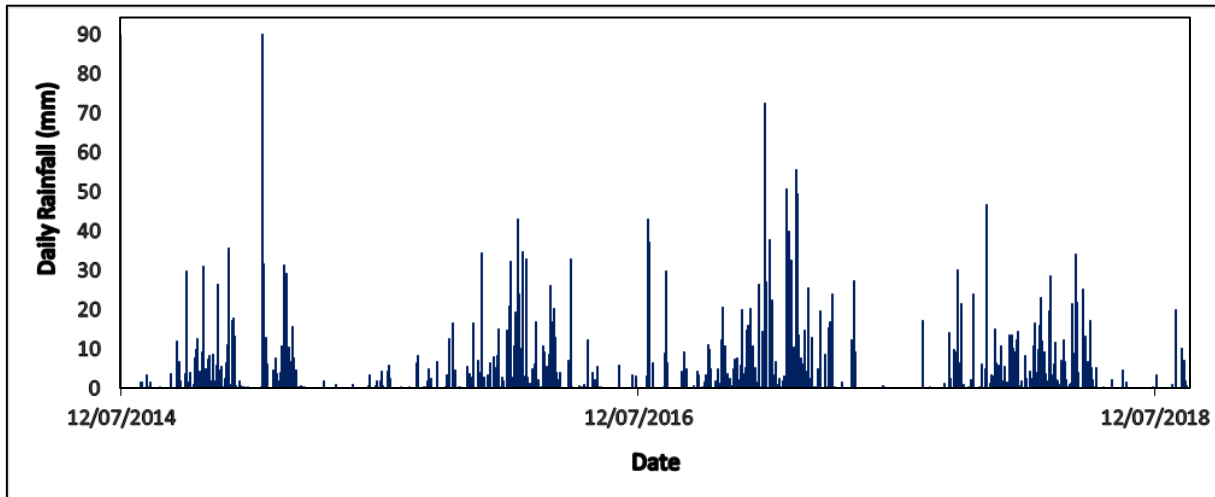


Figure 3.5:     Daily rainfall for Cathedral Peak Catchment VI for July 2014 to August 2018.

**b)      Evaporation**

Both observed and ACRU simulated actual evaporation were used in this study in order to test the robustness of the root-zone storage capacity methodology. However only the maximum and minimum temperatures were used to calculate the potential evaporation using Hargreaves and Samani (1985) daily was used in the modelling exercise. The actual evaporation was then estimated by the ACRU model.

### *i) Observed Evaporation*

The observed actual evaporation at both the Two Streams catchment (Figure 3.6) and Cathedral Peak Catchment VI (Figure 3.7) was obtained using the Eddy Covariance (EC) method. The EC method is a micrometeorological technique for high-frequency flux measurements within the atmospheric boundary layer. The flux was calculated as a mean value of the product of instantaneous deviations in vertical wind speed and instantaneous deviations in the water vapour. The flux obtained was directly applied to

determine the latent heat of the shortened energy balance equation which is equal to the estimated actual evaporation using the eddy covariance method.
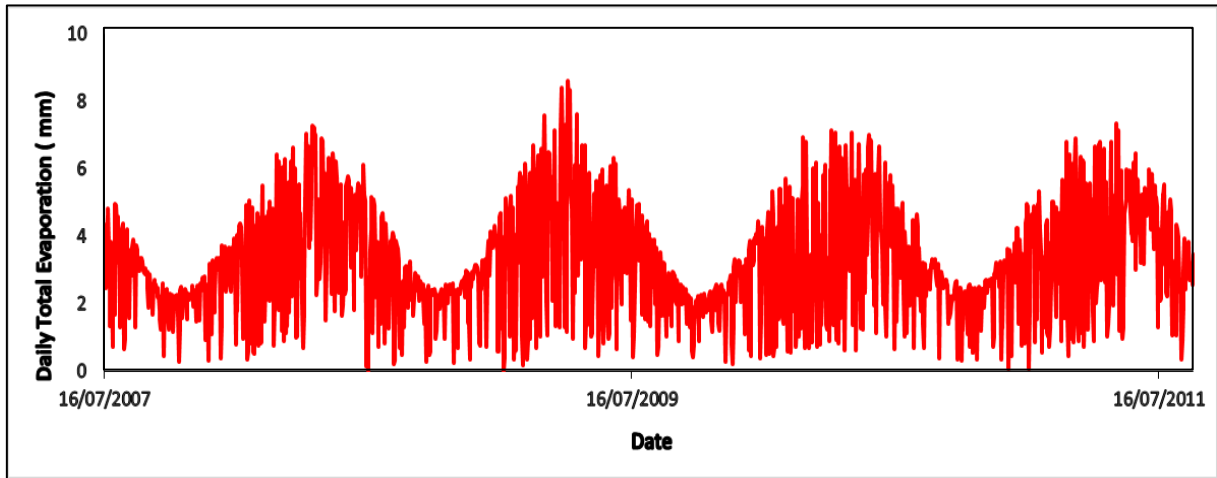


Figure 3.6:      Daily total evaporation for the Two Streams catchment from March 2007 to October 2013.
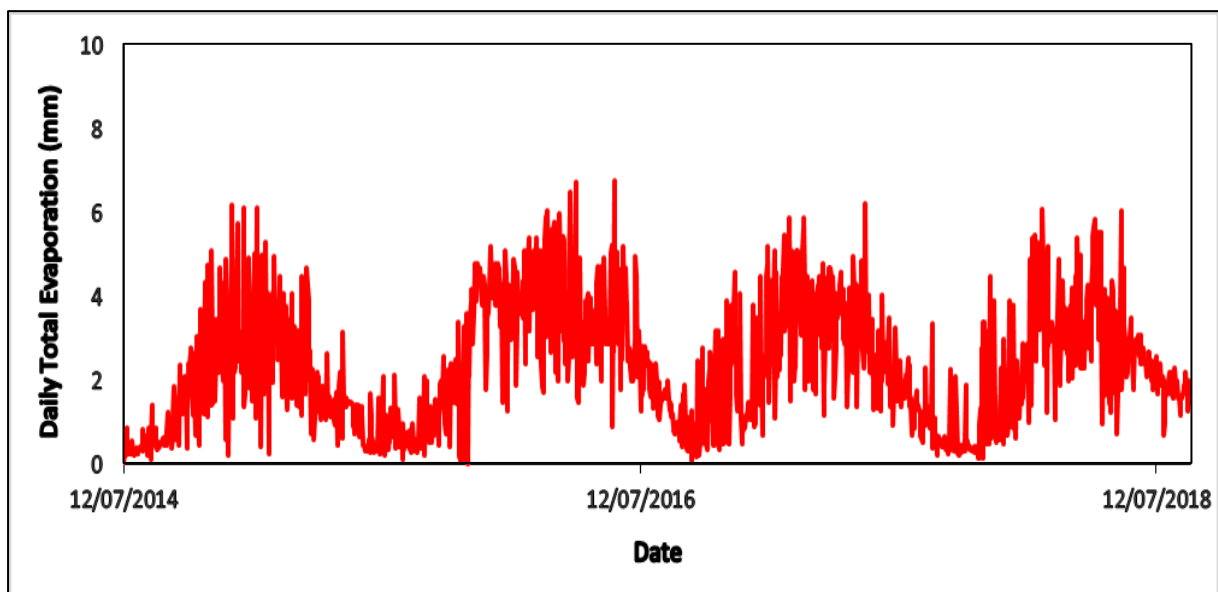


Figure 3.7:      Daily total evaporation for Cathedral Peak Catchment VI for July 2014 to August 2018.

*ii) Potential Evaporation*

ACRU requires an Apan equivalent potential evaporation in order to estimate the actual evaporation. The potential evaporation was calculated using two methods to ensure that the evaporation error was not due to the Hargreaves and Samani to Apan equivalent conversion routine in the ACRU model.

The first method was providing ACRU with daily maximum and minimum temperatures. The model internally converts the temperatures to grass equivalent potential evaporation using Hargreaves and Samani (1985) daily functionality followed by the multiplication by a value of 1.2 to convert the Apan equivalent and then multiplying by the crop coefficient. This potential evaporation is then used to determine with actual evaporation within the model.

The second method used an R script (Appendix C) to convert daily minimum and maximum temperatures to grass equivalent evaporation using the Hargreaves and Samani (1985) equation. The values were converted to an A-pan equivalent evaporation using monthly factors derived by Kunz *et al.* (2015) and then to potential evaporation using the crop coefficient. This potential evaporation was input into the ACRU model as an Apan equivalent to determine the actual evaporation.

The following procedure was followed to calculate the Apan equivalent potential evaporation for ACRU input. This was calculated for each Quinary catchment using the following methodology.

Kunz *et al*. (2015) used the following equations (Eq 3.1- Eq 3.6) representing an unscreened A-pan evaporation obtained from McMahon *et al.* (2013) and Roderick *et al.* (2007):

$$f(u_2) = 1.201 + 1.621u_2 \qquad \text{(Eq 3.1)}$$

where:

u$_2$ = daily average wind speed (m.s$^{-1}$), and

f(u$_2$) = aerodynamic term for an unscreened A-pan (mm day$^{-1}$ kPa$^{-1}$).

Since Kunz *et al.* (2015) assumed a constant wind speed of 2 m.s$^{-1}$, f(u$_2$) equates to 4.44 mm day$^{-1}$ kPa$^{-1}$. To account for direct solar radiation reaching the A-pan water surface, Linacre (1994) used the following equation (Eq 3.2):

$$R = 1.32 + \frac{4A}{10^4} + \frac{8A^2}{10^5} \qquad \text{(Eq 3.2)}$$

where:

R = A- pan radiation factor, and

A = latitude (degrees decimal).

To account for the diffuse radiation reaching the A-pan's wall, McMahon *et al.* (2013) and Rotstayn *et al.* (2006) used the following equation (Eq 3.3):

$$F = -0.11 + \frac{1.31R_S}{R_a} \qquad \text{(Eq 3.3)}$$

where:

F = diffuse radiation factor,

R$_s$ = incoming solar radiation (MJ m$^{-2}$ day$^{-1}$), and

R$_a$ = extra-terrestrial radiation (MJ m$^{-2}$ day$^{-1}$).

Linacre (1994) combined the above direct and diffuse radiation terms and a term to account for

the reflection of solar radiation from the A-pan's surroundings onto its wall, to derive the following relationship (Eq 3.4):

$$H = F \cdot R + 1.42(1 - F) + 0.42\alpha_s \qquad \text{(Eq 3.4)}$$

where:

H = heat augmentation factor,

R  = A-pan radiation factor,

F  = diffuse radiation factor, and

$\alpha_s$  = albedo of the A-pan's surroundings.

Net radiation was estimated using the methodology of Linacre (1994) as follows (Eq 3.5):

$$R_n = 0.71H \cdot R_s - R_{nl} \qquad\qquad \text{(Eq 3.5)}$$

where:

$R_n$  = net radiation (MJ m$^{-2}$ day$^{-1}$),

H  = heat augmentation factor,

$R_s$  = incoming solar radiation (MJ m$^{-2}$ day$^{-1}$), and

$R_{nl}$  = constant net longwave radiation loss (MJ m$^{-2}$ day$^{-1}$).

The following *PENPAN* equation was used in this study to calculate unscreened A-pan evaporation (Eq 3.6):

$$E_p = \frac{\Delta}{\Delta + a\gamma} \cdot \frac{R_n}{\lambda} + \frac{a\gamma}{\Delta + a\gamma} \cdot \frac{f(u_2)}{1} \qquad\qquad \text{(Eq 3.6)}$$

where:

$E_p$  = *PENPAN* evaporation (mm day$^{-1}$),

$\Delta$  = slope of the vapour pressure curve (kPa °C$^{-1}$),

a  = parameter set to 2.4,

$\gamma$  = psychometric constant (kPa °C$^{-1}$),

$R_n$  = net radiation (MJ m$^{-2}$ day$^{-1}$),

$\lambda$  = latent heat of vapourisation (2.45 MJ m$^{-2}$ mm$^{-1}$), and

$f(u_2)$  = Aerodynamic term (mm day$^{-1}$ kPa$^{-1}$).

The *PENPAN* evaporation values were then divided by reference grass evaporation calculated using the FAO56 (i.e. Penman-Monteith) method as described by Allen *et al.* (1998) to derive correction factors, from which monthly averages were obtained. The Quinary catchment for both Cathedral Peak Catchment VI (CP6) and the Two Streams catchment (TS) were identified as 4841 and 4729 respectively (Figure 3.8). From Kunz *et al.* (2015), the monthly *PENPAN* correction factors for each Quinary were extracted and applied to the relevant catchment. The

grass reference evaporation calculated using the Hargreaves and Samani (1985) equation was multiplied by the monthly *PENPAN*-derived correction factors to determine A-pan equivalent evaporation. The latter was then multiplied by the monthly crop coefficient to estimate daily total (i.e. actual) evaporation. The monthly crop coefficients and *PENPAN* correction factors can be found in Table 3.1.
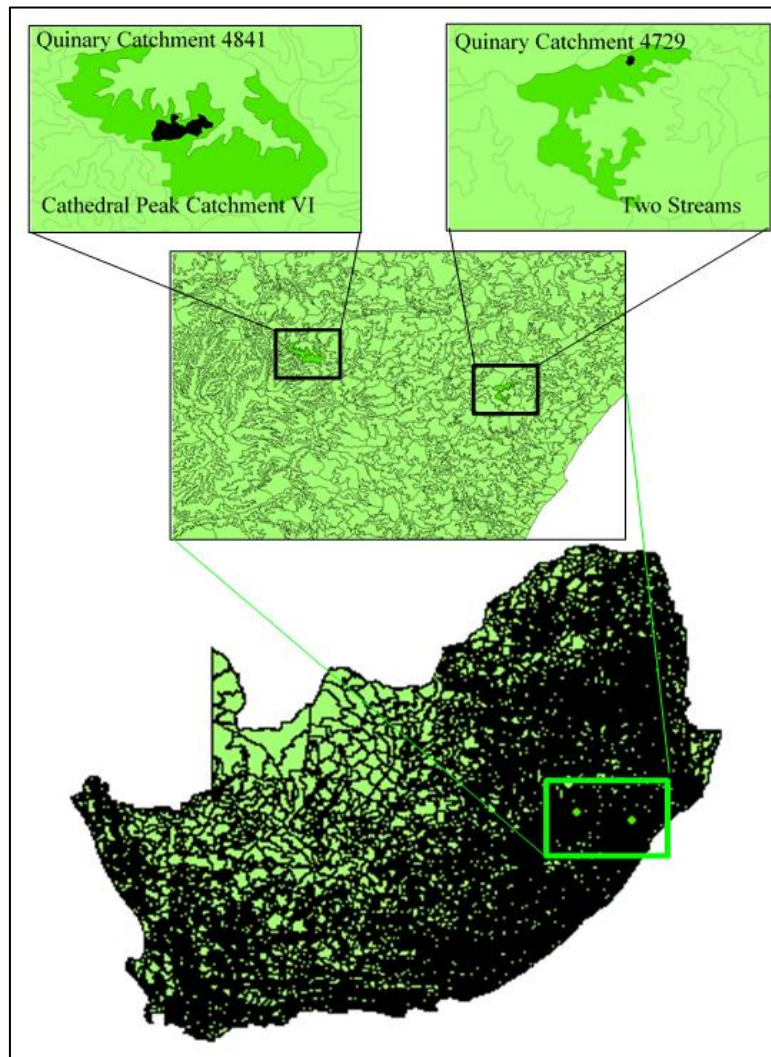


Figure 3.8:     The determination of Quinary catchment location

Table 3.1     Table showing the monthly crop coefficient (CAY) and PENPAN correction factors for both Cathedral Peak Catchment VI (CP6) and the Two Streams (TS) catchment

| CAY | JAN | FEB | MAR | APR | MAY | JUN | JUL | AUG | SEP | OCT | NOV | DEC |
|---|---|---|---|---|---|---|---|---|---|---|---|---|
| CP6 | 0.70 | 0.70 | 0.70 | 0.50 | 0.30 | 0.20 | 0.20 | 0.20 | 0.50 | 0.65 | 0.70 | 0.70 |
| TS | 0.90 | 0.90 | 0.90 | 0.88 | 0.85 | 0.86 | 0.89 | 0.90 | 0.92 | 0.92 | 0.90 | 0.90 |
| **PENPAN** | **JAN** | **FEB** | **MAR** | **APR** | **MAY** | **JUN** | **JUL** | **AUG** | **SEP** | **OCT** | **NOV** | **DEC** |

| | | | | | | | | | | | |
|---|---|---|---|---|---|---|---|---|---|---|---|
| CP6 | 1.29 | 1.29 | 1.31 | 1.34 | 1.39 | 1.41 | 1.39 | 1.36 | 1.34 | 1.31 | 1.29 | 1.29 |
| TS | 1.31 | 1.32 | 1.34 | 1.38 | 1.42 | 1.44 | 1.43 | 1.39 | 1.36 | 1.32 | 1.31 | 1.31 |

### c)    Streamflow

The streamflow has been monitored at Two Streams since 1999 using a 457.2 mm 90° V-notch weir originally using a Belfort Streamflow recorder (Everson *et al.*, 2018). In 2011, a logger (CR200X, Campbell Scientific) and pressure transducer (CS451, Campbell Scientific) were installed to continuously monitor streamflow (Figure 3.9).
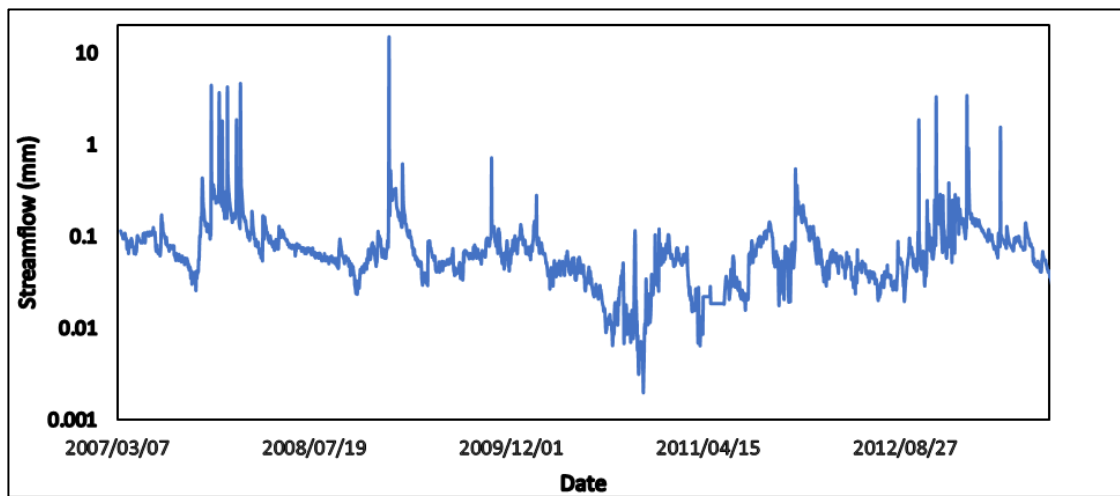


Figure 3.9:    Streamflow record for the Two Streams catchment from March 2007 to October 2013

Weir data for the outflow of Cathedral Peak Catchment VI was obtained from SAEON. The data was provided in metres along with a ratings table. Using the regressions found in the ratings table for the weir's multistage infrastructure, the measurement, in metres, was converted to cumecs ($m^3. s^{-1}$), and then to a daily time step (Figure 3.10).
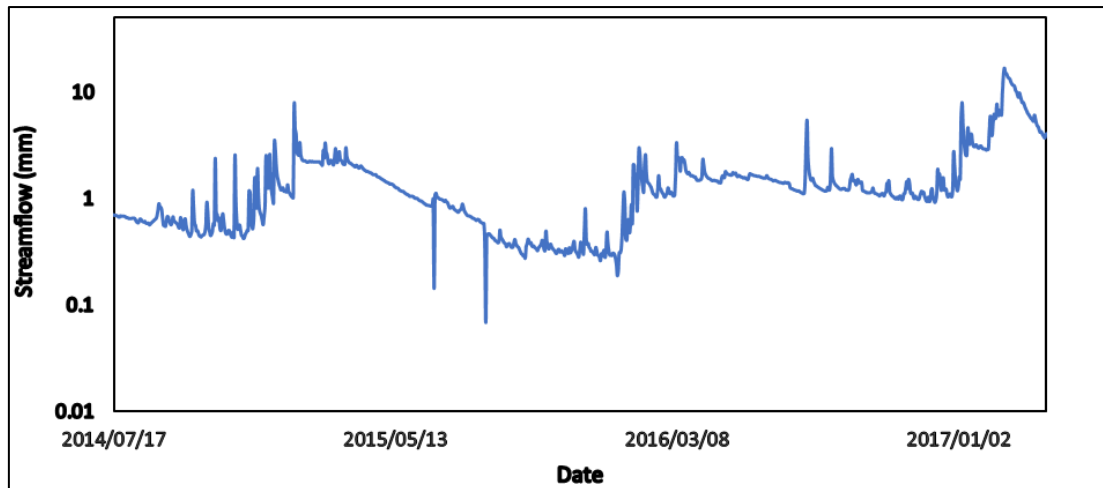
Figure 3.10:    Streamflow record for Cathedral Peak Catchment VI for July 2014 to August 2018

*d)    Interception*

The estimation of interception loss for the Two Streams catchment was taken from the work of Bulcock and Jewitt (2011) who found that the water available for infiltration into the soil was 56.7% of the gross precipitation (Table 3.2). The gross precipitation for each day was multiplied by 0.567 to produce a daily time series of interception over the study period, March 2007 to October 2013.   (Figure 3.11).   This method was chosen at Two Streams as the measurements were taken in- situ over the same period as the climate data was obtained.

Table 3.2:    Interception losses of *Acacia mearnsii* at Two Streams (Bulcock and Jewitt, 2011).

| Genus | Gross Precipitation (mm) | Observed water drained to soil (mm) | Observed water drained to soil (%) |
|---|---|---|---|
| *Acacia mearnsii* | 1884.7 | 1237.7 | 65.7 |

65
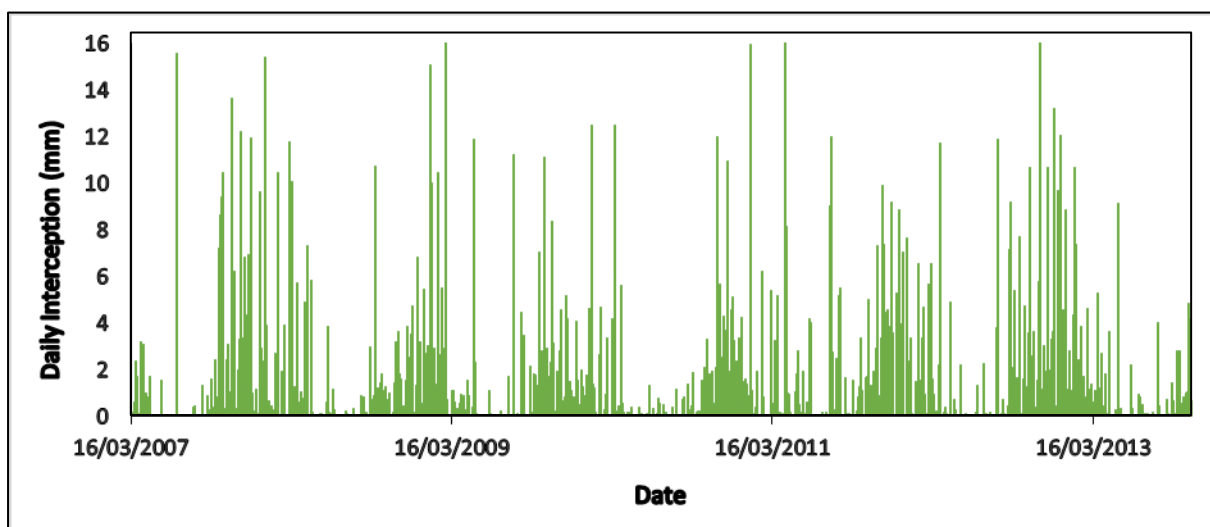
Figure 3.11:    Interception loss record for Two Streams from March 2007 to October 2013

The daily interception loss for the Cathedral Peak Catchment VI was calculated using the variable storage Gash model developed by Bulcock and Jewitt (2011). Using this method, the Water Research Commission (WRC) project K5/2437, calculated the interception loss values (Table 3.2) for the Cathedral Peak catchments. The methodology for the variable storage Gash Model can be found in the WRC Research project K5/2437 report. The values were applied to all raindays where the rainfall exceeded the interception value. Where the interception value exceeded the rainfall, all the rainfall was assumed to be intercepted and thus allocated to interception. On non- raindays the interception value was assigned as zero.

Table 3.2: The monthly daily maximum interception (DMI) values for Cathedral Peak catchment VI grassland.

|  | JAN | FEB | MAR | APR | MAY | JUN | JUL | AUG | SEP | OCT | NOV | DEC |
|---|---|---|---|---|---|---|---|---|---|---|---|---|
| DMI (mm) | 2.94 | 2.56 | 2.36 | 1.75 | 1.54 | 1.39 | 1.46 | 1.38 | 2.11 | 2.47 | 2.65 | 2.87 |
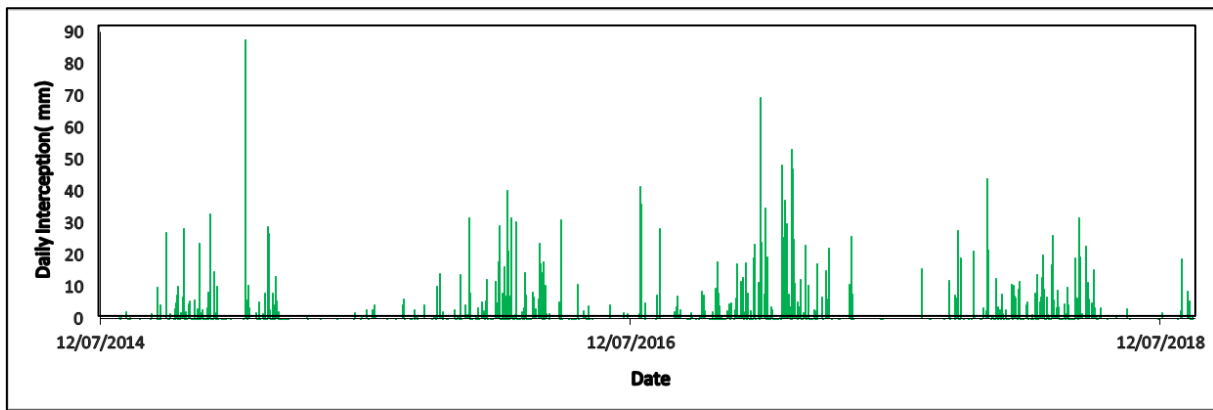
Figure 3.12:    Estimated interception loss values for Cathedral Peak Catchment VI from July 2014 to August 2018

### e) Soil Water Measurements

Soil water measurements were limited to Two Streams. Soil moisture was measured using Time domain reflectometry methodology which measures the travel time for a pulsed electromagnetic signal. Six CS616 probes were installed into a pit to a depth of 2.4 at 0.4 m intervals and measured the dielectric constant at hourly intervals.  The dielectric constant of water relatively high compared with other soil constituents.  Thus, changes in volumetric water content can be related to changes in the dielectric constant of the soil material. Issues investigated during the probe design process were probe length, configuration and the practicalities involved in probe insertion. The stainless steel probes have a length of 75 mm, a spacing of 15 mm and have a straight configuration.  The probes were used with a Campbell Scientific TDR100 system with multiplexers allowing the installation and automated monitoring of more than 350 TDR probes from a single CR1000 logger.

The soil parameters utilised in the soil water calculations can be found in Appendix A. The volumetric water content was converted to a millimetre depth using the soil depth. The observed and ACRU simulated soil moisture used in the model validation was converted to a millimetre depth for both the A and B horizon. Whilst the observed and ACRU simulated soil moisture used in the root-zone storage capacity validation was converted to a millimetre depth through the entire profile.

## 3.3 Calibration of the ACRU model

The ACRU model setups were not calibrated to their full potential but to the full extent possible with commonly available data as mentioned previously. The ACRU model setups were previously calibrated for Two Stream by Clulow et al. (2011) and for Cathedral Peak Catchment VI by Horan (2017) for different time periods. The models were calibrated further where possible under the set- out data constraints for the new time period

The model was run for Cathedral Peak Catchment VI using the new climate forcing data. The model under- simulated the low flows and over-simulated the magnitude of the high flows. The model is not retaining enough water during the receding limb of the hydrograph. This implies that total soil depth is too deep, the A-B and B-F response is too high or the effective depth of soil which is considered to be contributing to the stormflow generation process (SMDDEP) is too deep (Smithers and Schulze, 1995). From the list of possible causes listed above, parameters were adjusted systematically to improve the simulation. The soil depths for the A and/or B horizons were altered and it was decided that an A horizon depth of 0.34 m and B horizon of 1.4 m provided the best simulation of streamflow. The model was run using the altered soil depths and the simulation was much improved. The SMDDEP was altered to various depths. A SMDDEP of 0.3 m yielded the best result when compared to the observed data.

The model was run for Two Streams using the new climate forcing data. The model simulated the low flows well but the magnitude of the high flows are significantly under simulated whilst the duration of high flow is over-simulated. This implies that total soil depth is too deep, the quick flow response is too low, the A-B and B-F response is too high or the effective depth of soil which is considered to be contributing to the stormflow generation process (SMDDEP) is too deep (Smithers and Schulze, 1995). From the list of possible causes listed above, parameters were adjusted systematically to improve the simulation. The soil depths for the A and/or B horizons were altered and it was decided that an A horizon depth of 0.2 m and B horizon of 0.57 m provided the best simulation of streamflow. The model was run using the altered soil depths and the simulation was much improved. The SMDDEP was altered to various depths. A SMDDEP of 0.2 m yield the best result when compared to the observed data.

## 3.4 The Estimation of the Root-Zone Storage Capacity

Three methods were used to potentially estimate the root-zone storage capacity for both Cathedral Peak Catchment VI and Two Streams. For each catchment, identical datasets are used between the three methods to allow for comparison of results. Each dataset consisted of precipitation, actual evaporation, interception and streamflow at a daily time step. For the validation of the calculated root- zone storage capacity, the root- zone storage capacity needed to be adjusted to reflect a water content within the soil profile. The root- zone storage is the water available for plant uptake and thus can be defined as the water content above the permanent wilting point. The permanent wilting point was added to the root- zone storage content estimations to reflect the water content in the soil profile.

The different methods used in the estimation of the root-zone storage capacity are described below.

### 3.4.1 Nijzink Method

The change in interception storage over time was calculated by subtracting the actual evaporation and effective precipitation from the gross precipitation (Eq 3.7).

$$\frac{dI}{dt} = P_g - E_t - P_e \qquad \text{(Eq 3.7)}$$

where:

I= Interception (mm)

t= time (days)

$P_g$= Gross Precipitation (mm)

$E_t$= Actual evaporation (mm)

$P_e$= Effective Precipitation (mm)

The maximum root-zone storage capacity was calculated using the integral of the subtraction of the effective precipitation from the evapotranspiration over the time period (Eq 3.9).

$$RZSC = max \int_{t0}^{t1} (E_t - P_e)dt \qquad \text{(Eq 3.8)}$$

$$RZSC = ([E_t - P_e]_1 - [E_t - P_e]_0) \qquad \text{(Eq 3.9)}$$

where:

RZSC= Root-zone storage (mm)

$E_t$= Actual evaporation (mm)

$P_e$= Effective Precipitation (mm)

The absolute values of the root-zone storage were calculated for each time period, the maximum value was determined for the time series and assumed to be the maximum root-zone storage capacity of the catchment.

### 3.4.2  *Wang Method*

Although the Wang method was derived for use with remote sensing datasets, in this study the fundamental equations from Wang- Erlandsson *et al*. (2014) were applied to in-situ point climate data. As the first step, the inflow (Eq 3.10) and the outflow (Eq 3.11). of the system were calculated using daily datasets of precipitation, actual evaporation and interception. The interception values were estimated in Section 2.3.4. It was assumed that no irrigation was applied.

$$F_{out} = E = E_t + I \qquad \text{(Eq 3.10)}$$

where:

$F_{out}$= Flow out of the system (mm)

$E_t$= Actual Evaporation (mm)

I=Interception (mm)

$$F_{in} = P_g + F_{irr} \qquad \text{(Eq 3.11)}$$

where:

$F_{in}$= inflow to the system (mm)

$P_g$= Precipitation (mm)

$F_{irr}$= Irrigation applied within the system (mm)

The difference between the inflow and the outflow was calculated for each time step and the accumulated difference was defined as follows (Eq 3.13).

$$A = \int_{tn}^{tn-1} F_{out} - F_{in} \, . \, dt \qquad \text{(Eq 3.12)}$$

$$A = [F_{out} - F_{in}]_{tn-1} - [F_{out} - F_{in}]_{tn} \qquad \text{(Eq 3.13)}$$

where:

A= The accumulated difference (mm)

$F_{out}$= Flow out of the system (mm)

$F_{in}$= Flow into the system (mm)

$t_n$= final time interval

$t_{n-1}$= initial time interval

The soil moisture deficit is calculated. The soil moisture deficit, by definition, cannot be negative as it is to be considered as a running estimate of the root-zone storage capacity. Thus the following is assumed (Eq 3.14):

$$D_{(tn)} = F_{out} - F_{in} \qquad \text{(Eq 3.14)}$$

where:

$D_{(tn)}$= Soil moisture deficit (mm)

$F_{out}$= Flow out of the system (mm)

$F_{in}$= Flow into the system (mm)

If $D_{(tn)} < 0$ then $D_{(tn)}$ becomes 0

If $D_{(tn)} > 0$ then remains the initial value

71

The soil moisture deficit for the previous time interval is calculated as follows (Eq 3.15 and Eq 3.16):

When $D_{(tn)} < 0$

$$D_{(tn-1)} = (0 + A) \qquad \text{(Eq 3. 15)}$$

And when $D_{(tn)} > 0$:

$$D_{(tn-1)} = \left(D_{(tn)} + A\right) \qquad \text{(Eq 3.16)}$$

where:

$D_{(tn-1)}$= Soil moisture deficit over the previous time interval (mm)

$D_{(tn)}$= Soil moisture deficit over the initial time interval (mm)

A= The accumulated difference (mm)

As the final step, the root-zone storage capacity is calculated (Eq 3.17):

$$RZSC = (D(t_1), D(t_2), D(t_3) \dots D(t_{end})) \qquad \text{(Eq 3.17)}$$

where:

RZSC= Root-zone storage capacity (mm)

$D(t_n)$= Soil moisture deficit over a specific time interval (mm).

### 3.4.3    DiCaSM Routine

The DiCaSM model runs a simple routine to calculate the root-zone storage capacity. This routine requires the groundwater recharge per time interval, which was not available as an observed measurement.

The method used to estimate the groundwater recharge is an empirical relationship developed by Kumar (1977) for use in cases where recharge observation measurements are limited. The empirical relationship is defined as (Eq 3.18):

$$G = 0.63 \times P_e^{0.76} \tag{Eq 3.18}$$

where:

G = Groundwater recharge (mm)

$P_e$ = Effective precipitation (mm)

With groundwater recharge estimates, the root-zone storage capacity method within the DiCaSM model (Ragab, 2010) could be applied. The root-zone storage capacity was calculated using (Eq 3.19):

$$RZSC = P_e - G - E_t \tag{Eq 3.19}$$

where:

RZSC = change in root-zone storage capacity (mm)

$P_e$- Effective precipitation (mm)

G- Groundwater recharge (mm)

$E_t$- Actual Evaporation (mm)

The results from the three root-zone storage capacity methods are presented in Chapter 4.

## 3.5  Statistics and Measures of Model Efficiency

The mean, variance and range were calculated using daily observed and simulated data using the equations in Appendix E. Five goodness of fit parameters (Nash- Sutcliffe, Kling- Gupta, Root Mean Squared Error, Correlation coefficient and percent bias) were calculated using daily observed and simulated data the R scripts in Appendix D and the equations in Appendix E.

# CHAPTER 4: RESULTS

1. The ACRU model was run, with commonly available input data in South African research catchments, for both the Two Streams Catchment and Cathedral Peak Catchment VI.

2. The simulated streamflow was compared to the observed streamflow in both catchments.

3. The simulated soil water from Two Streams was compared to the observed soil water from the catchment.

4. The simulated evaporation, estimated using both the potential evaporation generated by the model and potential evaporation inputted into the model, was compared to the observed evaporation in both catchments.

5. The root- zone storage capacity calculated using both the observed and simulated evaporation was evaluated.

6. The calculated root-zone storage capacity was compared to the observed and simulated soil water to determine the performance of the root- zone storage concept under commercial afforestation and potential use in the hydrological modelling of grasslands in South Africa.

## 4.1 Results from the ACRU modelling: Comparison of Observed and Simulated Data

The ACRU simulations were compared to the observed data.

### 4.1.1 Comparison of Observed and Simulated Streamflows

The streamflow at the outlets of the Two Streams catchment and Cathedral Peak catchment VI were simulated using the ACRU model. The streamflow was simulated for the Two Streams catchment from March 2007 until October 2013. The performance of the model to simulate the streamflow was assessed using Nash-Sutcliff Efficiency (NSE), Kling-Gupta Efficiency (KGE), Root Mean Squared Error (RMSE), $R^2$ and percent bias (Table 4.1).

In comparison to the observed streamflow, the model produced a poor simulation of streamflow at Two Streams as evident from the negative NSE and KGE values (Table 4.1). ACRU under-simulates the magnitude of the high flows but over- simulates the duration of high flow and over- simulates of the low flows (Figure 4.1) resulting in an over- simulation of the total streamflow by 125% over the time period. The summer months were simulated better than the winter months (Table 4.1). Based on the suggestions in Smithers and Schulze (1995), the poor simulation could be attributed to errors in the soil parameters used or the actual evaporation. The streamflow was simulated for Cathedral Peak catchment VI from July 2014 to April 2017. In comparison to the observed streamflow, the model produced a fair simulation of streamflow with NSE and KGE values between 0.45 and 0.55 (Table 4.1). ACRU is over- simulating the magnitude of the high flow but receding too quickly and under-simulating the low flows resulting in a 12% under- simulation of the total discharge over the time period. The winter months were better simulated than the summer months (Table 4.1). The simulated hydrograph receded too rapidly, and the low flows were not maintained well (Figure 4.2). Based on the suggestions in Smithers and Schulze (1995), the concerns in the simulated streamflow could be attributed to errors in the soil parameters used or the actual evaporation.

Table 4.1: The overall and seasonal streamflow goodness of fit statistics for the Two Streams (TS) and Cathedral Peak Catchment VI (CP6) calculated using the daily streamflow values.

| Catchment | TS | CP6 |
|---|---|---|
| NSE | -0.28 | 0.45 |
| KGE | -0.64 | 0.52 |
| RMSE | 0.44 | 1.48 |
| $R^2$ | 0.03 | 0.65 |
| Bias (%) | 125 | -12 |
| Summer NSE | -0.21 | 0.46 |
| Winter NSE | -1.88 | 0.51 |
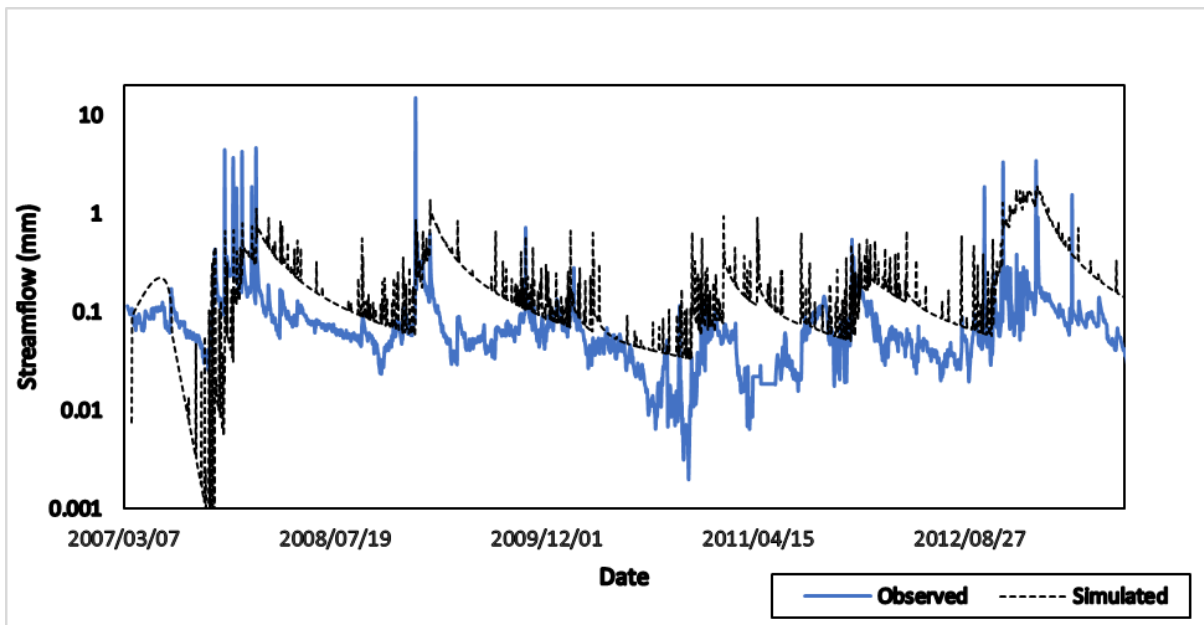
Figure 4.1: The log of the daily simulated streamflow (black dashed line) and the daily observed streamflow (blue line) from March 2007 to October 2013 at the outlet of Two Streams catchment.
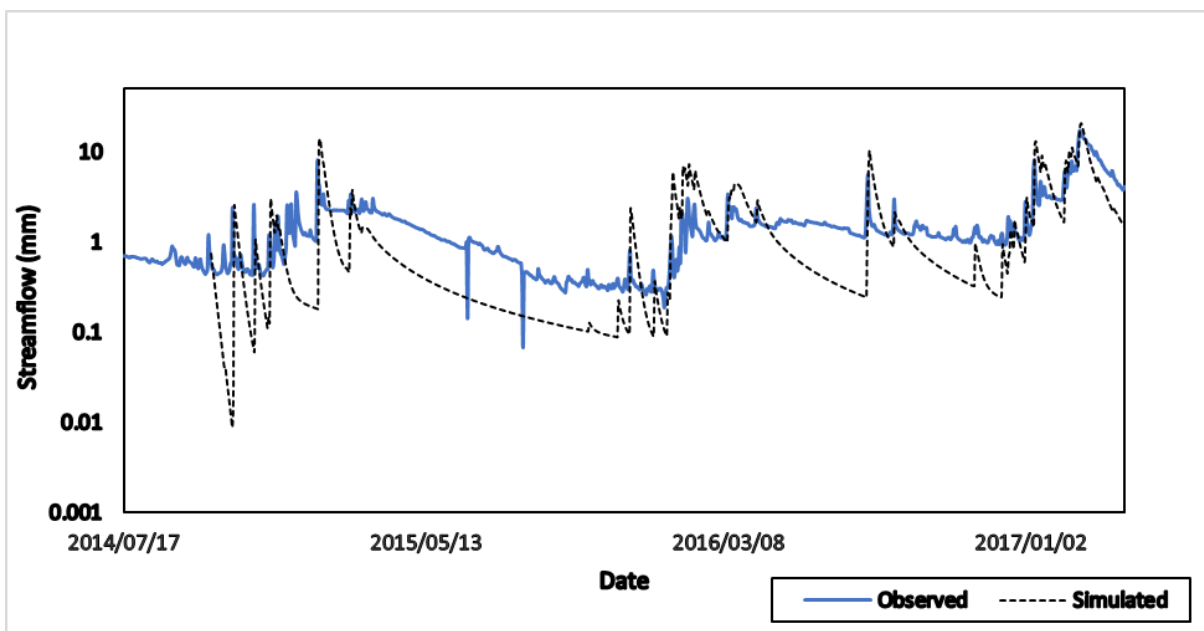


Figure 4.2: The log of the daily simulated streamflow (black dashed line) and the daily observed streamflow (blue line) from July 2014 to April 2017 at the outlet of Cathedral Peak Catchment VI.

### 4.1.2 Observed and ACRU Simulated Soil Water

Due to data availability, the verifications using observed soil water could only be undertaken for the Two Streams catchment from November 2011 until October 2013. The observed data was obtained from Time Domain Reflectometer (TDR) soil water probes at 0.4 m intervals through the soil profile to a depth of 2.4 m. The soil water storage for the A and B horizons was selected as an output from the ACRU model simulation for the Two Streams catchment. The simulated soil water storage was compared to the observed data for the relevant horizons (Figure 4.3 and Figure 4.4). In the A horizon, the observed and simulated soil water fluctuated within the range of plant available water, the fluctuations have a visibly fair correlation and good seasonal trend (Figure 4.3) but statistically the simulation is poor with an NSE of -0.29, and $R^2$ of 0.17 (Table 4.2). The simulated soil water is more responsive to rainfall than the observed soil water causing the temporal correlation of the peaks to be weak and 23% over simulation. The simulated soil water reduced to the permanent wilting point in the dry season whereas the observed soil water did not. In the B horizon, the model produced a poor simulation with an NSE of -0.47 and $R^2$ of 0.27 (Table 4.2). The ACRU model over- simulated the magnitude and flux of the soil water (Table 4.2 and Figure 4.4). The observed data formed a smooth curve with a single peak within the bounds of the plant available water whilst the simulated soil water was far more responsive.

There is not always a response to rainfall in the A soil horizon. This could be due to multiple factors such as low rainfall intensity, high levels of canopy interception, litter interception, immediate water uptake by water stressed trees and possibly surface sealing of the soil below the canopy which affects the infiltration. The simulated soil water in the B horizon fluctuated to a greater extent than the observed soil water. The B horizon is much deeper than the A horizon and therefore the response to rainfall events is lagged. Soil water in the B horizon tends to be taken up immediately by the trees as there is evidence that they are continuously stressed.

Table 4.2:    The soil water goodness of fit statistics for the Two Streams catchment
calculated using the daily soil water values.

|  | NSE | $R^2$ | Bias (%) |
|---|---|---|---|
| A Horizon | -0.29 | 0.17 | 23 |
| B Horizon | -0.47 | 0.27 | 10 |
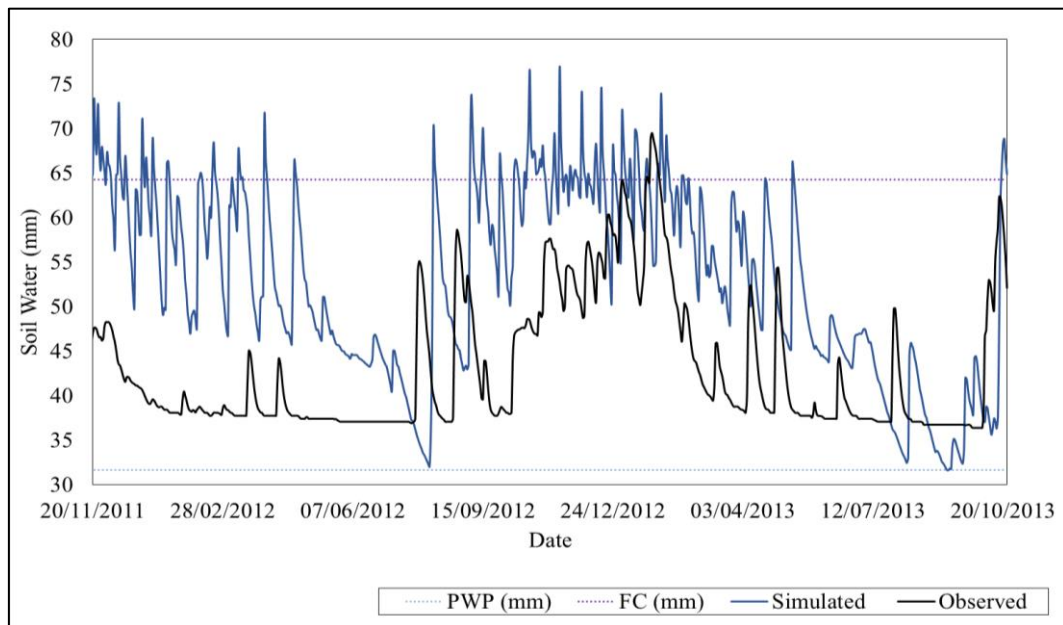


Figure 4.3:    The daily simulated soil water (blue line) and the daily observed soil water
(black line) in the A horizon plotted within the field capacity (purple dashed
line) and the wilting point (blue dashed line) for the period of November 2011
until October 2013.
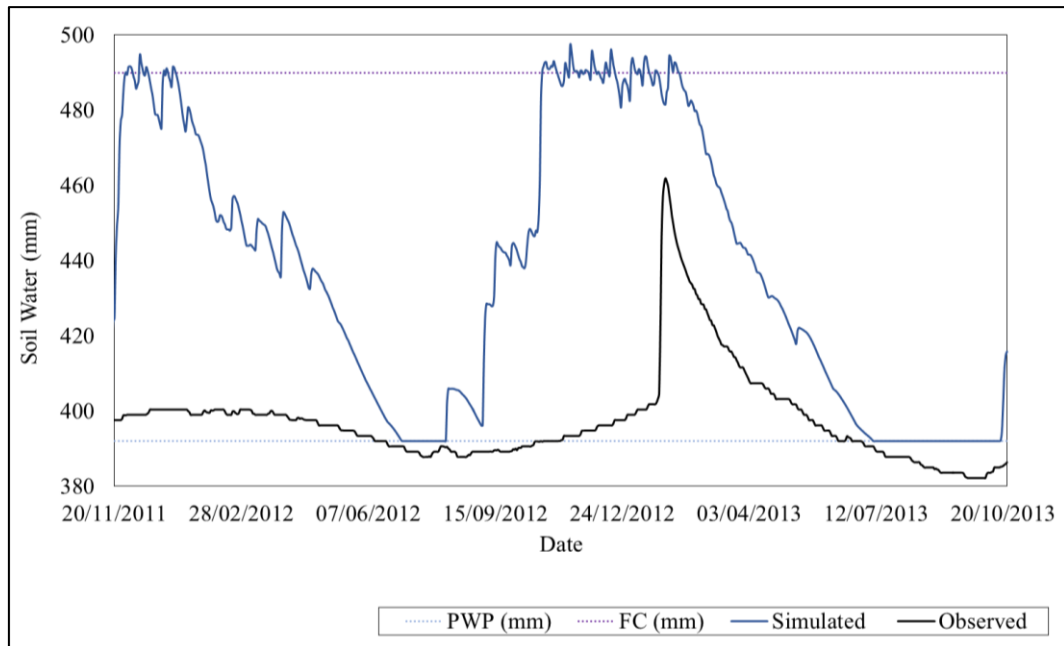
Figure 4.4: The daily simulated soil water (blue line) and the daily observed soil water (black line) in the B horizon plotted within the field capacity (purple dashed line) and the wilting point (blue dashed line) for the period of November 2011 until October 2013.

### 4.1.3    *Observed and Simulated Actual Evaporation*

The actual evaporation was simulated by the ACRU model (using the maximum and minimum temperatures) was compared to the observed records for the respective catchments from March 2007 until October 2013. The actual evaporation simulated by the model was used to determine the accuracy of the partitioning of water into the components of the water balance in the ACRU model. The overall and seasonal performance of the model to simulate the actual evaporation was assessed using NSE, KGE, RMSE, $R^2$ and percent bias (Table 4.3).

Table 4.3:    The overall and seasonal actual evaporation goodness of fit statistics for the Two Streams (TS) and Cathedral Peak Catchment VI (CP6) calculated using the daily observed and simulated actual evaporation values.

| Catchment | TS | CP6 |
|---|---|---|
| NSE | -0.06 | -0.19 |
| KGE | -0.17 | 0.165 |
| RMSE | 2.3 | 1.9 |
| $R^2$ | 0.17 | 0.10 |
| Bias (%) | -50 | -33 |
| Summer NSE | -0.17 | -0.44 |
| Winter NSE | -0.04 | 0.15 |

The model produced a very poor simulation of the actual evaporation resulting in negative NSE and KGE values and a large RMSE for both catchments (Table 4.3). At Two Streams, the actual evaporation was under simulated by 50% over the time period (Table 4.3) and this was particularly evident in the daily time series (Figure 4.5). The seasonal NSE suggests that the winter months are simulated slightly better than the summer months (Table 4.3), however, the under- simulations in the dry season are more evident than in the wet season in the daily time series (Figure 4.5). The model reduced the actual evaporation to zero in periods of the dry season because of the soil water drying out. This is not realistic as the catchment was afforested with evergreen *Acacia mearnsii* that continues to transpire throughout the year as confirmed by the observed evaporation (Figure 4.5).
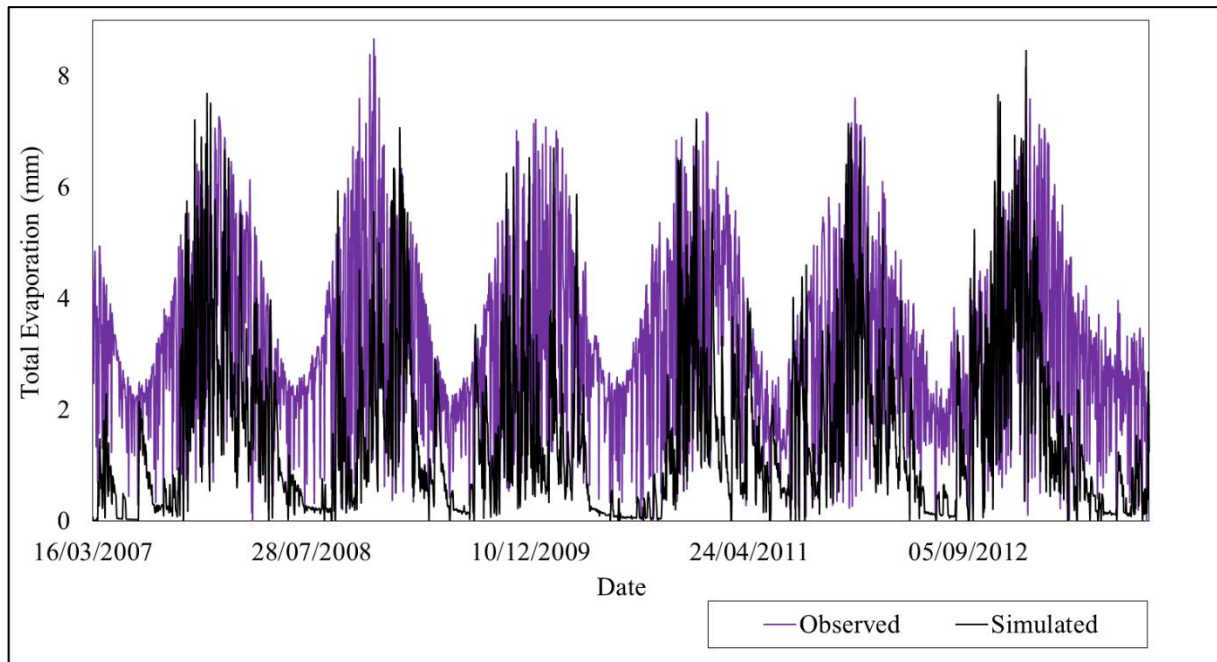
Figure 4.5:     The daily observed l evaporation (purple line) and the daily actual evaporation estimated by the ACRU model (using the maximum and minimum temperatures) (blacked dashed line) at the Two Streams Catchment over the period of March 2007 until October 2013.

The actual evaporation was simulated by ACRU (using the minimum and maximum temperatures) at Cathedral Peak Catchment VI from July 2014 until August 2018. In comparison to the observed evaporation records, the model poorly simulated the actual evaporation as evidenced by low NSE and KGE values, a large RMSE and a negative bias of 33% over the time period (Table 4.3). The seasonal NSE suggests that the winter months were simulated better than the summer months (Table 4.4), however, from the daily time series the under- simulations in the dry, winter season were more evident (Figure 4.7). The poor temporal simulation in comparison to the observed data is evident from the daily time series (Figure 4.7), for example, due to late rains in (April) 2016 and the re-sprouting of the vegetation following initial senesce, the observed evaporation was at a maximum for a longer time than the simulated actual evaporation suggests. ACRU was unable to account for the re-sprouting of senescing vegetation (due to intra-annual variation of rainfall) within the modelling period as stationary monthly crop coefficients are input for each year, thus the model simulates the same transpiration trend every year of the modelling period. Furthermore, the input crop coefficients suggest senesce of all the vegetation whereas the

82

observed evaporation data indicates that some of the vegetation continue to transpire during winter.
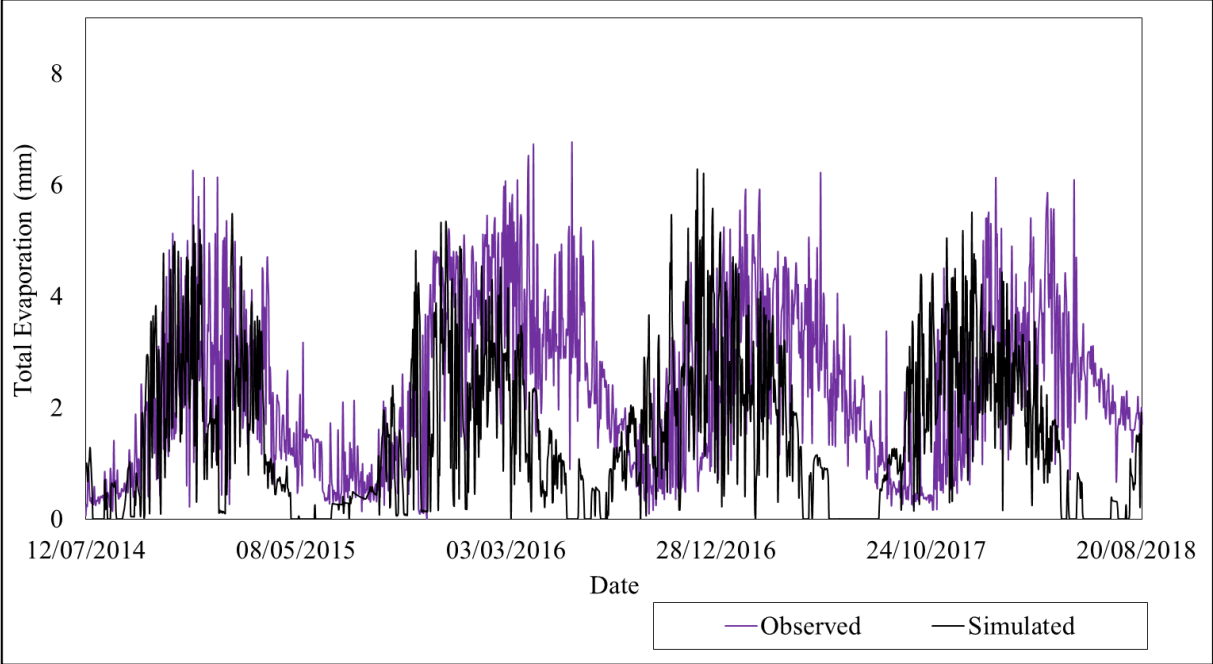


Figure 4.6:    The daily observed evaporation (red line) and the daily actual evaporation estimated by the ACRU model (blacked dashed line) at Cathedral Peak Catchment VI over the period of July 2014 until August 2018.

Within the ACRU model evaporation can be estimated using several methods. The potential evaporation estimated by a user- chosen method (e.g. Hargreaves and Samani, Penman-Monteith), are internally converted to a daily A Pan equivalent value and the crop coefficient which is the potential evaporation used in the model simulation. There is potential for discrepancies in the actual evaporation estimate due to the conversion from Hargreaves and Samani (1985) daily to A pan equivalent as a simple multiplication factor of 1.2 is used throughout the year. To eliminate the possibility of the conversion factor resulting in the poor simulation of the actual evaporation, the Hargreaves and Samani daily evaporation was calculated outside of the model and multiplied by a varying PENPAN correction factor (derived from work by Kunz *et al*. (2015), see section 3.2.1) followed by the crop coefficient for both catchments. This Apan equivalent potential evaporation was fed into the model to produce the actual evaporation. The actual evaporation estimated using the PENPAN conversion factor (Hargreaves and Samani PENPAN (HSPP)

83

estimation) was plotted against the actual evaporation estimated using the Apan equivalent conversion factor from within ACRU (1.2) for the Two Streams catchment (Figure 4.7) and for the Cathedral Peak Catchment VI (Figure 4.8). This comparison showed that the model estimated actual evaporation has a slightly wider range of values but there was no significant difference in the evaporation values for either site. Thus, it can be determined that the Apan equivalent conversion was not the source of error in the actual evaporation estimation within the model. The actual evaporation generated using the PENPAN Apan conversion factor will be used in all the following calculations.
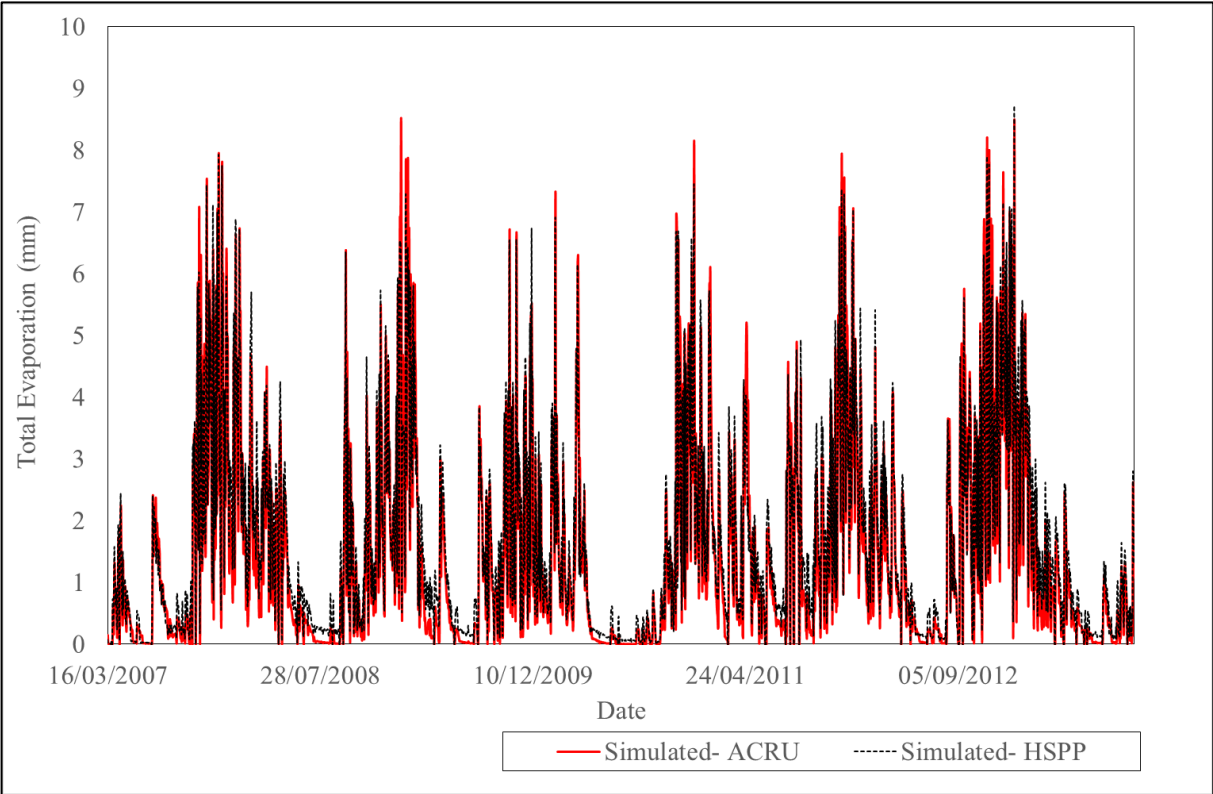


Figure 4.7:    The daily actual evaporation simulated using ACRU model Hargreaves and Samani to A-Pan conversion factor of 1.2 (purple line) and the daily actual evaporation estimation using the monthly factor derived by Kunz *et al.* (2015) (black dashed line) from March 2007 until October 2013.
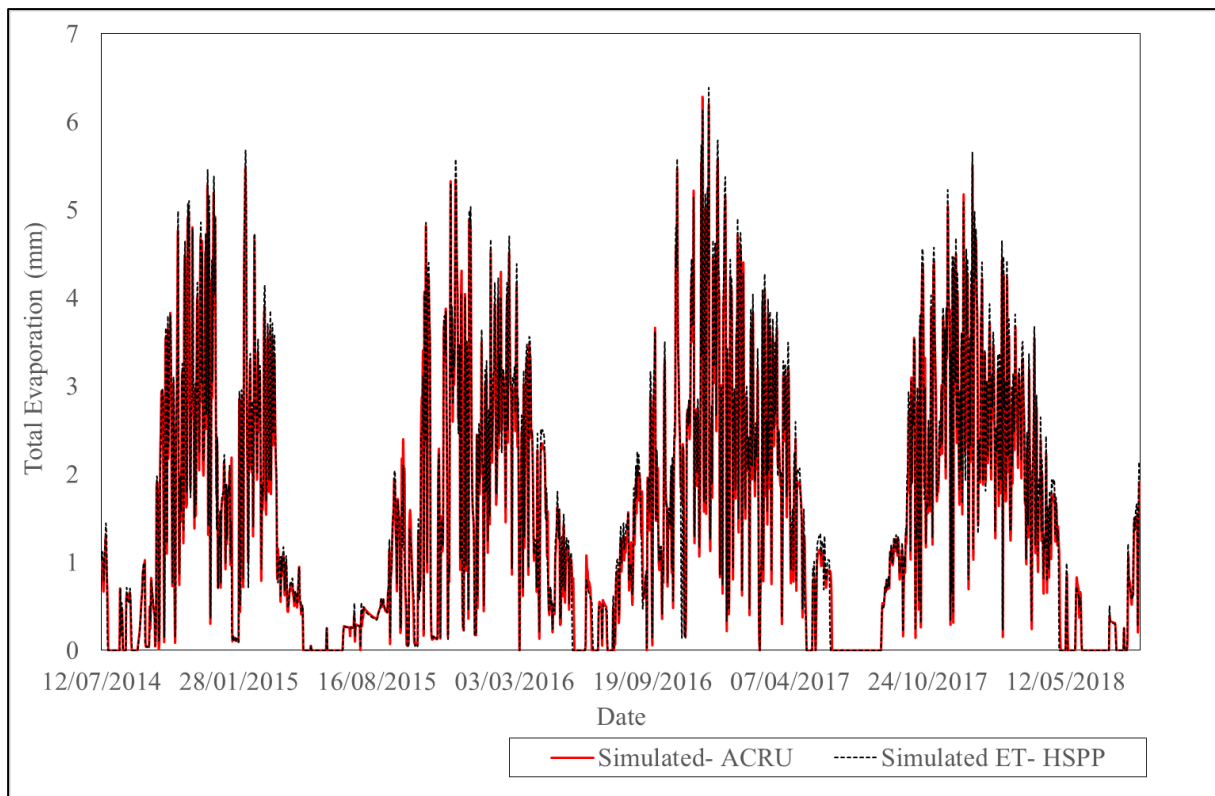
Figure 4.8:   The daily actual evaporation simulated using ACRU model Hargreaves and Samani to A-Pan conversion factor of 1.2 (red line) and the daily actual evaporation estimation using the monthly factor derived by Kunz *et al.* (2015) (black dashed line) from July 2014 until August 2018.

The ACRU model performed poorly at Cathedral Peak VI and more so at Two Streams. The streamflow simulations at Cathedral Peak Catchment VI were fair however the actual evaporation and soil water simulations were poor. At Two Streams the simulation of the streamflow, actual evaporation and soil water were all poor. McNamara (2018) illustrated that the ACRU model output is highly sensitive to the crop coefficient parameter. Thus, the conceptualisation of and uncertainty with the use of the crop coefficient (Allen *et al*., 2005 and Kunz *et al*., 2015) in the estimation of actual evaporation in the ACRU model could be contributing to the poor simulations of actual evaporation and consequently the soil water. In South Africa, there is a lack of site- specific crop coefficient data and thus estimations from FAO and other sources are commonly used. Added to this, the lack of adequate root depth and distribution information, and poor soils data further compounds the poor estimation of the soil water. The use of the root- zone storage capacity concept could potentially be used in addressing the uncertainties with the crop

85

coefficient and the data deficits. It incorporates both climatic and vegetation conditions into a single dynamic hydrological parameter and represents all the combinations of the vegetation in a catchment (de Boer-Euser *et al.*, 2019) and thus removing the reliance on the crop coefficient, rooting and soils data.

## 4.2 Root-zone Storage Capacity

Three methods were used to estimate the root-zone storage capacity for each of the catchments. The first, the Nijzink *et al.* (2016) method is based on a complex long-term water balance principle which supersedes the second method developed by Wang-Erlandsson *et al.* (2014). The final method is adapted from the DiCaSM model root-zone storage routine, which requires a groundwater recharge calculation, and for the purposes of this study, the method developed by Kumar (1977) was used. The results from the three methods are presented for each catchment.

### *4.2.1 Two Streams Catchment*

All three methods produced root-zone storage capacities that displayed strong seasonal trends throughout the study period with sporadic high peaks in the summer months in response to large rainfall events in the catchment (Figure 4.9). The median root- zone storage capacity (Table 4.4), the frequency distribution (Figure 4.10) and the daily root- zone storage time series (Figure 4.9) show that the Nijzink method estimates the greatest root- zone storage capacities and the Wang method estimates the lowest root- zone storage capacities. The Nijzink method results have the greatest variability in the calculated root- zone storage capacities and were very responsive to rainfall events. The root- zone storage capacities calculated using the DiCaSM method were the least variable (Table 4.4 and Figure 4.10). The DiCaSM method produced a root- zone storage capacity similar to that of the Nijzink method (Table 4.4) but did not produce sporadic peaks in response to the rainfall events evident from the range and the time series plot (Table 4.4 and Figure 4.9).

Table 4.4    Statistics of the root- zone storage capacities estimated using the Nijzink, Wang and DiCaSM methods at Two Streams.

|               | Nijzink | Wang | DiCaSM |
|---------------|---------|------|--------|
| Mean (mm)     | 6.1     | 4.0  | 6.04   |
| Median (mm)   | 5.3     | 3.1  | 5.6    |
| Variance (mm) | 17.6    | 14.4 | 7.8    |
| Range (mm)    | 39.7    | 29.8 | 16.7   |
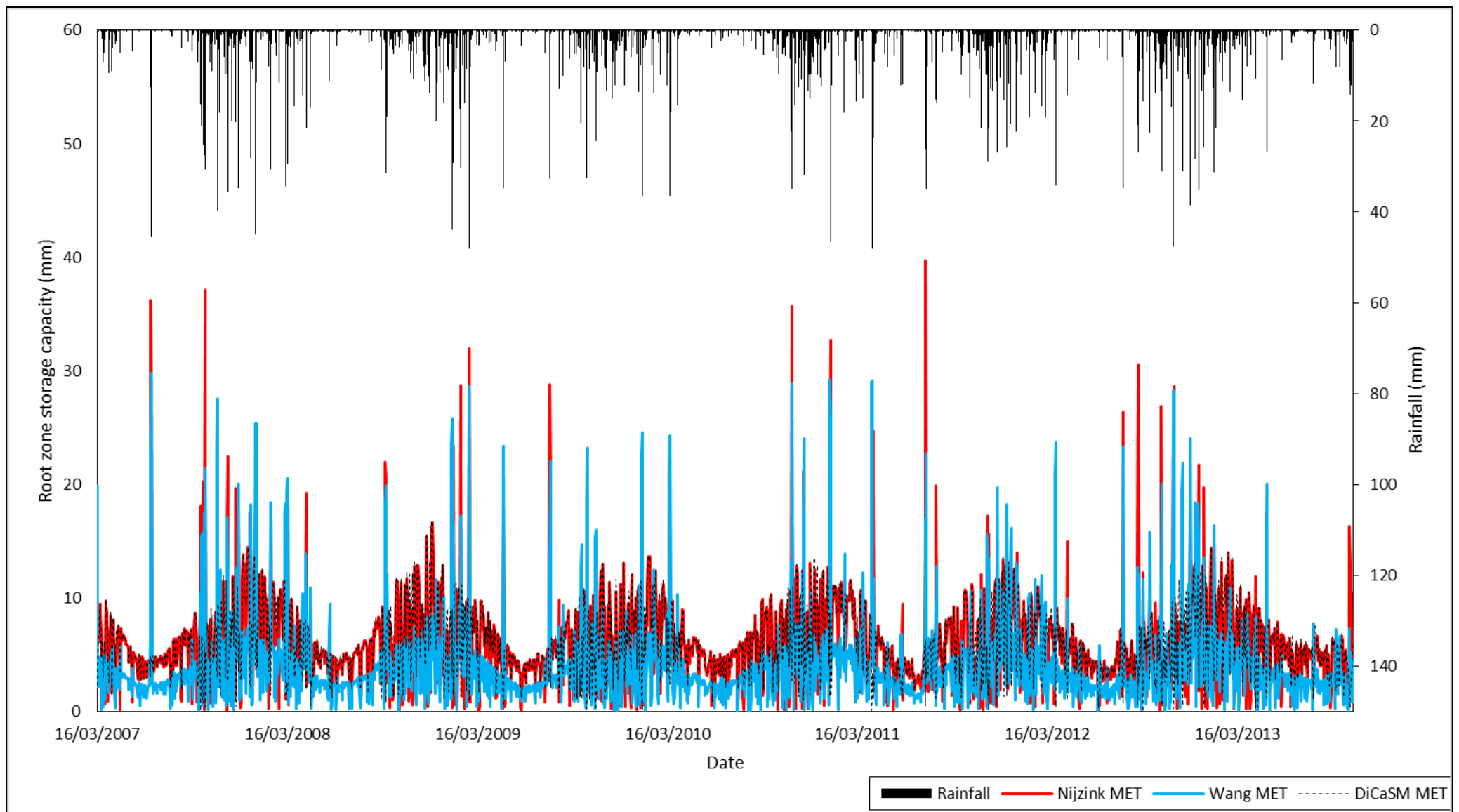
Figure 4.9:     Estimated daily root-zone storage capacity for the Nijzink (red line), Wang (blue line) and DiCaSM (dashed black line) methods and daily rainfall (black line) at the Two Streams catchment for March 2007 to October 2013.
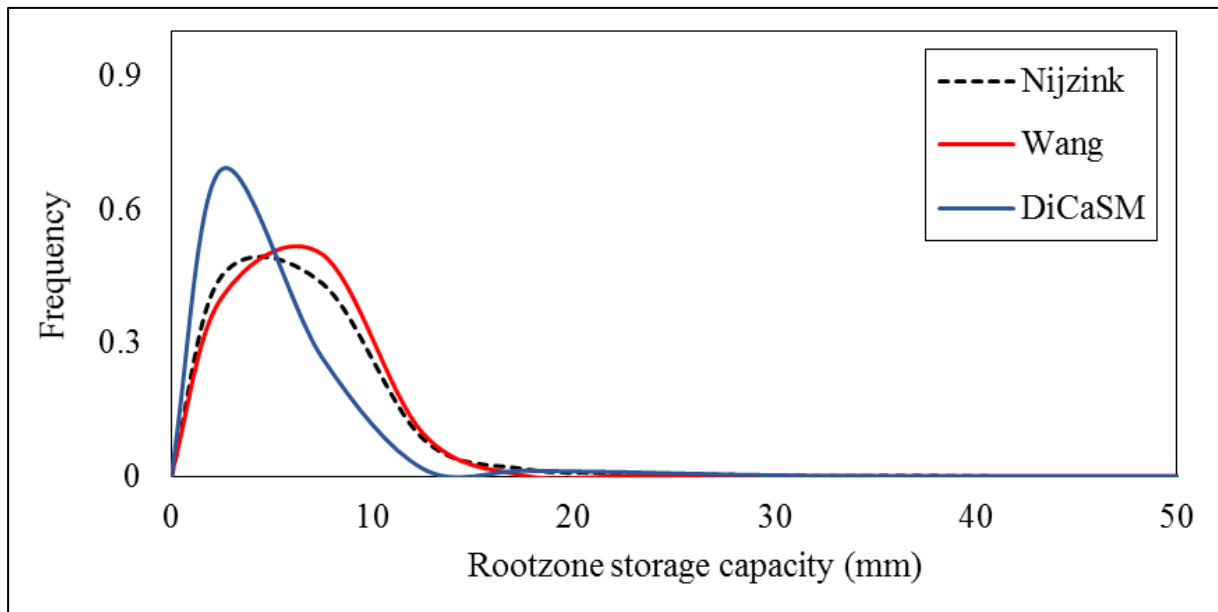
Figure 4.10:  Frequency distribution curve for the estimated root-zone storage capacity using the Nijzink (black dashed line), Wang (red line) and DiCaSM (blue line) methods for Two Streams Catchment from March 2007 to October 2013.

The root-zone storage capacities were re-calculated using the same methodologies (Nijzink, Wang and DiCaSM) however, the observed evaporation was replaced with the simulated actual evaporation using the PENPAN correction factor (hereafter referred to as the simulated actual evaporation) calculated in Section 4.3.1 to determine the sensitivity to the actual evaporation input in the root- zone storage capacity and to investigate the robustness of this method to data scarcity.

Using the simulated actual evaporation in the Nijzink method decreased the mean root-zone storage capacity however, it increased the variance and the range over the time period (Table 4.5 and Figure 4.11). Higher peaks in the root- zone storage were evident in the time series calculated using the simulated actual evaporation although the mean and median were lower than those derived using the observed evaporation (Figure 4.12). During periods where the simulated actual evaporation was significantly under- simulated (Figure 4.5), the calculated root- zone storage was lower, and the root- zone storage capacity decreased into the dry season. In spring 2010 the root- zone storage capacity estimated with the simulated actual evaporation significantly lagged the root- zone storage capacity estimated with the observed evaporation (Figure 4.12). The Nijzink method was

89

most sensitive to evaporation in the dry season, whereas in the wet season it was most sensitive to precipitation.

Table 4.5    Statistics of the root- zone storage capacities estimated using the Nijzink, Wang and DiCaSM methods with observed evaporation (OET) and simulated actual evaporation (SET) for the Two Streams catchment.

| | Nijzink | | Wang | | DiCaSM | |
|---|---|---|---|---|---|---|
| | OET | SET | OET | SET | OET | SET |
| Mean (mm) | 6.1 | 4.1 | 4.0 | 2.9 | 6.04 | 2.7 |
| Median (mm) | 5.3 | 2.6 | 3.1 | 1.6 | 5.6 | 2.1 |
| Variance (mm) | 17.6 | 23.0 | 14.4 | 159 | 7.8 | 5.2 |
| Range (mm) | 39.7 | 40.2 | 29.8 | 30.8 | 16.7 | 11.6 |
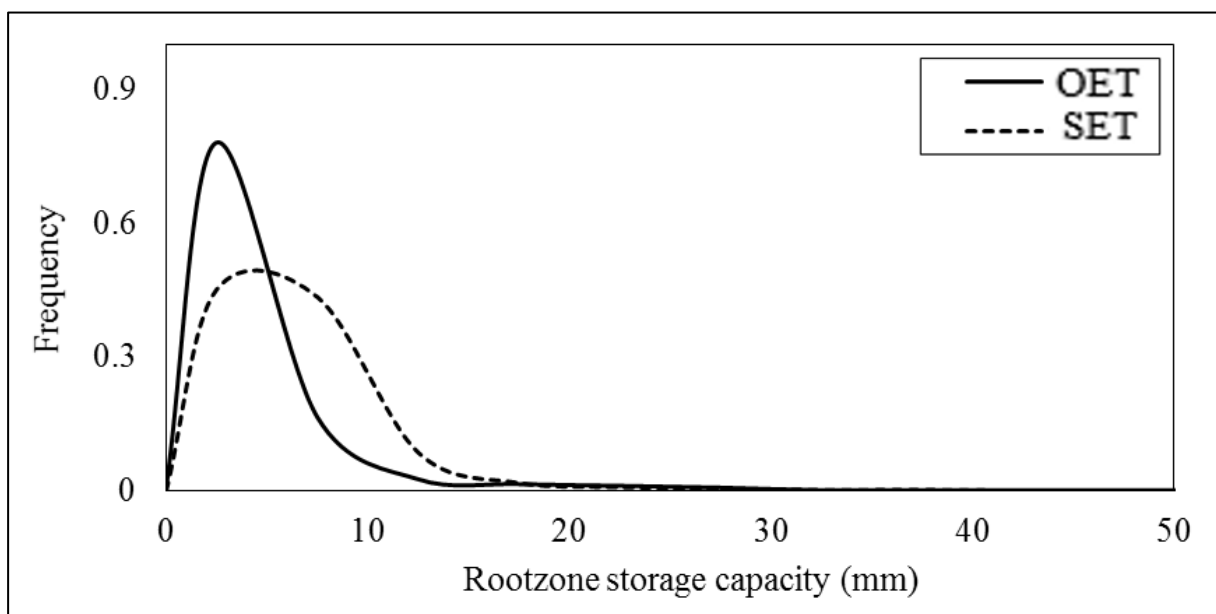


Figure 4.11:    Frequency distribution curve for the estimated root-zone storage capacity using the Nijzink method with observed evaporation (black line) and simulated actual evaporation (black dashed line) for the Two Streams Catchment from March 2007 to October 2013.
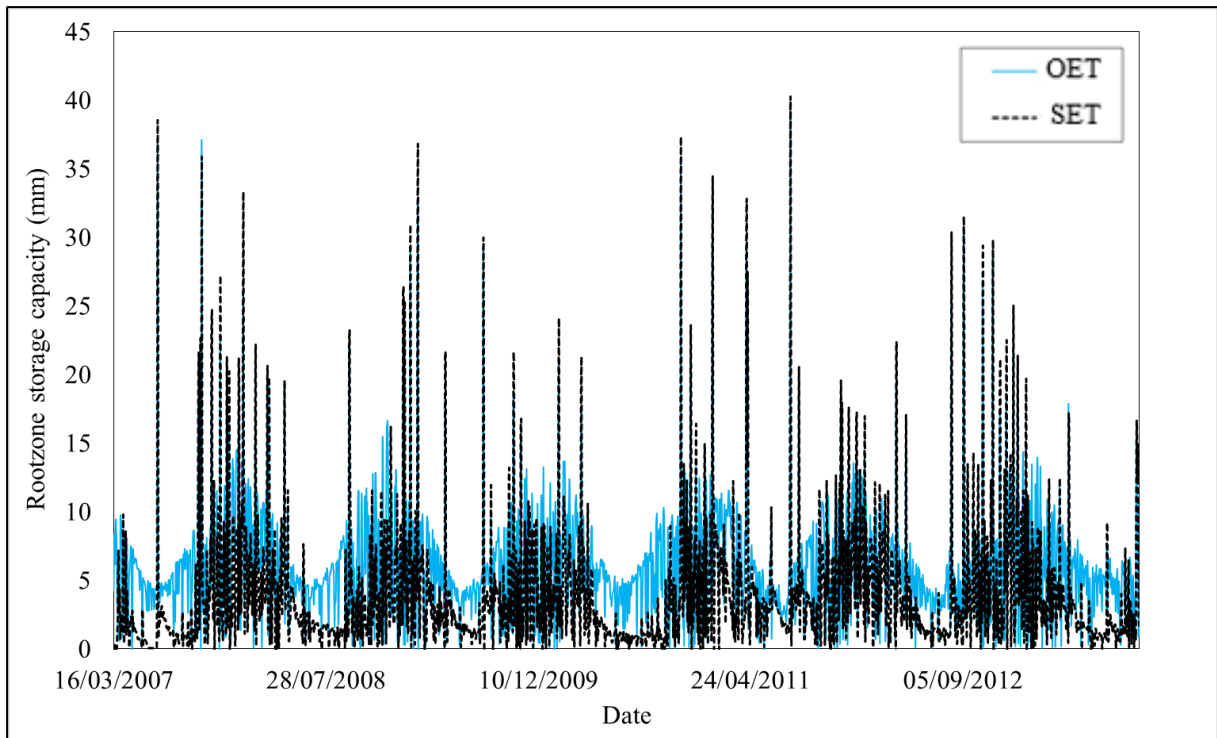
Figure 4.12:    Daily root-zone storage estimated using the Nijzink method with both the observed evaporation (blue line) and the simulated actual evaporation (black dashed line) for the Two Streams catchment.

Using the simulated actual evaporation in the Wang method decreased the mean root- zone storage capacity and slightly increased the variance and the range over the time period (Table 4.7 and Figure 4.13). A significant decrease in the root- zone storage capacity using the simulated actual evaporation was seen in the dry season (Figure 4.14) when the simulated actual evaporation was significantly under- simulated (Figure 4.5). The Wang method is sensitive to both the evaporation and precipitation in the wet season and the evaporation in the dry season.
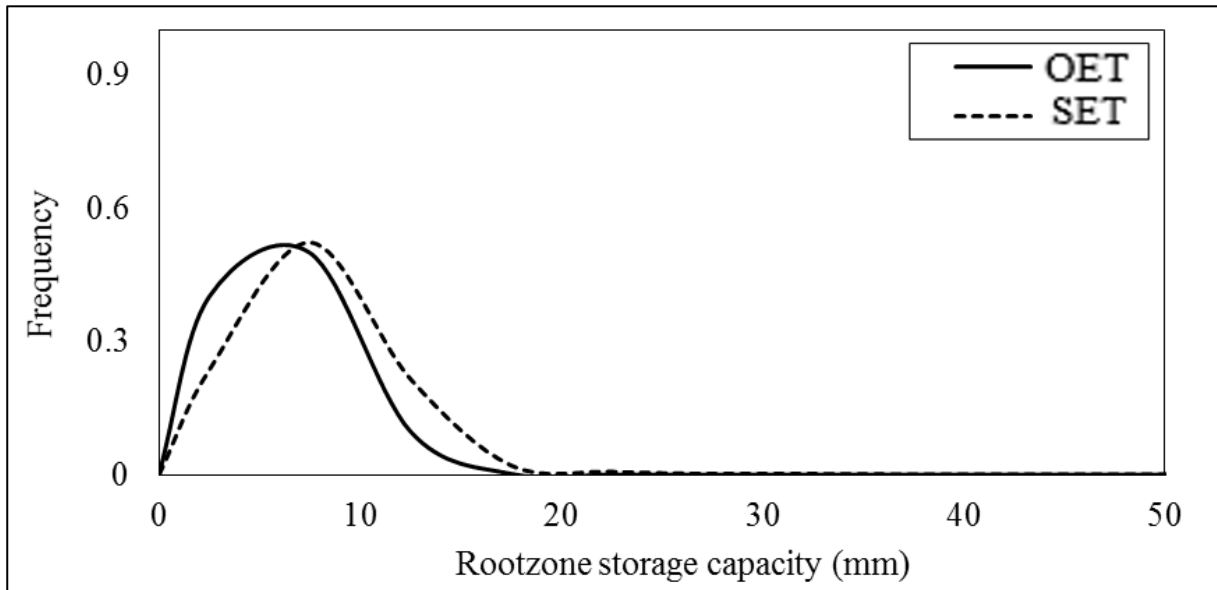
Figure 4.13:   Frequency distribution curve for the estimated root-zone storage capacity using the Wang method with observed evaporation (black line) and simulated actual evaporation (black dashed line) for the Two Streams Catchment from March 2007 to October 2013.
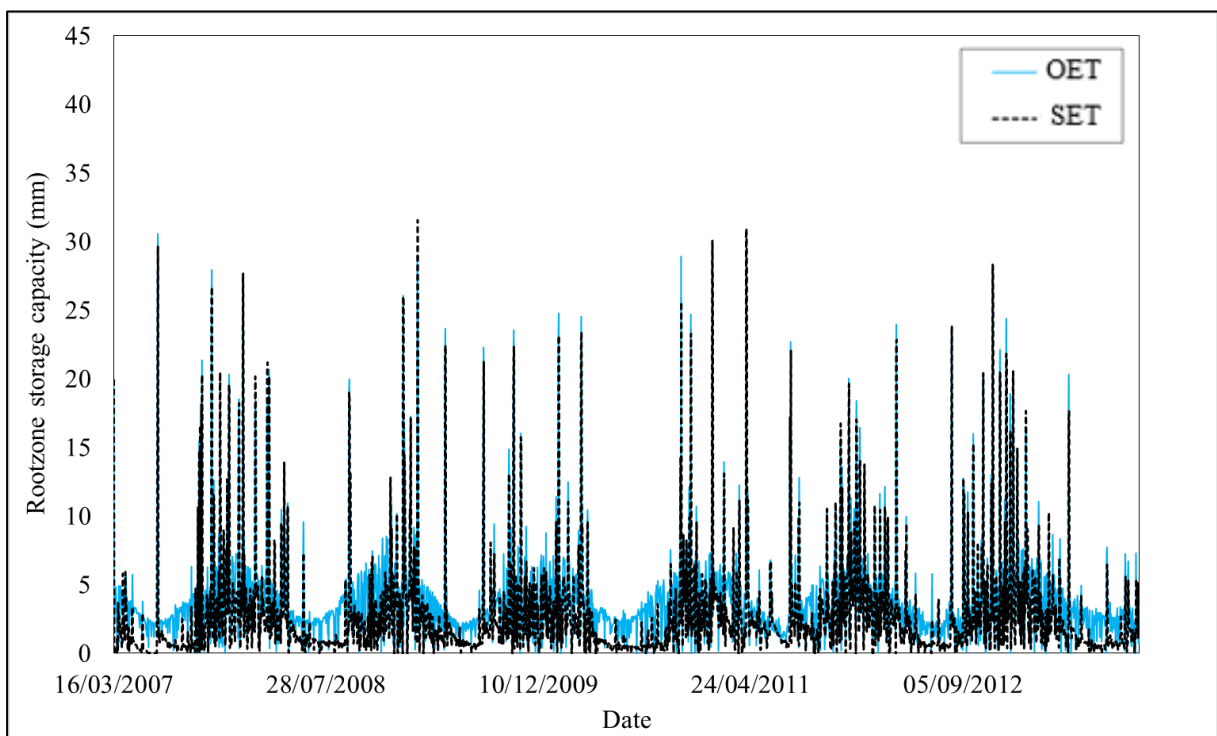


Figure 4.14:   Daily root-zone storage estimated using the Wang method with both the observed evaporation (blue line) and simulated actual evaporation (black dashed line) for the Two Streams catchment

92

Using the simulated actual evaporation in the DiCaSM method decreased the mean root-zone storage capacity, the variance and the range over the time period (Table 4.8 and Figure 4.15). Throughout the time period, the root- zone storage capacity estimated using the simulated actual evaporation was significantly lower than when using the observed evaporation. The DiCaSM method was highly sensitive to the evaporation component but less sensitive to the precipitation as the time series does not show high peaks (and large range) as the Nijzink and Wang methods.
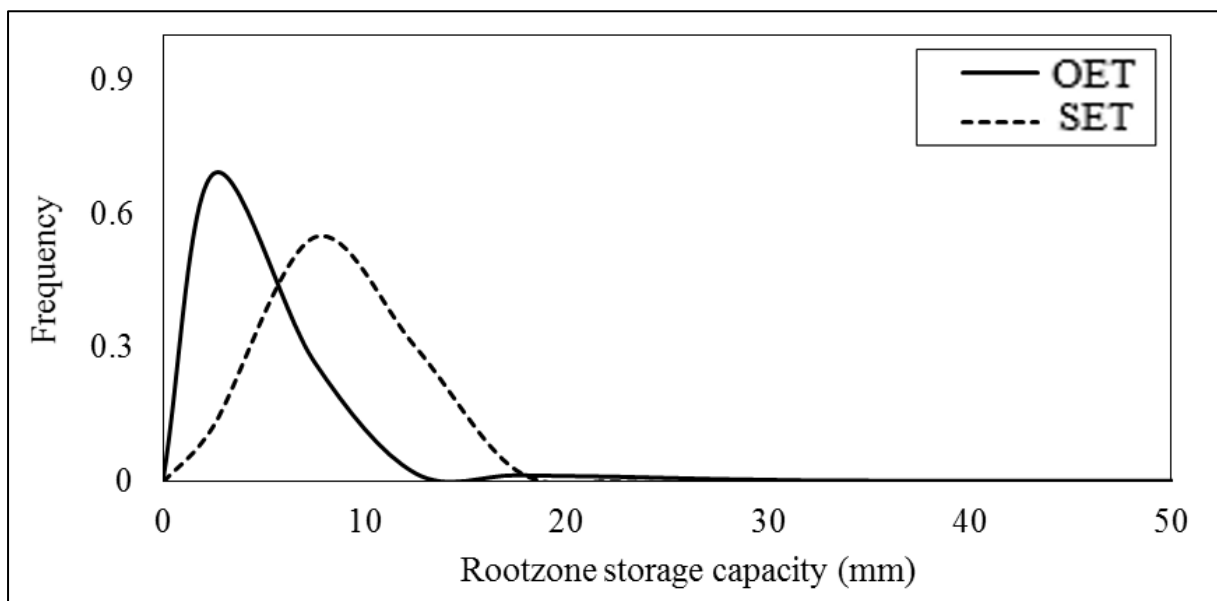


Figure 4.15:    Frequency distribution curve for the root-zone storage capacity estimated using the DiCaSM method with observed evaporation (black line) and simulated actual evaporation (black dashed line at Two Streams Catchment from March 2007 to October 2013.
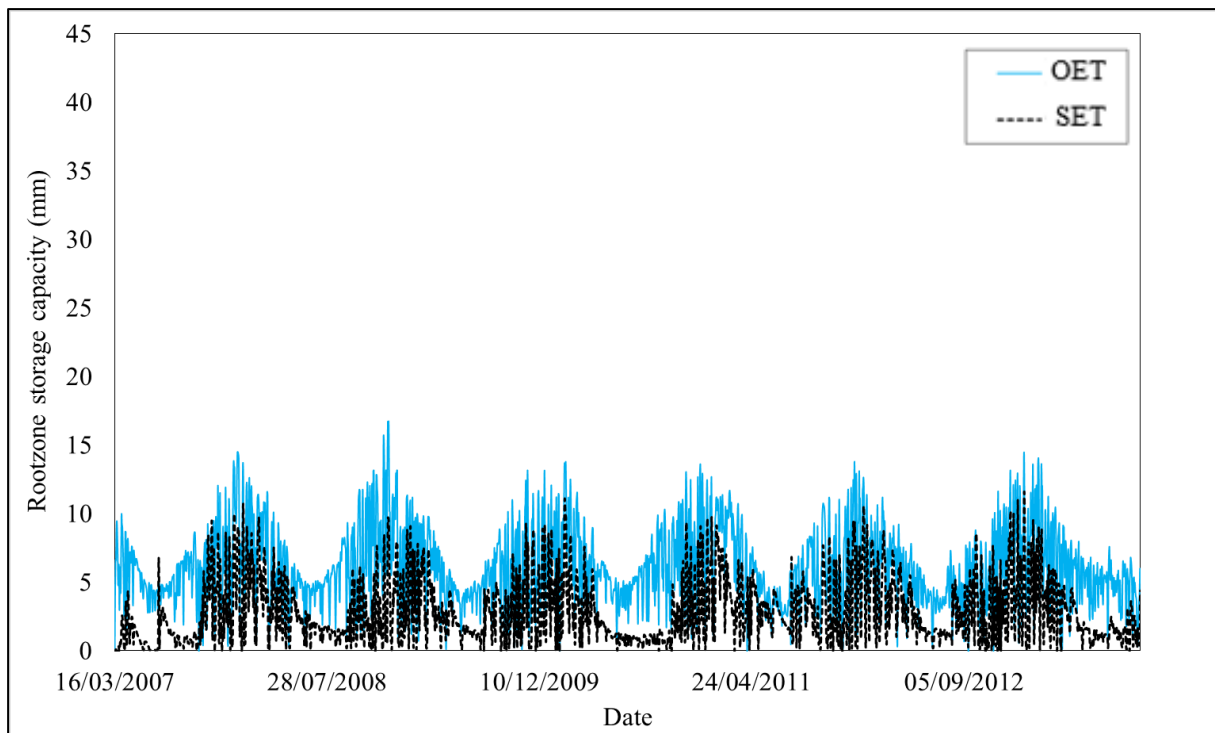
Figure 4.16:    Daily root-zone storage estimated using the DiCaSM method with both the observed evaporation (blue line) and the simulated actual evaporation (black dashed line) for the Two Streams catchment.

### 4.2.2    *Cathedral Peak Catchment VI*

The Nijzink, Wang and DiCaSM methods produced very similar root-zone storage capacities for Cathedral Peak catchment VI that displayed strong seasonal trends throughout the study period with sporadic high peaks in the summer months in response to rainfall events in the catchment (Figure 4.18). The median root- zone storage capacity (Table 4.6), the frequency distribution (Figure 4.17) and the daily root- zone storage time series (Figure 4.18) show that the Nijzink and DiCaSM methods estimated the greatest root- zone storage capacities and the Wang method estimated the lowest root- zone storage capacities. The Nijzink method resulted in the greatest variability within the calculated root- zone storage capacities and was highly responsive to rainfall events. The root- zone storage capacities calculated using the DiCaSM method were the least variable and did not respond rapidly to rainfall.

Table 4.6:    Statistics of the root- zone storage capacity estimated using the Nijzink, Wang and DiCaSM methods at Cathedral Peak catchment VI over the period July 2014 to August 2018.

|                 | Nijzink | Wang | DiCaSM |
| --------------- | ------- | ---- | ------ |
| Mean (mm)       | 8.4     | 6.8  | 8.6    |
| Median (mm)     | 7.0     | 5.5  | 8.0    |
| Variance (mm)   | 61.3    | 33.2 | 23.0   |
| Range (mm)      | 110.5   | 83.0 | 77.7   |
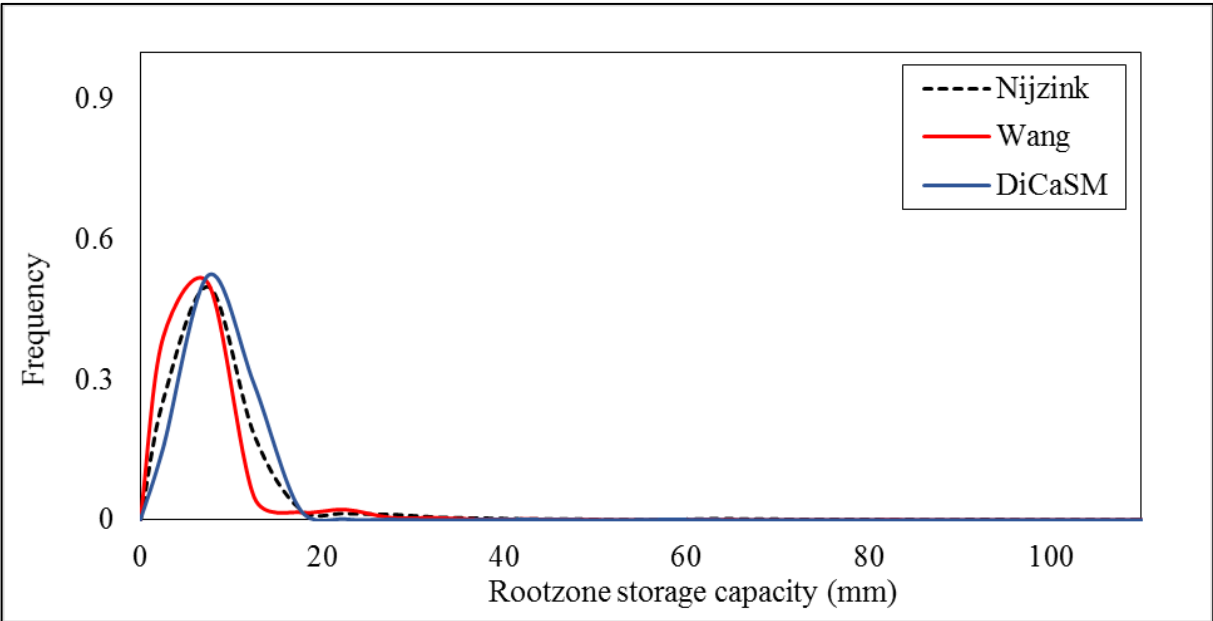


Figure 4.17:    Frequency distribution curve of the root-zone storage capacity estimated using the Nijzink (black dashed line), Wang (red line) and DiCaSM (blue line) methods for the Cathedral Peak Catchment VI (July 2014 to August 2018).
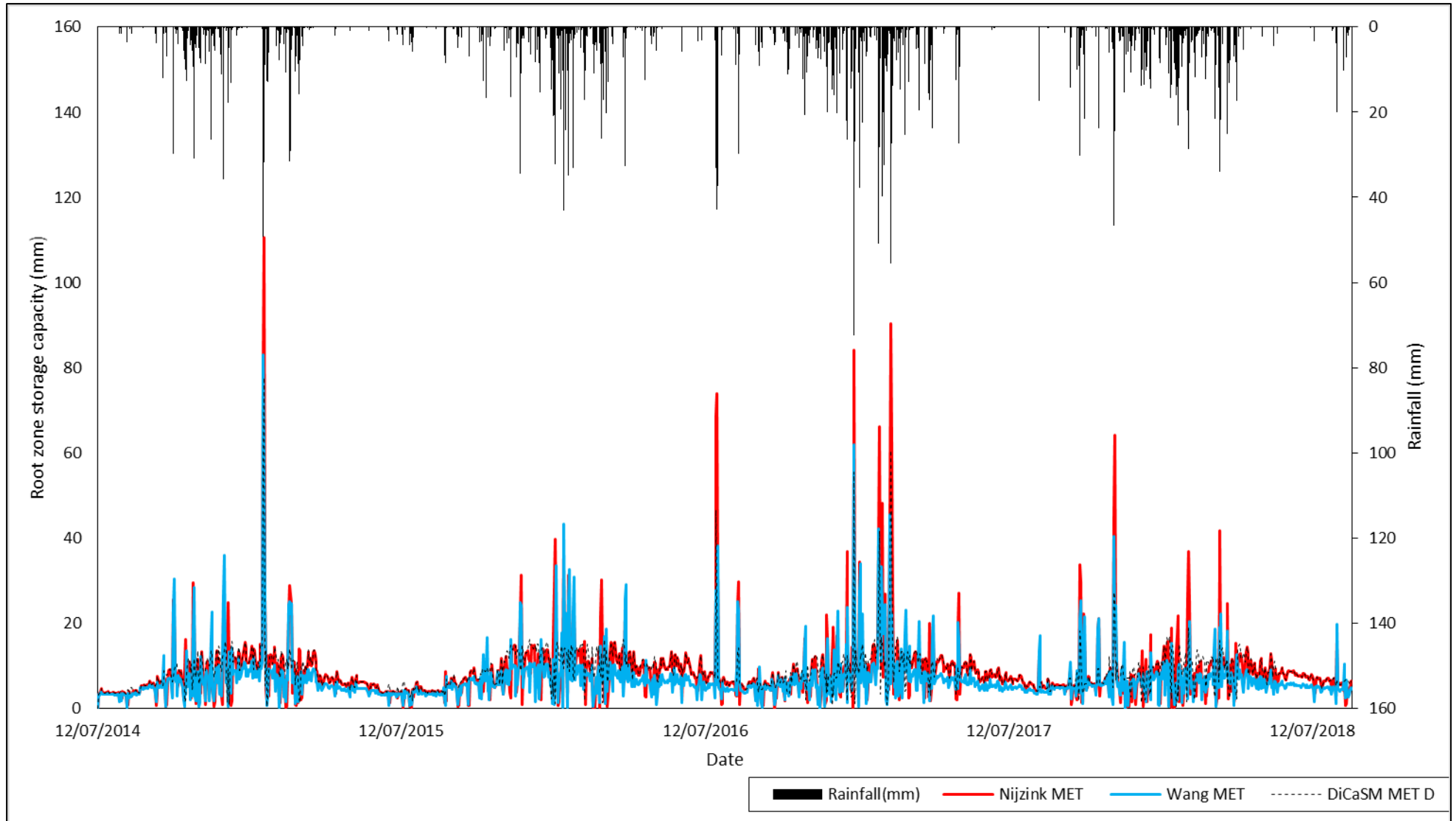
Figure 4.18:    Daily root-zone storage capacity calculated using the Nijzink (purple line), Wang (green line) and DiCaSM (blue line) methods and the daily rainfall (black line) for the Cathedral Peak Catchment VI from July 2014 to August 2018.

The root-zone storage capacities were re-calculated using the same methodologies (Nijzink, Wang and DiCaSM) however, the observed evaporation was replaced with the simulated actual evaporation using the PENPAN correction factor (hereafter referred to as the simulated actual evaporation) calculated in Section 4.3.1 to determine the sensitivity to the actual evaporation input in the root- zone storage capacity and to investigate the robustness of this method to data scarcity.

Using the simulated actual evaporation in the Nijzink method decreased the mean root-zone storage capacity and more markedly decreased the median, as well as slightly increasing the variance and range over the time period (Table 4.7 and Figure 4.20). In the dry, winters of 2016, 2017 and 2018 the root- zone storage capacity decreased slowly into the winter when using the observed evaporation, corresponding with the prolonged higher actual evaporation period due to late April rains (Figure 4.6). However, the root- zone storage derived with the simulated actual evaporation declines quickly during the autumn months. The winter root- zone storage capacity is sensitive to the evaporation whilst the summer root- zone storage capacity was sensitive to the precipitation and the evaporation.

Table 4.7:    Statistics describing the root- zone storage capacity estimated using the Nijzink, Wang and DiCaSM methods with observed evaporation (OET) and simulated actual evaporation (SET) for the Cathedral Peak catchment VI.

| | Nijzink | | Wang | | DiCaSM | |
|---|---|---|---|---|---|---|
| | OET | SET | OET | SET | OET | SET |
| Mean (mm) | 8.4 | 7.5 | 6.8 | 6.3 | 8.6 | 7.48 |
| Median (mm) | 7.0 | 5.2 | 5.5 | 4.7 | 8.0 | 6.3 |
| Variance (mm) | 61.3 | 71.8 | 33.2 | 34.7 | 23.0 | 28.7 |
| Range (mm) | 110.5 | 113.6 | 83.0 | 84.7 | 77.7 | 80.7 |
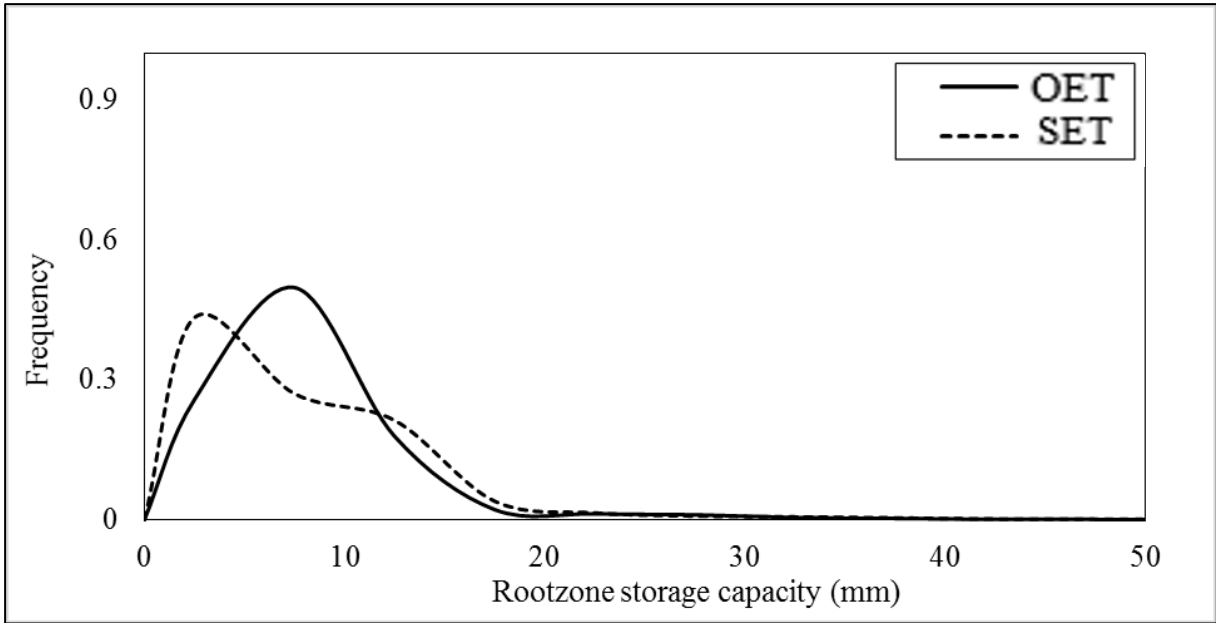
Figure 4.19:    Frequency distribution curve for the calculated root-zone storage capacity using the Nijzink method with observed evaporation (black line) and simulated actual evaporation (black dashed line) for Cathedral Peak Catchment VI over the period July 2014 to August 2018.
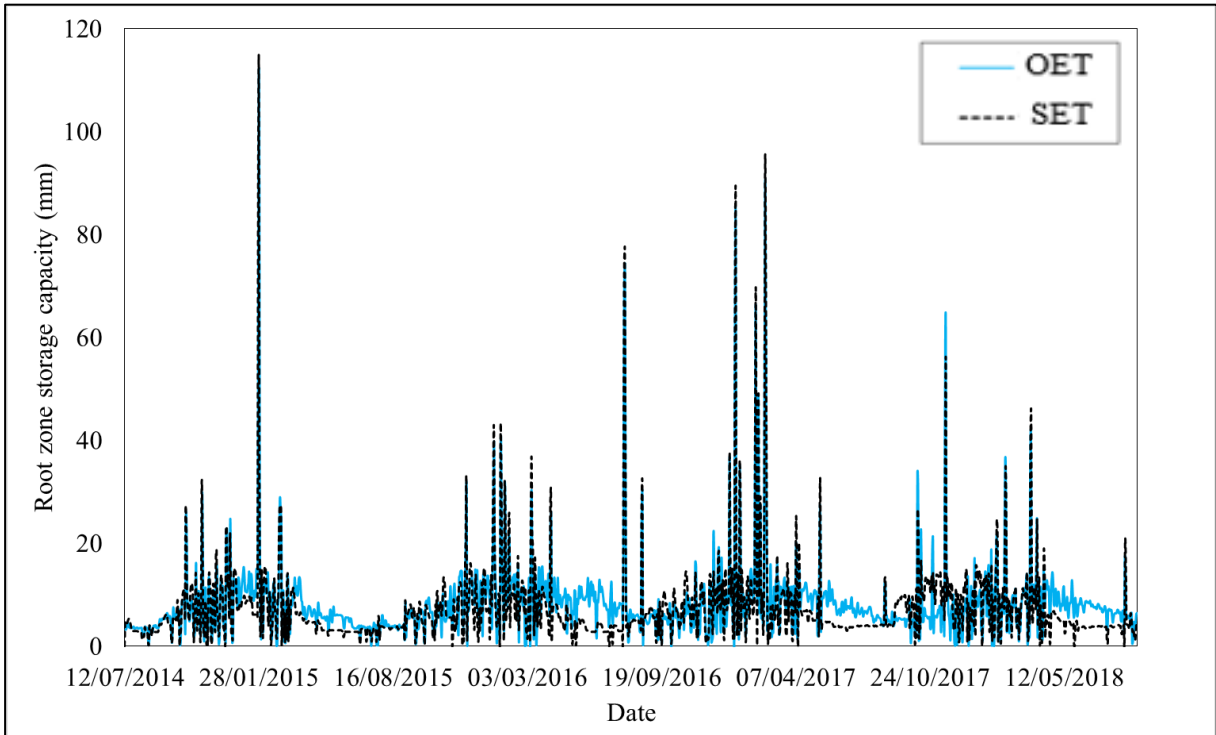


Figure 4.20:    Daily root-zone storage estimated using the Nijzink method with both observed evaporation (blue line) and simulated actual evaporation (black dashed line) for Cathedral Peak Catchment VI from July 2014 to August 2018.

Using the simulated actual evaporation in the Wang method resulted in little difference in the mean root- zone storage capacity, variance or range (Table 4.11 and Figure 4.21). A higher winter root- zone storage using the observed evaporation was seen although it was not as prominent as with the Nijzink method (Figure 4.22). The Wang method was less sensitive to evaporation in the winter than the Nijzink method. In summer the Wang method was sensitive to the precipitation and less so to the evaporation.
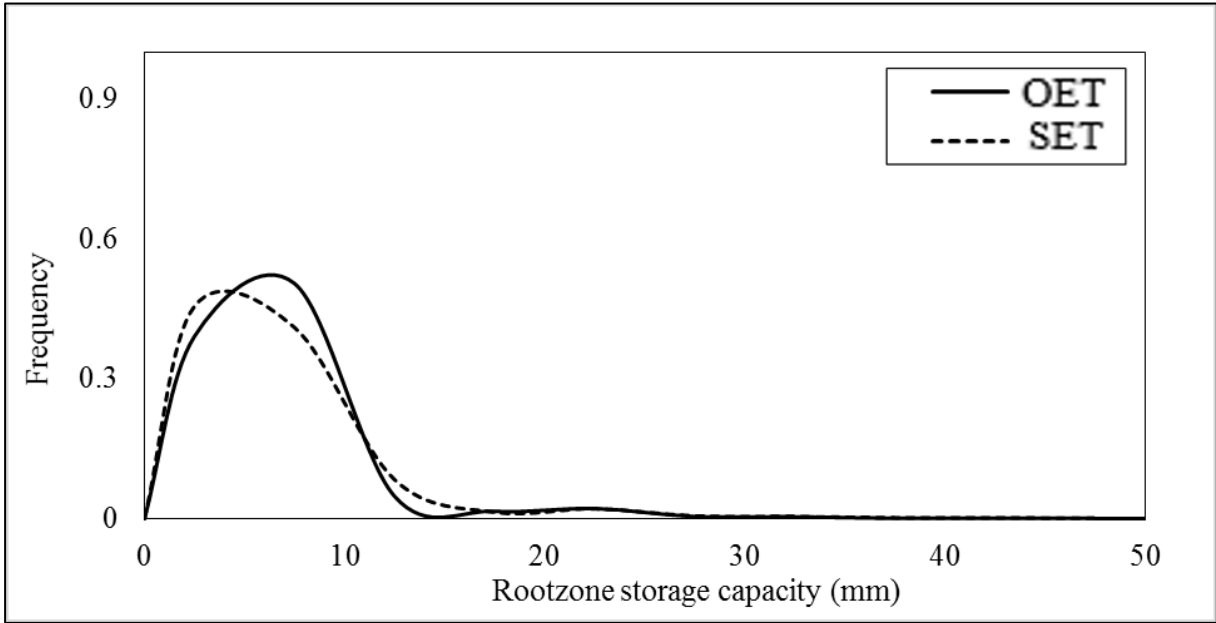


Figure 4.21:   The frequency distribution curve for the calculated root-zone storage capacity using the Wang method with observed evaporation (black line) and simulated actual evaporation (black dashed line) for Cathedral Peak Catchment VI from July 2014 to August 2018
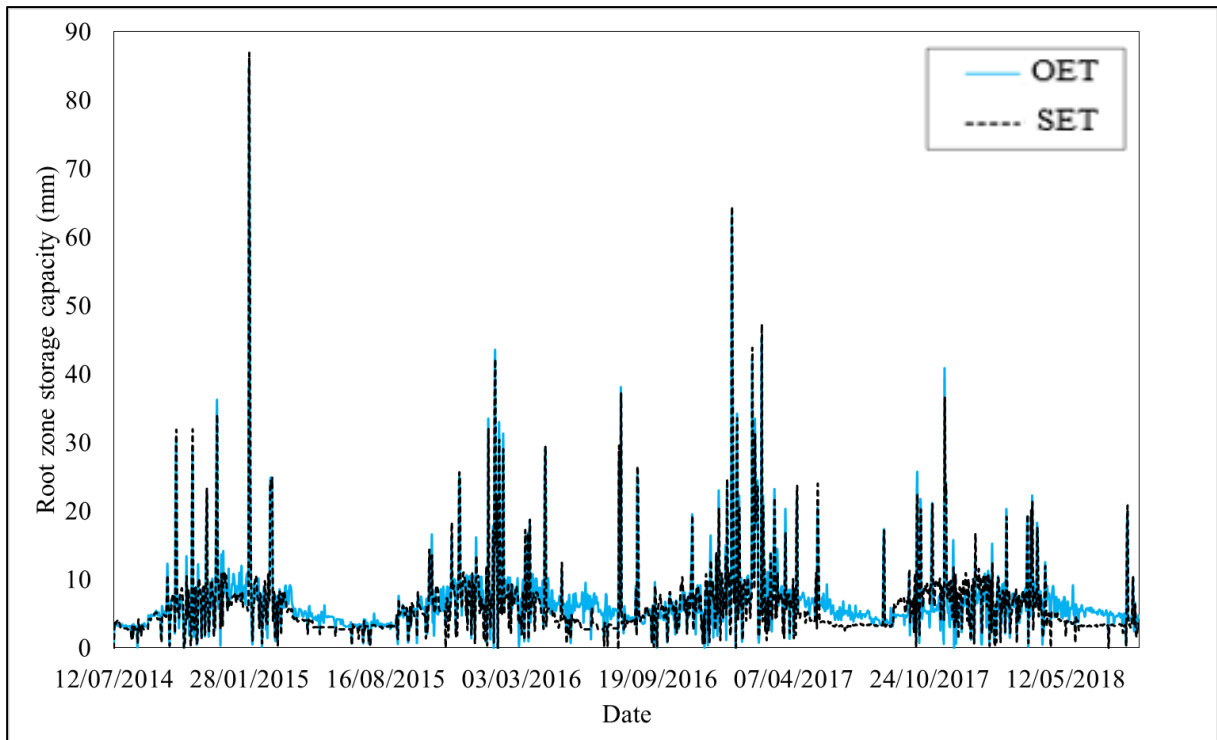
Figure 4.22:    Daily root-zone storage estimated using the Wang method with both observed
                evaporation (blue line) and simulated actual evaporation (black dashed line) at
                Cathedral Peak Catchment VI from July 2014 to August 2018

Using the simulated actual  evaporation in the DiCaSM method decreased the mean root-
zone storage capacity and increased the variance and the range over the time period (Table
4.12 and Figure 4.23). From the summer of 2016, there is a significant lag of the root- zone
storage capacity calculated with the observed evaporation. The lag can be seen throughout
the summer and winter periods suggesting that the DiCaSM method was highly sensitive
to the evaporation and less sensitive to the precipitation. Additionally, the DiCaSM method
did not produce as many sporadic high peaks as Nijzink and Wang methods did, thus
further suggesting less sensitivity to precipitation. Following the calculations and
understanding of the sensitivities of the three root- zone storage capacity methods, it was
necessary to validate the calculated root- zone storage capacities with the observed soil
water measurements.
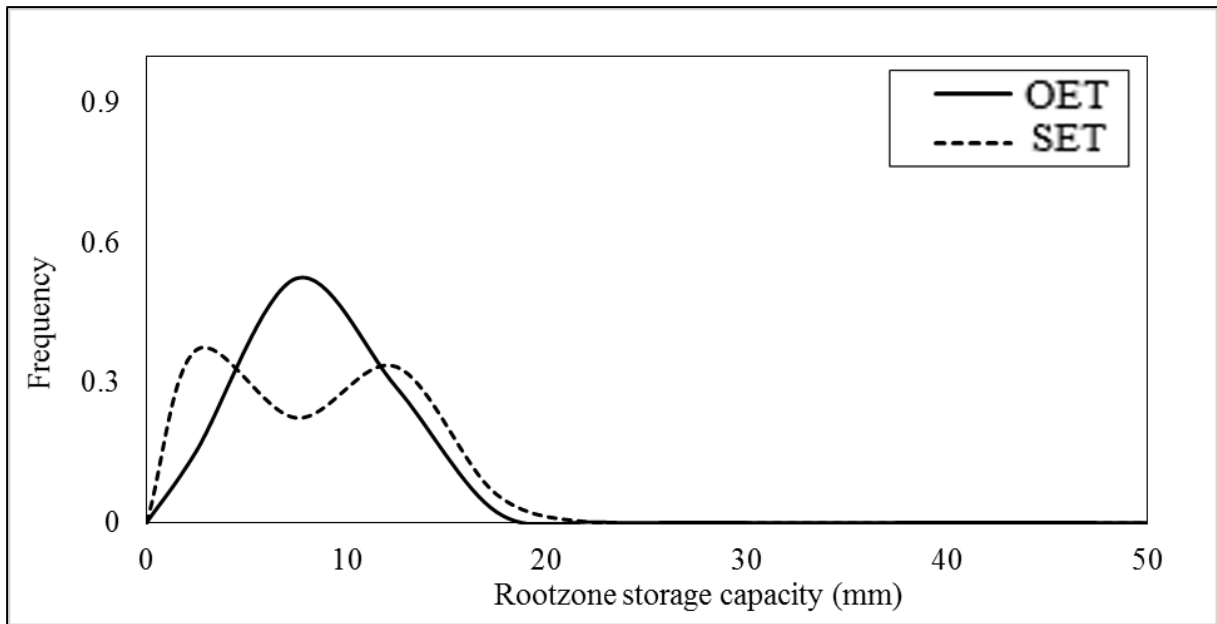
Figure 4.23:    Frequency distribution curve for the calculated root-zone storage capacity using the DiCaSM method with observed evaporation (black line) and simulated actual evaporation (black dashed line) at Cathedral Peak Catchment VI for July 2014 to August 2018.
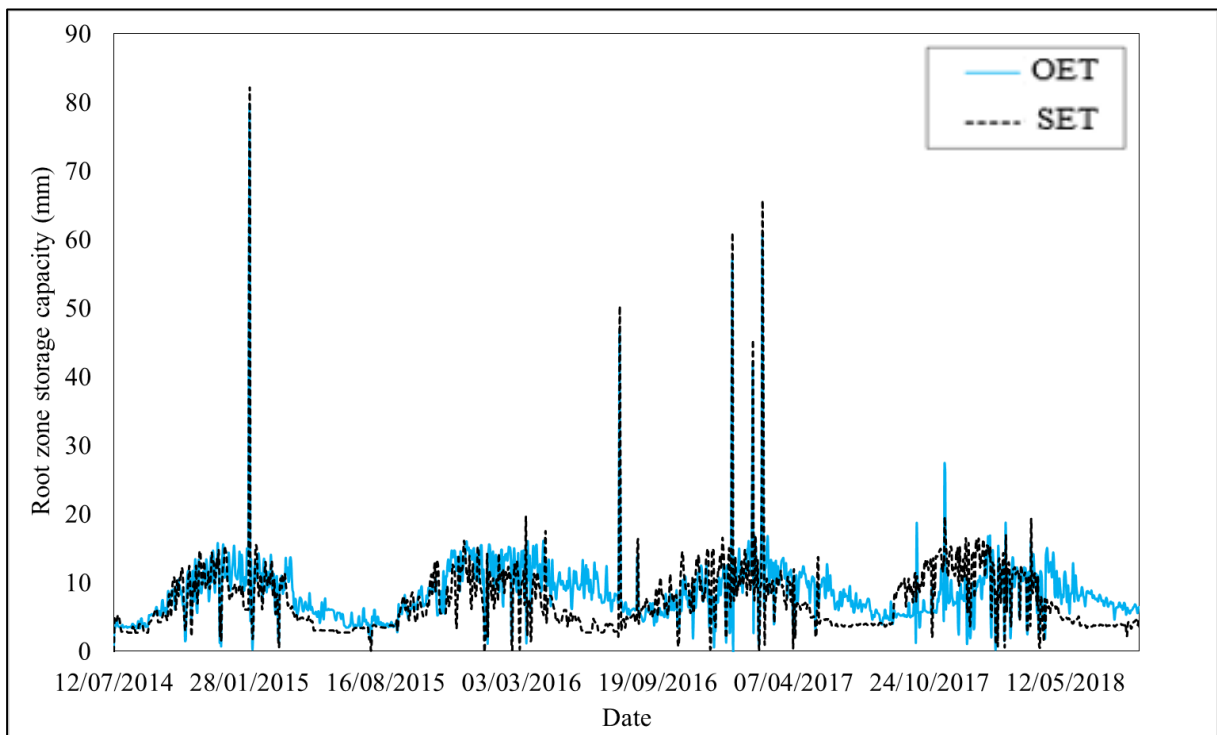


Figure 4.24:    Daily root-zone storage estimated using the DiCaSM method with both the observed evaporation (blue line) and the simulated actual evaporation (black dashed line) for Cathedral Peak Catchment VI from July 2014 to August 2018

## 4.3 Validation of the Root-zone Storage Capacity in Hydrological Modelling

The validation of the calculated root-zone storage capacity was undertaken in both catchments with the modelled simulated soil water. However, validation of the calculated root-zone storage capacity with observed soil water data was only undertaken at Two Streams as there is no soil water data available for Cathedral Peak Catchment VI. The root-zone storage capacity was defined as the water in the root-zone available to the plant and thus the calculated root-zone storage capacities were adjusted using the permanent wilting point for the profile. The observed soil water and the ACRU simulated soil water were produced as a soil water content value (meters per meter). The water content for each horizon was weighted by the depth of the soil horizon to produce a depth of water in millimetres. To account for the soil water throughout the extent of the soil profile the depth of soil water in the A and B horizons were summed.

### 4.3.1 Two Streams Catchment

Across the soil profile, the root- zone storage capacity methods produced better simulation of the soil water than the ACRU model at the Two Streams catchment. The goodness of fit statistics showed a poor simulation for all the root- zone storage capacity methods and the ACRU simulation compared to the observed data (Table 4.8). However, the estimated root-zone storage capacity methods produced better statistics compared to the ACRU simulation. The estimated root- zone storage capacity methods all produce an accurate bias, which indicates that the volume of water within the soil profile was comparable to observed values but the root-zone storage capacities were substantially more reactive to the rainfall compared to the observed data (Figure 4.25). The goodness of fit statistics suggest that the DiCaSM method produced the best simulation of the observed soil water although all three methods produced less variance than the observed data.

.

Table 4.8: Statistics and goodness of fit measures describing the root- zone storage capacity estimated using the Nijzink, Wang and DiCaSM methods and the ACRU simulated soil water at Two Streams.

| | Observed | Simulated | Nijzink | Wang | DiCaSM |
|---|---|---|---|---|---|
| Mean (mm) | 440.69 | 480.97 | 435.77 | 437.75 | 445.80 |
| Median (mm) | 437.87 | 476.81 | 434.23 | 435.23 | 443.86 |
| Range (mm) | 109.50 | 150.58 | 79.47 | 88.53 | 68.34 |
| KGE | - | -0.47 | 0.047 | 0.142 | 0.235 |
| NSE | - | -0.39 | -0.02 | -0.10 | 0.11 |
| Bias (%) | - | 10 | -1.5 | -0.64 | 1.09 |

.
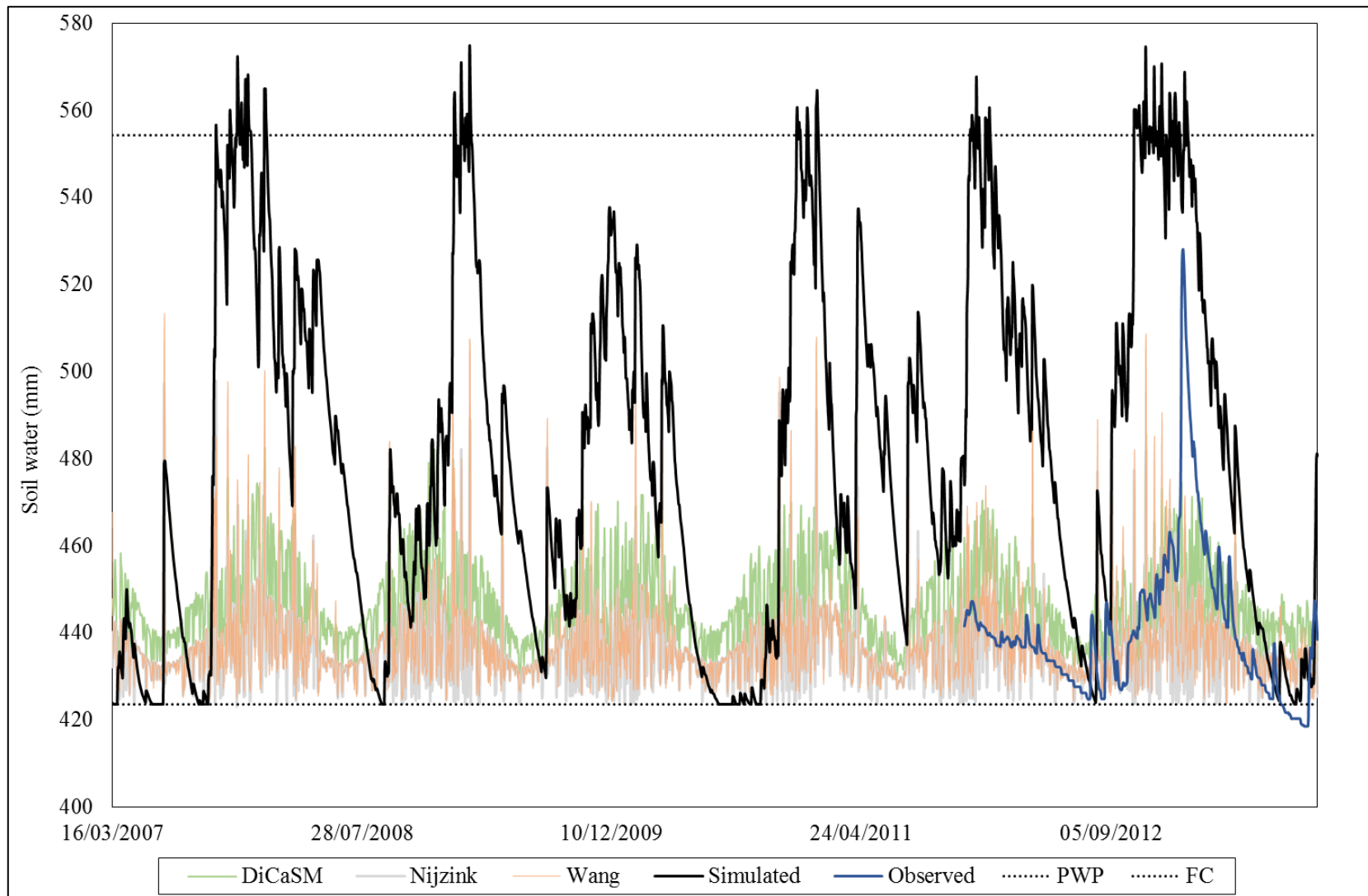
Figure 4.25: Daily estimated root-zone storage capacity using the Nijzink (grey line), Wang (pink line) and the DiCaSM (green line) methods with the observed soil water (blue line) and ACRU simulated soil water (black line) in the soil profile at Two Streams.

### 4.3.2    Cathedral Peak Catchment VI

The calculated root-zone storage capacity was compared to the ACRU simulated soil water at Cathedral Peak Catchment VI over the period of July 2014 until December 2016.  The peaks of the ACRU simulated soil water and root- zone storage capacity estimations coincided seasonally (Figure 4.26). It was difficult to understand the accuracy of the root- zone storage capacities without observed data. However, based on the seasonality and magnitude of the root-zone storage capacity estimation, it could be a promising alternative to detailed soil water modelling.
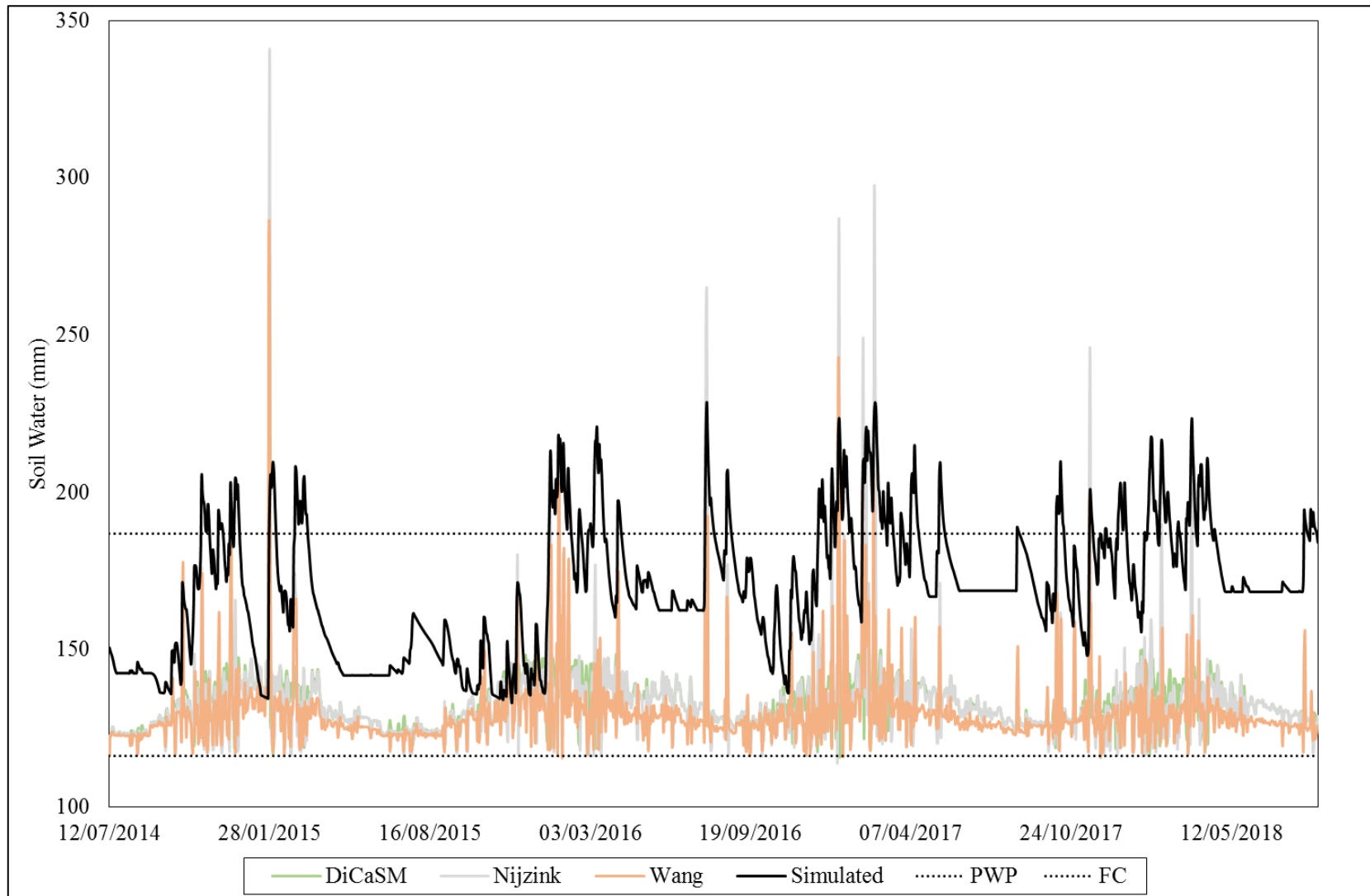
Figure 4.26:    Daily estimated root-zone storage capacity using the Nijzink (grey line), Wang (pink line) and the DiCaSM (green line) methods with the observed soil water (blue line) and ACRU simulated soil water (black line) in the soil profile at Cathedral Peak Catchment VI

# CHAPTER 5: DISCUSSION

The limited calibration of the ACRU model at Two Streams, utilising data commonly available in South Africa, yielded a poor simulation of the streamflow (Table 4.1 and Figure 4.1) and additionally through an independent validation of the actual evaporation (Figure 4.5) and soil water (Figure 4.3) it was found that these were simulated poorly. The model under- simulates the high flows and actual evaporation whilst over- estimating the low flows and soil water. The model is retaining too much water in the soil profile resulting in the magnitude of high flows being reduced and lag time being extended in the summer. Both soil layers store excess soil water in the wet season and dry out in the dry season. The over- estimation of the soil water in B horizon maintains the water available in the intermediate zone (Figure 4.4). The baseflow is generated as a function of water available in the intermediate zone. Baseflow occurs year around which maintains the low flows in the stream through the winter. In reality the soils would retain less water and the baseflow would cease in the winter. The model reduces the transpiration minimum in the winter months as the soil water in the B horizon is at PWP. In reality the trees would continue to transpire through the deep rooting system during the winter. The inaccuracies in the simulations could be occurring for the conceptualisations of the soil profile and baseflow generation in the model.

The limited calibration of the ACRU model at Cathedral Peak Catchment VI, utilising data commonly available in South Africa, yielded a fair simulation of the streamflow (Table 4.1 and Figure 4.2) and additionally through an independent validation of the actual evaporation (Figure 4.6) it was found that it was simulated poorly. The model over- simulates the high flows whilst under- estimating the low flows and actual evaporation. The model does not retain the receding limb of the hydrograph as in reality. Due to the conceptualisation of the soil profiles and rooting structure in the model it was found that there were periods in the winter where the soil water flatlines in the B horizon (Figure 4.26). This is due to all the roots retreating to the A horizon and thus no water can evaporate/transpire from the B horizon and because the soil water is far below DUL it cannot drain to the intermediate zone (The ACRU assumption is that drainage only occurs downwards and then only when the soil is above or some value close to DUL), so it remains stationary at this level until big rains or roots return to the B horizon. The model can only release baseflow through the intermediate zone. If this zone is dry no baseflow will occur. The catchment seems to have a large storage that is released (probably laterally through bank

discharge or shallow groundwater uprising) in the winter but ACRU struggles to simulate this and thus cannot replicate the low flows well. For the Cathedral Peak Catchment VI, the model simulation of the actual evaporation followed a seasonal pattern as the monthly crop coefficients for the grassland repeated consistently through the years. However, the observed evaporation data showed evidence of late April rains resulting in the grass continuing to transpire into winter. This transpiration in April and May was not accounted for when estimating the actual evaporation using the potential evaporation and crop coefficients. It would be recommended to utilise observed evaporation, where available, to account for varying climatic conditions and abnormalities which the inter-annual stationarity of the monthly crop coefficient values does not. However, for most sites in South Africa no observed records of actual evaporation are readily available.

The uncertainty in the conceptualisation of the soils routine within ACRU and the limited availably of soils and rooting data provided an opportunity to investigate the root-zone storage capacity concept. Literature suggests that the root zone storage capacity is independent of the soil depth, the number of horizons in the soil profile and the vegetation rooting depth. Three methods were used to calculate the root-zone storage with both observed and calculated actual evaporation. The variation between the root-zone storages produced using the three different methods with the same input data were significant. These variations increased when using the simulated actual evaporation. The Nijzink and DiCaSM methods produced the highest root-zone storage capacities at both the Two Streams catchment and Cathedral Peak Catchment VI (Table 4.4 and 4.6). The Nijzink method had the greatest variance and was highly responsive to rainfall events (Figure 4.12). The DiCaSM method had the least variance (Figure 4.16). The Nijzink and Wang methods (Figure 4.12 and 4.14) were shown to be sensitive to evaporation in the wet and dry season but more sensitive to the precipitation in the wet season. The Wang method was less sensitive to evaporation in the winter than the Nijzink method. The DiCaSM method was highly sensitive to the evaporation component but did not produce as many high peaks as the Nijzink and Wang methods, thus suggesting less sensitivity to precipitation.

The Nijzink method and the Wang method estimated a mean root- zone storage capacity of approximately 430 mm at Two Streams (Figure 4.25). This is in strong agreement with the work of Nijzink *et al* (2016) in the HJ Andrews catchment under a coniferous canopy

and with Wang- Erlandsson *et al*. (2014) under deciduous forest and less of an agreement with de Boer-Euser *et al*. (2019) where a root-zone storage capacity of approximately 410 mm, 395 mm and 325 mm respectively were estimated. The agreement with the work of Nijzink *et al* (2016) and Wang- Erlandsson *et al*. (2014) proves promising for the potential use of the root-zone storage concept in South Africa as it suggests that the both these methods are capturing the simplified forest hydrological processes, critical in the development of these internationally recognised methods, at Two Streams relatively accurately. The study area of de Boer-Euser *et al*. (2019) was vastly climatically different. Based on the conclusion of Wang-Erlandsson *et al*. (2014) that the vegetation had less effect on the root-zone storage capacity than the variation in climate, this could account for the lower root- zone storage capacity in the de Boer-Euser *et al*. (2019) study.

The Wang method estimated a mean root- zone storage capacity of approximately 130 mm at Cathedral Peak Catchment VI (Figure 4.26). This falls within the range of root- zone storage capacity (100 – 150mm) determined by Wang- Erlandsson *et al*. (2014) for grassland vegetation. The strong correlation of the Wang method at both Two Streams and Cathedral Peak Catchment VI with the results of Wang- Erlandsson *et al*. (2014) highlights the strength of the concept in being independent of vegetation within the catchment. This finding could demonstrate that one method can be utilised for a multiple vegetation types. The results for the three methods are relatively similar and thus it could be said with caution that the three methods could be used under various vegetation types. It would be recommended that additional studies in more climatically, vegetative and spatially diverse catchments are necessary to confirm this finding.

Although soil depth at Cathedral Peak Catchment VI (0.77 m) is substantially shallower than at Two Streams (1.74 m), the mean calculated root-zone storage across the three methods was greater at Cathedral Peak Catchment VI than that at Two Streams. This could suggest that the root-zone storage capacity reflects the catchment climate and vegetative conditions rather than the soil depth. This is consistent with the work of Srinivasan *et al*. (2015) who describes that commercial plantations create unsaturated conditions in the root-zone and therefore reduce the immediate root-zone storage capacity even though the roots may be deeper. The work of Laio

(2006) who found that plants distribute their roots in soil depth-independent fashion to achieve soil moisture uniformity throughout the root-zone. At a local scale, it is likely that root development is not limited to climatic variation alone but also site conditions. However, studies such as Schenk and Jackson (2002) and Feddes *et al*. (2001) found that rooting depths very closely correlated with climatic factors such as MAP and potential evaporation.

The increase in effective rainfall and decrease in actual evaporation of grassland environments could be additional contributing factors. Wang-Erlandsson *et al*. (2014) recorded that the global mean root-zone storage capacity of a grassland ranges between 10 mm greater and 50 mm smaller than a deciduous forest, when using a variety of models and input datasets, and concluded that the vegetation had less effect on the root-zone storage capacity than the variation in climate. Additionally, de Boer-Euser *et al.* (2019) found that vegetation characteristics did not strongly correlate with the patterns of the estimated root-zone storage capacities. In consideration of the studies mentioned above, the difference in root-zone storage capacities at Two Streams and Cathedral Peak Catchment VI could be attributed to varying climate conditions between the two catchments rather than the soil depth or vegetation. The two catchments have a high variance in climatic conditions as well as elevation. Two Streams has an elevation of 1 000 m.a.s.l and a MAP of 964 mm whilst Cathedral Peak Catchment VI has a greater elevation and MAP of 1 952 m.a.s.l and 1 135 mm, respectively. The water balance approach to the root-zone storage estimation assumes a classical water balance approach and a non-leaky catchment for it to be successful along with accurate observed climate data.

At Two Streams the soil water contents estimated using the root-zone storage capacities provided a better simulation of the observed soil water than the ACRU model did. The results from the Two Streams catchment indicate that the calculated root-zone storage capacity could provide a viable alternative method of soil water estimation. The performance of ACRU and the root- zone storage capacity concept were evaluated on a daily timestep. This might not be the most appropriate and representative timestep for assessing soil water simulations as the long term or seasonal fluctuations could be of more significance. The model fit could improve when using a longer timestep as the fluctuations would be less impactful. The calculated root-zone storage capacity is independent of soil and rooting characteristics. Boer-Euser *et al*. (2016) determined that a climate derived root-zone storage capacity better reproduced soil water signatures than the traditional soil parameter derived root-zone storage capacity. Federer *et al.* (2003) stated that when utilising the BROOK90 and WBM models, increasing the number of

soil layers conceptualised in the models and the inclusion of the rooting depth parameters had an insignificant effect on the monthly soil water estimates compared with using a single soil layer without the rooting depth parameter. The study undertaken by Robock *et al.* (1994) showed no evidence that a complicated biosphere model better simulated the soil water compared to a simple bucket- type hydrological model. Similarly, Baroni *et al.* (2010) concluded that the soil water simulated using the simple ALHymus model had a smaller normalised root mean squared error and mean error than the soil water simulated by a more complex SWAP model. In agreement with these studies, Orth *et al.* (2015) determined that two complex models HBV and PREVAH performed better than the simple water balance model (SWBM) in the simulation of streamflow but not for the soil water component. SWBM had approximately 0.8 correlation with the observed soil water compared with an approximate 0.6 for the HBV and PREVAH models. The above-mentioned studies and the root- zone storage validation illustrate that a simple, one layer, climate- driven, water balance soils routine may provide a better representation of the soil water than a highly complex, multi-layered, parameter- based alternative. Overly complex models can suffer from over- parameterization in the simulation of soil water.

Intensive soils data and measured rooting depths were used in the modelling of both catchments however, the soil water results yielded, were poor.  This highlights the possibility that although there are uncertainties with the use of soils data and rooting characteristics in hydrological modelling, the model conceptualisation could be an equally significant source of error. The root-zone storage concept could provide an alternative method to decrease modelling uncertainty where limited soils data and rooting depths are available.

The use of the root- zone storage concept within the ACRU model could limit the model uncertainty and improve the simulations necessary SFRA licensing. The method could allow areas of limited soils and rooting data to be modelled more accurately and the implication of afforestation be fully understood. There is opportunity for the concept to be used with future climate data to provide predictions of the root-zone storage for the future. The improved prediction and modelling opportunity of the effects of afforestation is an important aspect of water resource management and water licensing procedures in South Africa now and in the future. Consistent improvements to the ACRU model and the forest decision support system

would allow this methodology to remain at the forefront of the viable options for estimating the impacts of commercial afforestation.

The study was limited to two small catchments in KwaZulu- Natal, Two Streams and Cathedral Peak Catchment VI, over a period of six and four years, respectively. The soil water data used in the validation was only representative of a two-year period under mature commercial forestry. A more spatially and temporally explicit study would improve the understanding and confidence in the methodology and concept. If observed evaporation is available the model could be run with the use of observed evaporation as well as with the use of maximum and minimum temperature to compare the impact on streamflow and soil water. Additionally both the root- zone storage calculated using the observed and simulated actual evaporation could be compared with the model simulations and observed data in order to full analysis the effects of evaporation and the appropriateness of the methodology to regions with and without observed evaporation. Undertaking a study in a catchment of dynamic land use change would provide a sound basis that the concept is independent of vegetation.  Although this study has its limitations, it's a step forward in the modelling of soil water in South Africa.

# CHAPTER 6: CONCLUSION

The ACRU model produced poor simulations of soil water and evaporation at both the Two Streams catchment and Cathedral Peak Catchment VI. The crop coefficient used in actual evaporation estimation, soil input parameters and a complex soil water budgeting routine were identified as causes of uncertainty in the modelling exercise. The calculated root-zone storage capacity using the Nijzink method at Two Streams and the Wang method at Two Streams and Cathedral Peak Catchment VI closely correlated to the original studies by Nijzink *et al.* (2016) and Wang- Erlandsson *et al.* (2014). This correlation with international studies provides evidence that the root- zone storage concept could be suitable for South African conditions.

The Nijzink and DiCaSM methods produced the deepest root-zone storage capacity whilst Nijzink was the most variable and DiCaSM the least variable in both catchments. Nijzink was sensitive to the actual evaporation in both the dry and wet periods and sensitive to the precipitation in the wet periods. The Wang method was less sensitive to actual evaporation than the Nijzink in the dry period and most sensitive to precipitation in the wet season. DiCaSM was not sensitive to the rainfall in either season but highly sensitive to the actual evaporation year-round.

The root-zone storage concept better reproduced the observed soil water throughout the soil profile at the Two Streams catchment than the ACRU model. The results from Two Streams and Cathedral Peak Catchment VI, suggest that the root-zone storage capacity concept is independent of soil depth and rooting characteristics and thus could provide an effective alternative method of modelling the below- ground processes and decreasing modelling uncertainty in areas with accurate climate data but limited soils and rooting data availability. The use of the root-zone storage capacity in the modelling of areas under, current or future, afforestation could provide more accurate simulations and reduced uncertainty for the purposed of SFRA assessments and water use licensing.

The key findings of this study are
- That although the ACRU model may be simulating the streamflows well, the simulation of the actual evaporation and soil water may be poor.

- Traditional methods of actual evaporation estimation within hydrological models (using the crop coefficient etc) are not always able to capture the variability in timing and magnitude of evaporation.

- The observed data and the modelling results suggest that root zone storage capacity reflects climate conditions rather than soil depth.

- The use of the root-zone storage concept accounts for climatic variations and is independent of vegetation, soils and rooting characteristics.

- the study has shown that a simple climate driven water balance routine could provide a better representation than a complex, layered model.

- Where uncertainty in the soils and rooting characteristics exist, the root-zone storage capacity may provide a more dynamic, robust and accurate conceptualisation of the soil water within the root-zone under South African conditions.

However, the recommendation is that further studies need to be undertaken to investigate the viability of the root-zone storage capacity methods in South Africa under different climates and vegetation types (especially different species of commercial forestry trees), as well as for a longer period of observed data.

# REFERENCES

Abbott MB, Bathurst JC, Cunge JA, O'Connell PE and Rasmussen J. 1986. An introduction to the European Hydrological System—Systeme Hydrologique Europeen"SHE" 1: History and philosophy of a physically-based distributed modelling system. *Journal of Hydrology,* 87(1-2): 45-59.

Acocks JPH. 1988. Veld types of South Africa. *Memoirs of the Botanical Survey of South Africa*, 57: 1–146

Afzal M, Ragab R, Blake J, Black A and McEwen L. 2018. April Impacts of the climatic change on the hydrology of the Eden catchment in Scotland UK using DiCaSM model approach. *EGU General Assembly Conference Abstracts* (Vol 20 p 9346)

Allen RG, Pereira LS, Smith M, Raes D and Wright JL. 2005. FAO-56 dual crop coefficient method for estimating evaporation from soil and application extensions. *Journal of irrigation and drainage engineering*, 131(1): 2-13.

Armstrong AJ and Van Hensbergen HJ. 1996. Impacts of afforestation with pines on assemblages of native biota. *South Africa South African Forestry Journal,* 175(1): 35-42.

Arnold JG, Srinivasan R, Muttiah RS and Williams JR. 1998. Large area hydrologic modeling and assessment part I: model development 1. *Journal of the American Water Resources Association,* 34(1): 73-89

Balestrini R, Lumini E, Borriello R and Bianciotto V. 2015. Plant-soil biota interactions. *Soil Microbiology, Ecology and Biochemisty,* 1(1): 311-338

Baroni G., Facchi A., Gandolfi C., Ortuani B., Horeschi D. and Van Dam J.C., 2010. Uncertainty in the determination of soil hydraulic parameters and its influence on the performance of two hydrological models of different complexity. *Hydrology and Earth System Sciences,* 14(2): 251-270.

Bates HW. 1921. *The naturalist on the river Amazons*. London

Baumgardner MF, Silva LF, Biehl LL and Stoner ER. 1986. Reflectance properties of soils. In *Advances in agronomy* (Vol. 38, pp. 1-44). Academic Press.

Beerling DJ and Berner RA .2005. Feedbacks and the coevolution of plants and atmospheric CO2. *Proceedings of the National Academy of Sciences of the United States of America*, 102: 1302–1305.

Benson ML, Landsberg JJ and Borough CJ. 1992. The Biology of Forest Growth experiment: an introduction. *Forest Ecology and Management,* 52(1-4): 1-16.

Berliner DD. 2009. Systematic Conservation Planning for South Africa's Forest Biome: An assessment of the conservation status of South Africa's forests and recommendations for their conservation. PhD dissertation. University of Cape Town

Beven K. 1989. Changing ideas in hydrology—the case of physically-based models. *Journal of Hydrology,* 105(1-2): 157-172.

Beven K. 1995. Linking parameters across scales: subgrid parameterizations and scale dependent hydrological models. *Hydrological Processes,* 9(5-6): 507-525.

Birkel C, Tetzlaff D, Dunn SM and Soulsby C. 2011. Using time domain and geographic source tracers to conceptualize streamflow generation processes in lumped rainfall-runoff models. *Water Resources Research*, *47*(2): 1-15.

Blasone RS, Vrugt JA, Madsen H, Rosbjerg D, Robinson BA and Zyvoloski GA. 2008. Generalized likelihood uncertainty estimation (GLUE) using adaptive Markov Chain Monte Carlo sampling. *Advances in Water Resources,* 31(4): 630-648.

Bleby TM, Mcelrone AJ and Jackson RB. 2010. Water uptake and hydraulic redistribution across large woody root systems to 20 m depth. *Plant Cell & Environment,* 33(12): 2132-2148.

Brown A.E., Zhang L., McMahon T.A., Western A.W. and Vertessy R.A., 2005. A review of paired catchment studies for determining changes in water yield resulting from alterations in vegetation. *Journal of Hydrology*, 310(1-4): 28-61.

Bugan RD. 2014. Modeling and regulating hydrosalinity dynamics in the Sandspruit river catchment (Western Cape). Doctoral dissertation. Stellenbosch University

Bulcock HH and Jewitt GPW. 2010. Spatial mapping of leaf area index using hyperspectral remote sensing for hydrological applications with a particular focus on canopy interception. *Hydrology and Earth System Sciences,* 14(2): 383-392.

Butts MB, Payne JT, Kristensen M and Madsen H. 2004. An evaluation of the impact of model structure on hydrological modelling uncertainty for streamflow simulation. *Journal of hydrology*, 298(1-4): 242-266.

Campos I., Balbontín C., González-Piqueras J., González-Dugo M.P., Neale C.M. and Calera A., 2016. Combining a water balance model with evapotranspiration measurements to estimate total available soil water in irrigated and rainfed vineyards. *Agricultural Water Management,* 165(1) :141-152.

Castillo VM, Gomez-Plaza A. and Martınez-Mena M. 2003. The role of antecedent soil water content in the runoff response of semiarid catchments: a simulation approach. *Journal of Hydrology*, 284(1-4): 114-130.

Chapagain AK and Hoekstra AY. 2008. The global component of freshwater demand and supply: an assessment of virtual water flows between nations as a result of trade in agricultural and industrial products. *Water international*, 33(1): 19-32.

Chen J and Adams BJ .2006. Integration of artificial neural networks with conceptual models in rainfall-runoff modelling. *Journal of Hydrology,* 318(1-4): 232-249.

Chen J, Xia J, Zhao Z, Hong S, Liu H and Zhao F. 2016. Using the RESC model and diversity indexes to assess the cross-scale water resource vulnerability and spatial heterogeneity in the Huai River Basin, China. *Water,* 8(10): 431.

Childs S. and Hanks R.J., 1975. Model of Soil Salinity Effects on Crop Growth 1. *Soil Science Society of America Journal*, 39(4): 617-622.

Chowdary VM, Desai VR, Gupta M, Jeyaram A and Murthy YVNK. 2012. Runoff simulation using distributed hydrological modeling approach, remote sensing and GIS techniques: A case study from an Indian agricultural watershed. *International Archives of the Photogrammetry, Remote Sensing and Spatial Information Sciences,* 39: B8.

Clinton BD. 2003. Light temperature and soil moisture responses to elevation evergreen understory and small canopy gaps in the southern Appalachians. *Forest Ecology and Management,* 186(1-3): 243-255.

Cloke H, Weisheimer A and Pappenberger F. 2011. Representing uncertainty in land surface hydrology: fully coupled simulations with the ECMWF land surface scheme. *ECMWF Technical Memorandum 729(1):* 1-48. European Centre for Medium Range Weather Forecasts, England.

Clulow AD, Everson CS and Gush MB. 2011. The long-term impact of Acacia mearnsii trees on evaporation streamflow and ground water resources. *Water Research Commission Report TT505/11*, Water Research Commission, Pretoria.

Collins D.B.G. and Bras R.L., 2007. Plant rooting strategies in water-limited ecosystems. *Water Resources Research*, 43(W06407): 1-10.

Coulson K., 2012. *Solar and terrestrial radiation: methods and measurements*. Elsevier, California.

Coppin NJ and Richards IG. 1990. *Use of vegetation in civil engineering* (pp 23-36). London: Construction Industry Research and Information Association.

D'Agostino DR, Trisorio LG, Lamaddalena N and Ragab R. 2010. Assessing the results of scenarios of climate and land use changes on the hydrology of an Italian catchment: modelling study. *Hydrological processes,* 24(19): 2693-2704.

Da Silva E.V., Bouillet J.P., de Moraes Gonçalves J.L., Junior C.H.A., Trivelin P.C.O., Hinsinger P., Jourdan C., Nouvellon Y., Stape J.L. and Laclau J.P., 2011. Functional specialization of Eucalyptus fine roots: contrasting potential uptake rates for nitrogen, potassium and calcium tracers at varying soil depths. *Functional Ecology*, 25(5): 996-1006.

de Boer-Euser T, McMillan HK, Hrachowitz M, Winsemius HC and Savenije HH. 2016. Influence of soil and climate on root-zone storage capacity. *Water Resources Research,* 52(3): 2009-2024.

de Boer-Euser T., Meriö L.J. and Marttila H., 2019. Understanding variability in root zone storage capacity in boreal regions, *Hydrology 10 and Earth System Sciences*, 23 (1): 125–138.

Dee DP, Uppala SM, Simmons AJ, Berrisford P, Poli P, Kobayashi S, Andrae U, Balmaseda MA, Balsamo G, Bauer DP and Bechtold P. 2011. The ERA-Interim reanalysis: Configuration and performance of the data assimilation system. *Quarterly Journal of the royal meteorological society*, 137(656): 553-597.

Dexter AR. 2004. Soil physical quality: Part I. Theory, effects of soil texture, density, and organic matter, and effects on root growth. *Geoderma*, *120*(3-4): 201-214.

D'Odorico P and Rigon R. 2003. Hillslope and channel contributions to the hydrologic response. *Water resources research,* 39(5): 1113- 1122.

Dupuy L, Gregory PJ and Bengough GA. 2010. Root growth models: towards a new generation of continuous approaches. *Journal of Experimental Botany,* 61(8): 2131–2143.

DWAF (2003a) Volume 1: Water Conservation And Water Demand Management - A Planning Framework for Catchment Management Agencies DRAFT Department of Water Affairs and Forestry Pretoria South Africa

DWAF (2003b) A Guideline To The Water Quality Management Component of a Catchment Management Strategy WMQ Series No MS 82 Department of Water Affairs and Forestry Pretoria South Africa

DWAF (2003c) Guidelines for undertaking a water conservation and water demand management situation assessment and development of a business plan within the water services sector. Department of Water Affairs and Forestry, Pretoria, South Africa.

DWAF (2003d) Volume 3: Guidelines for Implementing Water Conservation and Water Demand Management within the Water Services Sector Department of Water Affairs and Forestry, Pretoria, South Africa.

DWAF (Department of Water Affairs & Forestry) (2003) RDM module 1: Introductory Module Pretoria.

DWAF (Department of Water Affairs and Forestry) (1996) South African Water Quality Guidelines (second edition) Volume 1: Domestic Use Pretoria South Africa

Dye P and Versfeld D. 2007. Managing the hydrological impacts of South African plantation forests: An overview Forest Ecology and Management. *Forest Ecology Management*, 251: 121-128.

Eagleson PS. 1982. Ecological optimality in water-limited natural soil-vegetation systems: 1 Theory and hypothesis. *Water Resources Research,* 18(2): 325-340.

Eltahir EA. 1998. A soil moisture–rainfall feedback mechanism: 1 Theory and observations. *Water resources research,* 34(4): 765-776.

Etter S, Strobl B, Seibert J and Meerveld HJ. 2018. Value of uncertain streamflow observations for hydrological modelling. *Hydrology and Earth System Sciences,* 22(10): 5243-5257.

Ewen J., Parkin G. and O'Connell P.E., 2000. SHETRAN: distributed river basin flow and transport modeling system. *Journal of hydrologic engineering*, 5(3): 250-258.

Fan Y., Miguez-Macho G., Jobbágy E.G., Jackson R.B. and Otero-Casal C., 2017. Hydrologic regulation of plant rooting depth. *Proceedings of the National Academy of Sciences*, 114(40): 10572-10577.

FAO Regional Office for Asia, 2006. Rapid Growth of Selected Asian Economies: Lessons and Implications for Agriculture and Food Security. Food & Agriculture Organisation, Bankok.

Federer C.A., Vörösmarty C. and Fekete B., 2003. Sensitivity of annual evaporation to soil and root properties in two models of contrasting complexity. *Journal of Hydrometeorology*, 4(6):1276-1290.

Feddes RA, Hoff H, Bruen M, Dawson T, De Rosnay P, Dirmeyer P, Jackson RB, Kabat, P, Kleidon A, Lilly A and Pitman AJ. 2001. Modeling root water uptake in hydrological and climate models. *Bulletin of the American meteorological society*, *82*(12): 2797-2810

Feki H and Slimani M. 2015. A comparison of three geostatistical procedures for rainfall network optimization. *Proceedings of the International Association of Hydrological Sciences,* 366: 166-167.

Fenicia F, Kavetski D and Savenije HH. 2011. Elements of a flexible approach for conceptual hydrological modeling: 1 Motivation and theoretical development. *Water Resources Research,* 47(11): 1-13.

Gao H, Hrachowitz M, Schymanski SJ, Fenicia F, Sriwongsitanon N and Savenije HHG. 2014. Climate controls how ecosystems size the root-zone storage capacity at catchment scale. *Geophysical Research Letters,* 41(22): 7916-7923.

Gentine P., D'Odorico P., Lintner B.R., Sivandran G. and Salvucci G., 2012. Interdependence of climate, soil, and vegetation as constrained by the Budyko curve. *Geophysical Research Letters*, 39(L19404):1-9.

Gerten D, Schaphoff S and Lucht W. 2007. Potential future changes in water limitations of the terrestrial biosphere. *Climatic Change,* 80(3-4): 277-299.

Gimbel K.F., Felsmann K., Baudis M., Puhlmann H., Gessler A., Bruelheide H., Kayler Z.E., Ellerbrock R.H., Ulrich A., Welk E. and Weiler M., 2015. Drought in forest understory ecosystems-a novel rainfall reduction experiment. *Biogeosciences*, 12(4): 961-975.

Govender M and Everson CS. 2005. Modelling streamflow from two small South African experimental catchments using the SWAT model. *Hydrological Process,* 19: 683-692.

Graeff T, Zehe E, Blume T, Francke T and Schröder B. 2012. Predicting event response in a nested catchment with generalized linear models and a distributed watershed model. *Hydrological Processes,* 26(24): 3749-3769.

Greenwood A, Benyon RG and Lane P. 2011. A method for assessing the hydrological impact of afforestation using regional mean annual data and empirical rainfall–runoff curves. *Journal of Hydrology,* 411: 101016.

Greiner L, Keller A, Grêt-Regamey A and Papritz A. 2017. Soil function assessment: review of methods for quantifying the contributions of soils to ecosystem services. *Land use policy,* 69: 224-237.

Gu J., Zheng X., Wang Y., Ding W., Zhu B., Chen X., Wang Y., Zhao Z., Shi Y. and Zhu J., 2007. Regulatory effects of soil properties on background N 2 O emissions from agricultural soils in China. *Plant and Soil*, 295(1-2): 53-65.

Gush MB, Scott DF, Jewitt GPW, Schulze RE ,Hallowes LA and Görgens AHM. 2002. A new approach to modelling streamflow reductions resulting from commercial afforestation in South Africa. *The Southern African Forestry Journal,* 196(1): 27-36.

Hargreaves G.H. and Samani Z.A., 1985. Reference crop evapotranspiration from temperature. Applied engineering in agriculture, 1(2): 96-99.

Hill T.R., 1996. Description, classification and ordination of the dominant vegetation communities, Cathedral Peak, KwaZulu-Natal Drakensberg. *South African Journal of Botany*, 62(5): 263-269.

Hudak AT and Wessman CA. 1998. Textural analysis of historical aerial photography to characterize woody plant encroachment in South African savannah. *Remote sensing of environment,* 66(3): 317-330.

Hutson JL and Cass A. 1987. A retentivity function for use in soil–water simulation models. *Journal of Soil Science,* 38(1): 105-113.

Ibrahim MM and Aliyu J. 2016. Comparison of Methods for Saturated Hydraulic Conductivity Determination: Field Laboratory and Empirical Measurements (A Pre-view). *British Journal of Applied Science & Technology,* 15(3): 1-8.

Djaman K., Irmak S. and Futakuchi K., 2016. Daily reference evapotranspiration estimation under limited data in Eastern Africa. *Journal of Irrigation and Drainage Engineering,* 143(4): 601- 605.

Islam Z .2011. A review on physically based hydrologic modelling. PhD dissertation. University of Alberta

Jajarmizadeh M, Harun S and Salarpour M. 2012. A review on theoretical consideration and types of models in hydrology. *Journal of Environmental Science and Technolog*y, 5(5) 249-261.

Jewitt G. 2002. Can integrated water resources management sustain the provision of ecosystem goods and services? *Physics and Chemistry of the Earth Parts A/B/C,* 27(11-22): 887-895.

Jewitt G and Schulze RE. 1999. Verification of the ACRU model for forest hydrology applications. *Water SA*, 25: 483-489.

Jung JKHM and McCouch SRM. 2013. Getting to the roots of it: genetic and hormonal control of root architecture. *Frontiers in plant science,* 4(1):  1-32.

Kleidon A., 2004. Beyond Gaia: Thermodynamics of life and Earth system functioning. *Climatic Change*, 66(3): 271-319.

Kleidon A. and Heimann M., 1998. A method of determining rooting depth from a terrestrial biosphere model and its impacts on the global water and carbon cycle. *Global Change Biology*, 4(3): 275-286.

Koehler B, Corre MD, Veldkamp E, Wullaert H. and Wright SJ. 2009. Immediate and long-term nitrogen oxide emissions from tropical forest soils exposed to elevated nitrogen input. *Global Change Biology*, 15(8): 2049-2066.

Kuczera G, Kavetski D, Franks S and Thyer M. 2006. Towards a Bayesian total error analysis of conceptual rainfall-runoff models: Characterising model error using storm-dependent parameters. *Journal of Hydrology,* 331(1-2): 161-177.

Kuenene BT, Van Huyssteen CW and Hensley M. 2009. September Soil water saturation in the Cathedral Peak VI catchment KwaZulu-Natal. *South African Journal of Geology*, 114 (3): 525-534.

Kumar CP. 1977. Estimation of Natural Ground Water Recharge. *ISH Journal of Hydraulic Engineering,* 3(1): 61-74.

Kunz R.P., Mengistu M.G., Steyn J.M., Doidge I.A., Gush M.B., du Toit E.S., Davis N.S., Jewitt G.P.W. and Everson C.S., 2015. *Assessment of Biofuel Feedstock Production in South Africa: Synthesis Report on Estimating Water Use Efficiency of Biofuel Crops.* Water Research Commission, South Africa.

Laio F, Porporato A, Ridolfi L and Rodriguez-Iturbe I. 2001. Plants in water-controlled ecosystems: active role in hydrologic processes and response to water stress: II Probabilistic soil moisture dynamics. *Advances in Water Resources,* 24(7): 707-723.

Laio F. 2006. A vertically extended stochastic model of soil moisture in the root zone. *Water Resources Research*, 42(2): 1-10.

Lawrence P.J. and Chase T.N., 2009. Climate impacts of making evapotranspiration in the Community Land Model (CLM3) consistent with the Simple Biosphere Model (SiB). *Journal of Hydrometeorology*, 10(2): 374-394.

Legates DR ,Mahmood R, Levia DF, DeLiberty TL, Quiring SM, Houser C and Nelson FE. 2011. Soil moisture: A central and unifying theme in physical geography. *Progress in Physical Geography,* 35(1): 65-86.

Legesse D, Vallet-Coulomb C and Gasse F. 2003. Hydrological response of a catchment to climate and land use changes in Tropical Africa: case study South Central Ethiopia. *Journal of Hydrology,* 275(1-2): 67-85.

Li H., Zhang Y., Vaze J. and Wang B., 2012. Separating effects of vegetation change and climate variability using hydrological modelling and sensitivity-based approaches. Journal of Hydrology, 420 (1): 403-418.

Liang X. 1994. A Two-Layer Variable Infiltration Capacity Land Surface Representation for General Circulation Models. *University of Washington: Water Resources Series*, 140(1): 1-208.

Lin H. 2012. *Hydropedology: Synergistic integration of soil science and hydrology*. Elsevier Academic Press. United Kingdom. 3-40.

Linacre E.T., 1994. Estimating US Class A pan evaporation from few climate data. *Water International*, 19(1): 5-14.

Lindström G, Johansson B, Persson M, Gardelin M and Bergström S. 1997. Development and test of the distributed HBV-96 hydrological model. *Journal of Hydrology,* 201(1-4): 272-288.

Liu Y, Pereira LS and Fernando RM. 2006. Fluxes through the bottom boundary of the root-zone in silty soils: parametric approaches to estimate groundwater contribution and percolation. *Agricultural Water Management,* 84(1-2): 27-40.

Lobet G, Couvreur V, Meunier F, Javaux M and Draye X. 2014. Plant water uptake in drying soils. *Plant physiology,* 164(4): 1619-1627.

Longley PA, Goodchild MF, Maguire DJ and Rhind DW. 2005. GIS. *Teoria ipraktyka. Wydawnictwo naukowe PWN, Warszawa*, 164-182.

Maeght J-L, Rewald B. and Pierret A. 2013. How to study deep roots—and why it matters. *Frontiers in plant science*, 13(*4)*: 299- 313.

Mahe G, Paturel JE, Servat E, Conway D and Dezetter A. 2005. The impact of land use change on soil water holding capacity and river flow modelling in the Nakambe River Burkina-Faso. *Journal of Hydrology,* 300(1-4): 33-43.

Malan GJ. 2016. Investigating the suitability of land type information for hydrological modelling in the mountain regions of Hessequa South Africa. Doctoral dissertation. Stellenbosch University.

Manus C, Anquetin S, Braud I, Vandervaere JP, Creutin JD, Viallet P. and Gaume E. 2009. A modeling approach to assess the hydrological response of small mediterranean catchments to the variability of soil characteristics in a context of extreme events. *Hydrology and Earth System Sciences Discussions*, 13(2): 2687–2725.

Mao G and Liu J. 2019. A hydrological model for root zone water storage simulation on a global scale. Geoscientific Model Development Discussions (under review). 1-32.

Martínez-Fernández J. and Ceballos A. 2005. Mean soil moisture estimation using temporal stability analysis. *Journal of Hydrology*, *312*(1-4): 28-38.

McDonnell JJ, Sivapalan M, Vaché K, Dunn S, Grant G, Haggerty R, Hinz C, Hooper R, Kirchner J, Roderick ML and Selker J. 2007. Moving beyond heterogeneity and process complexity: A new vision for watershed hydrology. *Water Resources Research,* 43(W07301): 1-6.

McMahon T.A., Peel M.C., Lowe L., Srikanthan R. and McVicar T.R., 2013. Estimating actual, potential, reference crop and pan evaporation using standard meteorological data: a pragmatic synthesis. *Hydrology and Earth System Sciences*, 17(4): 1331-1363.

McMurtrie RE, Comins HN, Kirschbaum MUF and Wang YP. 1992. Modifying existing forest growth models to take account of effects of elevated $CO_2$. *Australian Journal of Botany,* 40(5): 657-677.

McNamara MA. 2018. Determination of below-ground vegetation and water use model parameters for a revised South African hydrological baseline land cover. MSc dissertation. University of KwaZulu-Natal, South Africa.

Meigh, J. R., McKenzie, A. A. & Sene, K. J. (1999) A grid-based approach to water scarcity estimates for eastern and southern Africa. *Water Resources Management.* 13(1): 85–115.

Milly PCD. 1994. Climate soil water storage and the average annual water balance. *Water Resources Research,* 30(7): 2143-2156.

Montanari A and Koutsoyiannis D. 2014. Modeling and mitigating natural hazards: Stationarity is immortal! *Water Resources Research,* 50(12): 9748-9756.

Montenegro A and Ragab R. 2010. Hydrological response of a Brazilian semi-arid catchment to different land use and climate change scenarios: a modelling study. *Hydrological Processes,* 24(19): 2705-2723.

Montenegro S and Ragab R. 2012. Impact of possible climate and land use changes in the semi arid regions: A case study from North Eastern Brazil. *Journal of Hydrology,* 434: 55-68.

Morris F, Toucher MW, Clulow A, Kusangaya S, Morris C and Bulcock H. 2016. Improving the understanding of rainfall distribution and characterisation in the Cathedral Peak catchments using a geo-statistical technique. *Water SA,* 42(4): 684-693.

Nauman TW and Thompson JA. 2014. Semi-automated disaggregation of conventional soil maps using knowledge driven data mining and classification trees. *Geoderma*, *213*: 385-399

Neitsch SL, Arnold JG, Kiniry JR and Williams JR. 2011. *Soil and water assessment tool theoretical documentation version 2009.* Neitsch SL, Arnold JG, Kiniry JR and Williams JR. 2011. *Soil and water assessment tool theoretical documentation version 2009.* Texas Water Resources Institute, United States of America.

Nijzink R, Hutton C, Pechlivanidis I, Capell R, Arheimer B, Freer J, Han D, Wagener T, McGuire K, Savenije H and Hrachowitz M. 2016. The evolution of root-zone moisture capacities after deforestation: a step towards hydrological predictions under change? *Hydrology and Earth System Sciences,* 20(12): 4775-4799.

Orth R., Staudinger M., Seneviratne S.I., Seibert J. and Zappa M., 2015. Does model performance improve with complexity? A case study with three hydrological models. *Journal of Hydrology*, 523(1): 147-159.

Nänni UW. 1970a. Trees water and perspective. *South African Forestry Journal*, 75(1): 9-17.

Nänni UW. 1970b. The effect of afforestation on streamflow at Cathedral Peak: report no 1. *South African Forestry Journal,* 74(1): 6-12.

Pappenberger F and Beven KJ. 2006. Ignorance is bliss: Or seven reasons not to use uncertainty analysis. *Water resources research*, *42*(W05302): 1-8.

Parker DC, Manson SM, Janssen MA, Hoffmann MJ and Deadman P. 2003. Multi-agent systems for the simulation of land-use and land-cover change: a review. *Annals of the association of American Geographers*, 93(2): 314-337.

Paterson G, Turner D, Wiese L, Van Zijl G, Clarke C and Van Tol J. 2015. Spatial soil information in South Africa: Situational analysis limitations and challenges. *South African Journal of Science,* 111(5-6): 1-7.

Pechlivanidis IG, Jackson BM, McIntyre NR and Wheater HS. 2011. Catchment scale hydrological modelling: a review of model types, calibration approaches and uncertainty analysis methods in the context of recent developments in technology and applications. *Global NEST journal*, 13(3): 193-214.

Phogat V, Šimunek J, Skewes MA, Cox JW and McCarthy MG. 2016. Improving the estimation of evaporation by the FAO-56 dual crop coefficient approach under subsurface drip irrigation. *Agricultural water management,* 178: 189-200.

Pierret A, Maeght JL, Clément C, Montoroi JP, Hartmann C and Gonkhamdee S. 2016. Understanding deep roots and their functions in ecosystems: an advocacy for more unconventional research. *Annals of botany,* 118(4): 621–635.

Pike A. and Schulze R.E., 1995. AUTOSOIL Version 3: A soils decision support system for South African soils. Department of Agricultural Engineering, University of Natal, Pietermaritzburg.

Pluntke T, Pavlik D and Bernhofer C. 2014. Reducing uncertainty in hydrological modelling in a data sparse region. *Environmental Earth Sciences*, 72(12): 4801-4816.

Quinn PFBJ, Beven K, Chevallier P and Planchon O. 1991. The prediction of hillslope flow paths for distributed hydrological modelling using digital terrain models. *Hydrological processes,* 5(1): 59-79.

Quinton J.N., Govers G., Van Oost K. and Bardgett R.D., 2010. The impact of agricultural soil erosion on biogeochemical cycling. *Nature Geoscience*, 3(5): 311.

Ragab R., Bromley J., Dörflinger G. and Katsikides S., 2010. IHMS—Integrated Hydrological Modelling System. Part 2. Application of linked unsaturated, DiCaSM and saturated

zone, MODFLOW models on Kouris and Akrotiri catchments in Cyprus. *Hydrological processes*, 24(19): 2681-2692.

Ragab R. 2012. Challenges and issues on measuring modelling and managing the water resources under changing climate and land use. *Integrated Water Resources Management in the Mediterranean Region,* 1(1): 91-107.

Refsgaard J.C., Abbott M.B. (1990) The Role of Distributed Hydrological Modelling in Water Resources Management. In: Abbott M.B., Refsgaard J.C. (eds) Distributed Hydrological Modelling. Water Science and Technology Library, 22. Springer, Dordrecht

Refsgaard JC and Storm B. 1990. Construction calibration and validation of hydrological models. In: Abbott M.B., Refsgaard J.C. (eds) Distributed Hydrological Modelling. Water Science and Technology Library, 22. Springer, Dordrecht

Reynolds C.A., Jackson T.J. and Rawls W.J., 2000. Estimating soil water-holding capacities by linking the Food and Agriculture Organization soil map of the world with global pedon databases and continuous pedotransfer functions. *Water Resources Research*, 36(12): 3653-3662.

Richardson AD, Duigan SP and Berlyn GP. 2002. An evaluation of noninvasive methods to estimate foliar chlorophyll content. *New Phytologist*, 153(1): 185-194.

Richter D and Markewitz D. 1995. How Deep Is the Soil? *BioScience,* 45: 600-609.

Rodríguez-Iturbe I and Porporato A. 2007. *Ecohydrology of water-controlled ecosystems: soil moisture and plant dynamics.* Cambridge University Press, New York, pp 10-12.

Robock A., Vinnikov K.Y., Schlosser C.A., Speranskaya N.A. and Xue Y., 1995. Use of midlatitude soil moisture and meteorological observations to validate soil moisture simulations with biosphere and bucket models. *Journal of Climate*, 8(1): 15-35.

Rochester R.E.L., 2010. Uncertainty in hydrological modelling: a case study in the Tern catchment, Shropshire, UK. Doctoral dissertation, University College London, London.

Roderick M.L., Hobbins, M.T. and Farquhar, G.D., 2009. Pan evaporation trends and the terrestrial water balance. II. *Energy balance and interpretation. Geography Compass*, 3(2): 761-780.

Rotstayn L.D., Roderick, M.L. and Farquhar, G.D., 2006. A simple pan-evaporation model for analysis of climate simulations: Evaluation over Australia. Geophysical Research Letters, 33(L17715): 1-5.

Rowe TJ. 2015. Development and assessment of rules to parameterise the ACRU model for design flood estimation. Masters dissertation. University of KwaZulu-Natal, South Africa.

Royappen M. 2002. Towards improved parameter estimation in streamflow predictions using the ACRU model. Doctoral dissertation. University of KwaZulu-Natal, South Africa.

Sala OE Lauenroth WK and Parton WJ. 1992. Long-term soil water dynamics in the shortgrass steppe. *Ecology*, *73*(4): 1175-1181.

Salvucci GD and Entekhabi D. 1994. Equivalent steady soil moisture profile and the time compression approximation in water balance modeling. *Water Resources Research*, *30*(10): 2737-2749.

Salvucci GD. 2001. Estimating the moisture dependence of root-zone water loss using conditionally averaged precipitation. *Water Resources Research,* 37(5): 1357-1365.

Saxton KE and Rawls WJ. 2006. Soil water characteristic estimates by texture and organic matter for hydrologic solutions. *Soil science society of America Journal,* 70(5): 1569-1578.

Schaake JC, Koren VI, Duan QY, Mitchell K. and Chen F. 1996. Simple water balance model for estimating runoff at different spatial and temporal scales. *Journal of Geophysical Research: Atmospheres*, 101(D3): 7461-7475.

Schenk HJ and Jackson RB. 2002. Rooting depths lateral root spreads and below-ground/above-ground allometries of plants in water-limited ecosystems. *Journal of Ecology,* 90(3): 480-494.

Schmidt E.J., Schulze R.E. and Dent M., 1987. SCS-based design runoff. *ACRU Report 24*. University of Natal, Pietermaritzburg, South Africa.

Schulze RE. 1979. Soil loss in the key area of the Drakensberg. *Agricultural Engineering in South Africa*, 13: 22–23.

Schulze RE, Hutson JL and Cass A. 1985. Hydrological characteristics and properties of soils in Southern Africa 2: Soil water retention models. *Water SA,* 11(3): 129-136.

Schulze RE. 1995. Hydrology and agrohydrology: A text to accompany the ACRU 300 agrohydrological modelling system. *Water Research Commission Report TT69/95*, Water Research Commission, Pretoria.

Schulze RE and Pike A. 2004. Development and Evaluation of an Installed Hydrological Modelling System. *Water Research Commission Report 1155/1*, Water Research Commission, Pretoria.

Schulze R and Horan M. 2005. *AUTOSOILS*. School of Bioresources Engineering and Environmental Hydrology University of KwaZulu-Natal, Pietermaritzburg, South Africa.

Schulze R., 2012, October. Mapping hydrological soil groups over South Africa for use with the SCS–SA design hydrograph technique: methodology and results. *In Sixteenth SANCIAHS National Hydrology Symposium*. pp. 1-3.

Schwinning S., 2010. The ecohydrology of roots in rocks. Ecohydrology: Ecosystems, Land and Water Process Interactions, *Ecohydrogeomorphology*, 3(2): 238-245.

Schymanski SJ, Sivapalan M, Roderick ML, Beringer J and Hutley LB. 2008. An optimality-based model of the coupled soil moisture and root dynamics. H*ydrology and earth system sciences,* 12(3): 913-932.

Scott DF and Gush MB. 2017. *Forest management and water in the Republic of South Africa*. United Nations Educational Scientific and Cultural Organization (UNESCO) Open Access Repository, Available at: http://www.unesco.org/open-access/terms-use-ccbysa-en. [Accessed 19 May 2018].

Scott DF and Lesch W. 1997. Streamflow responses to afforestation with *Eucalyptus grandis* and *Pinus patula* and to felling in the Mokobulaan experimental catchments South Africa. *Journal of Hydrology,* 199(3-4): 360-377.

Scott DF. 1999. Managing riparian zone vegetation to sustain streamflow: results of paired catchment experiments in South Africa. *Canadian Journal of Forest Research,* 29(7): 1149-1157.

Scott D.F., 2000. Soil wettability in forested catchments in South Africa; as measured by different methods and as affected by vegetation cover and soil characteristics. *Journal of Hydrology*, 231(1): 87-104.

Smithers J and Schulze R. 1995. ACRU Agrohydrological modelling system. *Water Research Commission Report TT70/95*, Water Research Commission, Pretoria.

Srinivasan, V., Thompson, S., Madhyastha, K., Penny, G., Jeremiah, K. and Lele, S., 2015. Why is the Arkavathy River drying? A multiple-hypothesis approach in a data-scarce region. *Hydrology and Earth System Sciences*, 19(4): 1905-1917.

Taha H, Akbari H, Rosenfeld A. and Huang J. 1988. Residential cooling loads and the urban heat island—the effects of albedo. *Building and environment*, *23*(4): 271-283.

Tewari DD. 2001. Is commercial forestry sustainable in South Africa? The changing institutional and policy needs. *Forest Policy and Economics,* 2(3-4): 333-353.

Thompson J.A., Roecker S., Grunwald S., Owens P.R., 2012. Digital Soil Mapping: Interactions with and Applications for Hydropedology. In: Lin, H. (Ed.), *Hydropedology: Synergistic Integration of Soil Science and Hydrology*. Academic Press, Elsevier B.V., pp. 665–709.

Troch PA, Martinez GF, Pauwels VR, Durcik M, Sivapalan M, Harman C, Brooks PD, Gupta H and Huxman T. 2009. Climate and vegetation water use efficiency at catchment scales Hydrological Processes. *An International Journal,* 23(16): 2409-2414.

Tron S, Bodner G, Laio F, Ridolfi L and Leitner D. 2015. Can diversity in root architecture explain plant water use efficiency? A modeling study. *Ecological modelling,* 312: 200-210.

Van Genuchten MT. 1980. A closed-form equation for predicting the hydraulic conductivity of unsaturated soils 1. *Soil science society of America journal*, 44(5): 892-898.

Van Tol JJ, Le Roux PAL, Lorentz SA. and Hensley M. 2013. Hydropedological classification of South African hillslopes. *Vadose Zone Journal*, 12(4): DOI: vzj2013.01.0007.

Van Zijl GM, Le Roux PA and Turner DP. 2013. Disaggregation of land types using terrain analysis expert knowledge and GIS methods. *South African Journal of Plant and Soil,* 30(3): 123-129.

Van der Zel DW. 1982. *The afforestation permit system*. Directorate of Forestry, South Africa.

Van der Zel DW. 1995. Accomplishments and dynamics of the South African afforestation permit system. *South African Forestry Journal,* 172(1): 49-58

Vereecken H, Schnepf A, Hopmans J, Javaux M, Or D, Roose T, Vanderborght J, Young M, Amelung W, Aitkenhead M, Allison S, Assouline S, Baveye P, Berli M, Brüggemann N, Finke P, Flury M, Gaiser T, Govers G and Young I. 2016. Modeling Soil Processes: Review Key Challenges and New Perspectives. *Vadose Zone Journal,* 15: 1-57

Vietz, F.G., 1972. Water deficits and nutrient availability. *Water deficits and plant growth*, 3(1): 217-239.

von Stackelberg N, Chescheir GM, Skaggs RW, Amatya DM. 2007. Simulation of the Hydrologic Effects of Afforestation in the Tacuarembó River Basin Uruguay. *Transactions of the ASABE. 50*(2):455-468.

Vrettas MD and Fung IY. 2017. Sensitivity of transpiration to subsurface properties: Exploration with a 1-D model. *Journal of Advances in Modeling Earth Systems,* 9(2): 1030-1045.

Vrugt JA, Ter Braak CJ, Clark MP, Hyman JM and Robinson BA. 2008. Treatment of input uncertainty in hydrologic modeling: Doing hydrology backward with Markov chain Monte Carlo simulation. *Water Resources Research,* 44(W00B09): 1-15.

Wagener T, McIntyre N, Lees MJ, Wheater HS, and Gupta HV. 2003 Towards reduced uncertainty in conceptual rainfall-runoff modelling: Dynamic identifiability analysis. *Hydrological Processes* 17(2) 455-476

Wagener T, Sivapalan M, Troch P and Woods R. 2007. Catchment classification and hydrologic similarity. *Geography compass,* 1(4): 901-931.

Wallner M., Haberlandt U. and Dietrich J. 2012. Evaluation of different calibration strategies for large scale continuous hydrological modelling. *Advances in Geosciences,* 31: 67-74.

Wang-Erlandsson L., Van Der Ent R.J., Gordon L.J. and Savenije H.H.G., 2014. Contrasting roles of interception and transpiration in the hydrological cycle–Part 1: Temporal characteristics over land. *Earth System Dynamics*, 5(2): 441-469.

Wang-Erlandsson L, Bastiaanssen WG, Gao H, Jagermeyr J, Senay GB, Van Dijk A, Guerschman JP, Keys PW, Gordon LJ and Savenije HH. 2016. Global root-zone storage capacity from satellite-based evaporation. *EGU General Assembly Conference Abstracts 18.*

Wattenbach M, Zebisch M, Hattermann F, Gottschalk P, Goemann H, Kreins P, Badeck F, Lasch P, Suckow F and Wechsung F. 2007. Hydrological impact assessment of afforestation and change in tree-species composition – A regional case study for the Federal State of Brandenburg (Germany). *Journal of Hydrology,* 346: 1-17.

Xu CY. and Singh VP. 2004. Review on regional water resources assessment models under stationary and changing climate. *Water resources management*, *18*(6): 591-612.

Yang Y., Donohue R.J. and McVicar T.R. 2016. Global estimation of effective plant rooting depth: Implications for hydrological modeling. *Water Resources Research*, 52(10): 8260-8276.

Zegre NP. 2008. Local and downstream effects of contemporary forest harvesting on streamflow and sediment yield. PhD dissertation. Oregon State University.

Zhang M and Wang S. 2016. A review of precipitation isotope studies in China: Basic pattern and hydrological process. *Journal of Geographical Sciences,* 26(7): 921-938.

Zhao Q., Poulson S.R., Obrist D., Sumaila S., Dynes J.J., McBeth J.M. and Yang Y., 2016. Iron-bound organic carbon in forest soils: quantification and characterization. Biogeosciences, 13(1): 4777-4788.

Zhao J., Chen S., Hu R. and Li Y., 2017. Aggregate stability and size distribution of red soils under different land uses integrally regulated by soil organic matter, and iron and aluminum oxides. *Soil and Tillage Research*, 167(1): 73-79.

Zhu YI, Ren LI, Lui H and Skaggs TH. 2006. Determination of root-zone water storage in a desert woodland using a two-layer moisture balance model Hydrological Research in

China: Process Studies Modelling Approaches and Applications. *IAHS publication*, 322 (1):246.

# APPENDIX A

|  | **Two Streams** | **Cathedral Peak Catchment VI** |
|---|---|---|
| **Area (km²)** | 0.65 | 0.619 |
| **Latitude (◦)** | 29.20 | 28.99 |
| **Elevation (m)** | 1000 | 1952 |
| **MAP (mm)** | 964 | 1135 |
| **LAG** | NA | Schmidt/ Schulze |
| **SLOPE (%)** | NA | 25 |
| **XI30 (mm/hour)** | NA | 74.16 |
| **CORPPT** | NA | 1.254 |
| **QFRSPP** | 0.05 | 0.2 |
| **COFRU** | 0.005 | 0.009 |
| **EVTR** | Es and Et calculated separately | Es and Et calculated separately |
| **Soil texture** | Sandy Loam |  |
| **SMDDEP (m)** | 0.34 | 0.2 |
| **VEGETATION PARAMETERS** | | |
| **CAY** | | |
| JAN | 0.9 | 0.7 |
| FEB | 0.9 | 0.7 |
| MAR | 0.9 | 0.7 |
| APR | 0.88 | 0.5 |
| MAY | 0.85 | 0.3 |
| JUN | 0.86 | 0.2 |
| JUL | 0.89 | 0.2 |
| AUG | 0.9 | 0.2 |
| SEP | 0.92 | 0.5 |
| OCT | 0.92 | 0.65 |
| NOV | 0.9 | 0.7 |
| DEC | 0.9 | 0.7 |
| **LAI** | | |
| JAN | 2.62 | |
| FEB | 20.61 | |
| MAR | 2.6 | |
| APR | 2.45 | |
| MAY | 2.24 | |
| JUN | 2.11 | |
| JUL | 2.04 | |
| AUG | 2.09 | |
| SEP | 2.2 | |
| OCT | 2.38 | |
| NOV | 2.48 | |
| DEC | 2.46 | |
| **COIAM** | | |
| JAN | 0.25 | 0.15 |
| FEB | 0.25 | 0.15 |

| MAR | 0.25 | | 0.25 | |
|-----|------|---|------|---|
| APR | 0.3 | | 0.3 | |
| MAY | 0.3 | | 0.3 | |
| JUN | 0.3 | | 0.3 | |
| JUL | 0.35 | | 0.3 | |
| AUG | 0.35 | | 0.3 | |
| SEP | 0.3 | | 0.3 | |
| OCT | 0.3 | | 0.3 | |
| NOV | 0.25 | | 0.2 | |
| DEC | 0.25 | | 0.15 | |
| **VEGINT** | | | | |
| JAN | 1.76 | | 1.6 | |
| FEB | 1.76 | | 1.6 | |
| MAR | 1.76 | | 1.6 | |
| APR | 1.73 | | 1.4 | |
| MAY | 1.7 | | 1.2 | |
| JUN | 1.68 | | 1 | |
| JUL | 1.67 | | 1 | |
| AUG | 1.68 | | 1 | |
| SEP | 1.7 | | 1.3 | |
| OCT | 1.72 | | 1.6 | |
| NOV | 1.74 | | 1.6 | |
| DEC | 1.76 | | 1.6 | |
| **BELOW GROUND PARAMETERS** | | | | |
| **ROOT** | **A horizon** | **B Horizon** | **A horizon** | **B Horizon** |
| JAN | 0.7 | 0.3 | 0.9 | 0.1 |
| FEB | 0.7 | 0.3 | 0.9 | 0.1 |
| MAR | 0.7 | 0.3 | 0.9 | 0.1 |
| APR | 0.7 | 0.3 | 0.95 | 0.05 |
| MAY | 0.7 | 0.3 | 1 | 0 |
| JUN | 0.7 | 0.3 | 1 | 0 |
| JUL | 0.7 | 0.3 | 1 | 0 |
| AUG | 0.7 | 0.3 | 1 | 0 |
| SEP | 0.7 | 0.3 | 0.95 | 0.05 |
| OCT | 0.7 | 0.3 | 0.9 | 0.1 |
| NOV | 0.7 | 0.3 | 0.9 | 0.1 |
| DEC | 0.7 | 0.3 | 0.9 | 0.1 |
| **SOIL PARAMETERS** | | | | |
| | **A horizon** | **B Horizon** | **A horizon** | **B Horizon** |
| Depth (m) | 0.34 | 1.4 | 0.2 | 0.57 |
| PWP (m/m) | 0.093 | 0.28 | 0.131 | 0.158 |
| FC (m/m) | 0.189 | 0.35 | 0.222 | 0.25 |
| Porosity (m/m) | 0.448 | 0.448 | 0.439 | 0.411 |
| ABRESP | 0.65 | NA | 0.4 | NA |
| BFRESP | NA | 0.65 | NA | 0.4 |
| SMANI | 0.2 | 0.3 | 0.5 | 0.5 |

# APPENDIX B

| Soil Pattern code | Description | Soil Pattern code | Description |
|---|---|---|---|
| Ae | Freely drained, red, eutrophic, apedal soils comprise >40% of the land type (yellow soils comprise <10%) | Fb | Shallow soils (Mispah & Glenrosa forms) predominate; usually lime in some of the bottomlands in landscape |
| Af | Freely drained, red, eutrophic, apedal soils comprise >40% of the land type (yellow soils comprise <10%); with dunes | Fc | Shallow soils (Mispah & Glenrosa forms) predominate; usually lime throughout much of landscape |
| Ag | Freely drained, shallow (<300 mm deep), red, eutrophic, apedal soils comprise >40% of the land type (yellow soils comprise <10%) | Gb | Podzols occur (comprise >10% of land type); dominantly shallow |
| Ca | Land type qualifies as Ba-Bd, but >10% occupied by upland duplex/margalitic soils | Ha | Deep grey sands dominant (comprise >80% of land type) |
| Db | Duplex soils (sandier topsoil abruptly overlying more clayey subsoil) comprise >50% of land type; <50% of duplex soils have non-red B horizons | Hb | Deep grey sands sub dominant (comprise >20% of land type) |
| Dc | Either red or non-red duplex soils (sandier topsoil abruptly overlying more clayey subsoil) comprise >50% of land type; plus >10% occupied by black or red clays | Ib | Rock outcrops comprise >60% of land type |
| Fa | Shallow soils (Mispah & Glenrosa forms) predominate; little or no lime in landscape | Ic | Rock outcrops comprise >80% of land type |

# APPENDIX C

```r
library('readr')
PET <- read_csv('N:/Temperature.csv')

Day<- PET$Day
Tmax<- PET$Tmax
Tmin<- PET$Tmin
#Tmean<- PET$Taverage

et0_H <- function(latitude,Day,Tmin,Tmax)

  coeff = 0.0022

Tmean = (Tmax+Tmin)/2                      # calcul de la T moyenne

j    = (29.20*2*(4*(atan(1))))/360                # latitude de la station (rad)

dr   = 1 + (0.033 * cos(((2*(4*(atan(1))))/365)*Day))  # distance Terre-Soleil relative inverse
(rad)

d    = 0.409 * sin((0.0172*Day)-1.39)      #(2*pi)/365      # declinaison solaire (rad)

ws   = acos(-tan(j)*tan(d))                # angle de levee (rad)

Gsc  = 0.0820;                                    # constante solaire (MJ/m2/min)

# Eq. 21

Ra <- (24*60/(4*(atan(1)))) * Gsc * dr * (ws*(sin(j)*sin(d)) + (cos(j)*cos(d)) * sin(ws));
# rayonnement extra-terrestre (MJ/m2/j)


EToH = 0.0022*(Tmean+17.8)*0.408*Ra*((Tmax-Tmin)^0.5)    # coeff=0.0022

return(EToH)

write.csv(EToH, 'N:/PET.csv', row.names=F)
write.csv(Tmean, 'N:/Tmean.csv', row.names=F)
write.csv(Tmax, 'N:/Tmax.csv', row.names=F)
write.csv(Tmin, 'N:/Tmin.csv', row.names=F)
```

# APPENDIX D

```
install.packages("zoo")
install.packages("xts")
install.packages("hydroGOF")
install.packages(c("tidyr", "devtools"))
install.packages(c("dplyr"))

library(hydroGOF)
library(zoo)
library(xts)

library(readr)
library(tidyr)
library(dplyr)

setwd("N:/Model_output/") #set working directory


Obs_SF_2ST= read.csv("Obs_SF_2ST.csv") #read in observed data
Obs_SF_CP6= read.csv("Obs_SF_CP6.csv")
Obs_ET_2ST= read.csv("Obs_ET_2ST.csv")
Obs_ET_CP6= read.csv("Obs_ET_CP6.csv")

Sim_SF_2ST= read.csv("Sim_SF_2ST.csv") #read in simulated data
Sim_SF_CP6= read.csv("Sim_SF_CP6.csv")
Sim_ET_2ST= read.csv("Sim_ET_2ST.csv")
Sim_ET_CP6= read.csv("Sim_ET_CP6.csv")


kling_SF_2ST<-KGE(Sim_SF_2ST,Obs_SF_2ST, na.rm=TRUE, method="2012")    ~calculation of KGE, NSE
and RMSE
NSE_SF_2ST<-NSE(Sim_SF_2ST,Obs_SF_2ST, na.rm=TRUE, FUN= NULL)
RMSE_SF_2ST<-RMSE(Sim_SF_2ST,Obs_SF_2ST, na.rm=TRUE)

kling_SF_CP6<-KGE(Sim_SF_CP6,Obs_SF_CP6, na.rm=TRUE, method="2012")
NSE_SF_CP6<-NSE(Sim_SF_CP6,Obs_SF_CP6, na.rm=TRUE, FUN= NULL)
RMSE_SF_CP6<-RMSE(Sim_SF_CP6,Obs_SF_CP6, na.rm=TRUE)

kling_ET_2ST<-KGE(Sim_ET_2ST,Obs_ET_2ST, na.rm=TRUE, method="2012")
NSE_ET_2ST<-NSE(Sim_ET_2ST,Obs_ET_2ST, na.rm=TRUE, FUN= NULL)
RMSE_ET_2ST<-RMSE(Sim_ET_2ST,Obs_ET_2ST, na.rm=TRUE)

kling_ET_CP6<-KGE(Sim_ET_CP6,Obs_ET_CP6, na.rm=TRUE, method="2012")
NSE_ET_CP6<-NSE(Sim_ET_CP6,Obs_ET_CP6, na.rm=TRUE, FUN= NULL)
RMSE_ET_CP6<-RMSE(Sim_ET_CP6,Obs_ET_CP6, na.rm=TRUE)


print(paste("kling_SF_2ST=",kling_SF_2ST))  #print out
print(paste("kling_SF_CP6=",kling_SF_CP6))

print(paste("kling_ET_2ST=",kling_ET_2ST))
print(paste("kling_ET_CP6=",kling_ET_CP6))

print(paste("NSE_SF_2ST=",NSE_SF_2ST))
print(paste("NSE_SF_CP6=",NSE_SF_CP6))

print(paste("NSE_ET_2ST=",NSE_ET_2ST))
print(paste("NSE_ET_CP6=",NSE_ET_CP6))

print(paste("RMSE_SF_2ST=",RMSE_SF_2ST))
print(paste("RMSE_SF_CP6=",RMSE_SF_CP6))

print(paste("RMSE_ET_2ST=",RMSE_ET_2ST))
print(paste("RMSE_ET_CP6=",RMSE_ET_CP6))
```

# APPENDIX E- Statistics and Measures of Model Efficiency

The mean, variance and range were calculated using the following equations:

$$\bar{x} = \frac{\sum x_i}{n}$$

Where:

x = population mean (mm)

$x_i$ = value in dataset (mm)

n= number of values in dataset

$$\sigma^2 = \frac{\sum(x_i - \mu)^2}{n}$$

Where:

$\sigma^2$ = population variance (mm)

$x_i$= term in dataset (mm)

$\mu$= population mean (mm)

n= number of values in dataset

$$range = x_{max} - x_{min}$$

Where:

$x_{max}$= Maximum value in dataset (mm)

$x_{min}$= Minimum value in dataset (mm)

The Nash–Sutcliffe efficiency (NSE) and Kling- Gupta efficiency (KGE) are used to evaluate the performance of a model to predict reality. NSE and KGE can range from $-\infty$ to 1. An efficiency of 1 represents a perfect simulation of the observed data. An efficiency of 0 suggests that the model predictions are as accurate as the mean of the observed data. An efficiency less than zero indicates that the observed mean better represents reality than the model. The closer the model efficiency is to 1, the more accurate the model is. The Rscript used to calculate the NSE, KGE, RMSE and percent bias can be found in Appendix D.

$$NSE = 1 - \frac{\sum_{t=1}^{T}(Q_m^t - Q_o^t)^2}{\sum_{t=1}^{T}(Q_o^t - \overline{Q_o})^2}$$

Where:

$Q_o$ = Mean of observed data (mm)

$Q_m$ = Simulated data (mm)

$Q_o^t$ = Observed data (mm)

$t$= time

$$KGE = 1 - \sqrt{(r-1)^2 + \left(\frac{\sigma_{sim}}{\sigma_{obs}} - 1\right)^2 + \left(\frac{\mu_{sim}}{\mu_{obs}} - 1\right)^2}$$

Where:

r = correlation coefficient between simulated and observed data

$\sigma_{obs}$= Standard deviation of observation data

$\sigma_{sim}$= Standard deviation of simulated data

$\mu_{obs}$= Mean of observation data

$\mu_{sim}$= Mean of simulated data

The Root Mean Square Error (RMSE) demonstrates how concentrated the data is around the line of best fit. It is calculated by determining the standard deviation of the prediction errors.

$$RMSE = \sqrt{\sum \frac{(y_{sim} - y_{obs})^2}{n}}$$

$y_{obs}$= Observed data value (mm)

$y_{sim}$= Simulated data value (mm)

n= Number of values in dataset

The bias is the average measure of the simulated data to differ from the observed.  The optimal value for the bias is zero. Positive values indicate a model under- estimation and negative values indicate an over- estimation.

$$Bias = \frac{\sum_{t=1}^{n}(y_{obs} - y_{sim})}{\sum_{t=1}^{n} y_{obs}} \; x \; 100$$

Where:

$y_{obs}$= Observed data value (mm)

$y_{sim}$= Simulated data value (mm)

t= time

APPENDIX F

| Parameters | Description | Unitt |
|---|---|---|
| $u_2$ | Daily average wind speed | $m.s^{-1}$ |
| $F(u_2)$ | Aerodynmaic term for a unscreened Apan | $m. day^{-1}.kPa^{-1}$ |
| R | Apan radiation factor | |
| A | Latitude | Decimal degrees |
| F | Diffuse Radiation Factor | |
| $R_s$ | Incoming solar radiation | $MJ.m^{-2}. Day^{-1}$ |
| $R_a$ | Extra-terrestrial radiation | $MJ.m^{-2}. Day^{-1}$ |
| H | Heat argument factor | |
| $\alpha_s$ | Albedo of Apan surrounds | |
| $R_n$ | Net radiation | $MJ.m^{-2}. Day^{-1}$ |
| $R_{ni}$ | Constant net longwave radiation loss | $MJ.m^{-2}. Day^{-1}$ |
| $E_p$ | Apan evaporation | $mm. day^{-1}$ |
| $\Delta$ | Slope of vapour pressure curve | $kPa \, ^{\circ}C^{-1}$ |
| a | Parameter = 2.4 | |
| $\Upsilon$ | Psychometric constant | $kPa \, ^{\circ}C^{-1}$ |
| $\lambda$ | Latent heat of vapourisation | $2.45 \, MJ.m^{-2}.mm^{-1}$ |
| I | Interception | mm |
| t | Time step | Day, month, year, etc |
| $P_g$ | Gross Precipitation | mm |
| $P_e$ | Effective Precipitation | mm |
| $E_t$ | Actual evaporation | mm |
| RZSC | Root-zone storage capacity | mm |
| $F_{out}$ | Flow out | mm |
| $F_{in}$ | Flow in | mm |
| A | Accumulated deficit | mm |
| $t_n$ | Final time period | Day, month, year, etc |
| $t_{n-1}$ | Initial time period | Day, month, year, etc |
| D | Soil moisture deficit | mm |
| G | Groundwater recharge | mm |
| **XI30** | | |
| **CORPPT** | Rainfall correction factor | |
| **QFRSPP** | Stormflow response fraction | |
| **COFRU** | Coefficient of baseflow response | |
| **EVTR** | Option for computation of total evapoartion | |
| **SMDDEP** | Critical depth of soil from which stormflow is generated | m |
| **CAY** | Average monthly crop coefficient | |
| **ELAIM** | Monthly LAI information | |
| **COIAM** | Coefficient of initial abstraction | |
| **VEGINT** | Interception loss by vegetation | |
| **ROOTA** | Fraction of effective root system in topsoil | |
| **ROOTB** | Fraction of effective root system in B horizon | |
| PWP | Permanent wilting point | m/m |
| FC | Field capacity | m/m |
| DUL | Drained upper limit | m/m |

| | | |
|---|---|---|
| ABRESP | Fraction of saturated soil to be redistributed daily from topsoil to subsoil when topsoil is above DUL | |
| BFRESP | Fraction of saturated soil to be redistributed daily from subsoil to intermediate zone when topsoil is above DUL | |
| SMANI | Soil water content at the start of simulation | |
| $x$ | Population mean | |
| $x_i$ | Value in dataset | |
| $n$ | Number of values in dataset | |
| $\sigma^2$ | Population variance | |
| $Q_o$ | Observed values | |
| $Q_s$ | Simulated values | |
| $r$ | Correlation coefficient | |
| $\sigma$ | Standard deviation | |
| $\mu$ | Mean of dataset | |
| $y$ | Value in dataset | |